

# On the Analysis of Alkaline Sulfite Pulps by means of Pyrolysis - Gas chromatography/Mass spectrometry

## Dissertation

Zur Erlangung der Würde des Doktors der Naturwissenschaften  
des Fachbereichs Biologie der Fakultät für Mathematik,  
Informatik und Naturwissenschaften  
der Universität Hamburg



vorgelegt von  
**Andreas Klingberg**  
aus Kopenhagen, Dänemark

Hamburg 2013

Genehmigt vom Fachbereich Biologie  
der Fakultät für Mathematik, Informatik und Naturwissenschaften  
an der Universität Hamburg  
auf Antrag von Professor Dr. R. PATT  
Weiterer Gutachter der Dissertation:  
Professor Dr. H. SIXTA  
Tag der Disputation: 17. April 2013

Hamburg, den 02. April 2013



Professor Dr. C. Lohr  
Vorsitzender des  
Fach-Promotionsausschusses Biologie

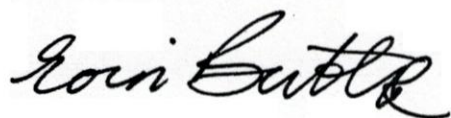
Eoin Butler  
Hafengasse 5  
D-72070 Tübingen

Tübingen, den 28.01.2013

**Bestätigung der Korrektheit der englischen Sprache**

Hiermit bestätige ich, Dr. Eoin Butler (irischer Staatsbürger), dass die Dissertation von Andreas Klingberg mit dem Titel „On the Analysis of Alkaline Sulfite Pulps by means of Pyrolysis-Gas chromatography/Mass spectrometry“ in korrektem und wissenschaftlichem englisch geschrieben wurde.

Mit freundlichen Grüßen

A handwritten signature in black ink, reading "Eoin Butler". The signature is written in a cursive, flowing style with a large initial 'E'.



# Danksagung

Die vorliegende Arbeit entstand an der Universität Hamburg und am Institut für Holztechnologie und Holzbiologie (HTB) des Johann Heinrich von Thünen-Instituts (TI, Hamburg), vormals Institut für Holzchemie und chemische Technologie des Holzes der Bundesforschungsanstalt für Forst- und Landwirtschaft (BFH).

Mein besonderer Dank gilt Herrn Prof. Dr. Patt für die Betreuung und Anleitung dieser Arbeit, Herrn Dr. Odermatt sowie Herrn Dr. Kordsachia für die ständige Diskussionsbereitschaft.

Des Weiteren sei den Mitarbeitern der Universität und des HTB für ihre Unterstützung meiner Analysen und für ein sehr angenehmes Arbeitsklima gedankt. Darüber hinaus möchte ich insbesondere Herrn Eidam und Frau Hamann für die Unterstützung im Labor danken sowie Herrn Dr. Wenig, Herrn Dr. Lehnen, Frau Heitmann und Herrn Dr. Meier für ihre ständige Bereitschaft, mir Hilfestellung bei Fragen und Problemen zu geben.

Für die finanzielle Unterstützung und das fördernde Interesse bedanke ich mich ganz herzlich bei Herrn Dr. Hans-Ludwig Schubert von der Firma Voith Paper Ravensburg.

Mein größter Dank gilt meiner Familie für ihre anhaltende Unterstützung während der Erstellung der Arbeit.

# Abbreviations

AMDIS .....	<b>A</b> utomated <b>M</b> ass <b>S</b> pectrometry <b>D</b> econvolution <b>A</b> nd <b>I</b> dentification <b>S</b> ystem
ANOVA .....	<b>A</b> nalysis <b>O</b> f <b>V</b> ariances
AS/AQ .....	<b>A</b> lkaline <b>S</b> ulfite <b>A</b> nthraquinone
ASAM .....	<b>A</b> lkaline <b>S</b> ulfite <b>A</b> nthraquinone <b>M</b> ethanol
BPC .....	<b>B</b> ase <b>P</b> eak <b>C</b> hromatogram
CAS .....	<b>C</b> hemical <b>A</b> bstracts <b>S</b> ervices
CI .....	<b>C</b> hemical <b>I</b> onization
DP .....	<b>D</b> egree of <b>P</b> olymerisation
EI .....	<b>E</b> lectronical <b>I</b> onisation
ESI .....	<b>E</b> lectrospray <b>I</b> onization
FID .....	<b>F</b> lame <b>I</b> onization <b>D</b> etector
G .....	<b>G</b> uaiacyl
GC .....	<b>G</b> as <b>C</b> hromatography
H .....	<b>p</b> -Hydroxyphenyl
HexA .....	<b>H</b> exenuronic of <b>A</b> cid
HPLC .....	<b>H</b> igh- <b>P</b> erformance- <b>L</b> iquid- <b>C</b> hromatography
HTB .....	Institut für <b>H</b> olz <b>t</b> echnologie und <b>H</b> olz <b>b</b> iologie
LC .....	<b>L</b> iquid <b>C</b> hromatography
MALDI .....	<b>M</b> atrix-assisted <b>L</b> aser <b>D</b> esoprtion/ <b>I</b> onization
MS .....	<b>M</b> ass <b>S</b> pectrometry
NIST .....	<b>N</b> ational <b>I</b> nstitute of <b>S</b> tandards and <b>T</b> echnology
NSSC .....	<b>N</b> eutral <b>S</b> ulfite <b>S</b> emi <b>M</b> echanical
PCA .....	<b>P</b> rincipal <b>C</b> omponent <b>A</b> nalysis
PLS .....	<b>P</b> artial <b>L</b> east <b>S</b> quares
Py .....	<b>P</b> yrolysis
S .....	<b>S</b> yringyl
TI .....	<b>T</b> hünen- <b>I</b> nstitut
TIC .....	<b>T</b> otal <b>I</b> on <b>C</b> hromatogram
TOF .....	<b>T</b> ime of <b>F</b> light
XIC .....	<b>E</b> xtracted <b>I</b> on <b>C</b> hromatogram

# Contents

<b>1</b>	<b>Introduction</b>	<b>6</b>
<b>2</b>	<b>Literature review</b>	<b>8</b>
2.1	Wood and pulp chemistry . . . . .	8
2.1.1	Polysaccharides . . . . .	9
2.1.1.1	Cellulose . . . . .	9
2.1.1.2	Hemicelluloses . . . . .	10
2.1.1.3	Dissolution and degradation of polysaccharides	11
2.1.2	Lignin . . . . .	12
2.1.2.1	Native lignin . . . . .	12
2.1.2.2	Delignification chemistry . . . . .	13
2.1.2.3	Residual lignin . . . . .	16
2.2	Alkaline Sulfite Pulping . . . . .	16
2.2.1	AS/AQ process . . . . .	17
2.2.2	ASAM process . . . . .	18
2.2.3	ASA process . . . . .	19
2.3	Chemical Characterization . . . . .	20
2.3.1	Benefits of instrumental chemistry . . . . .	22
2.3.2	Py-GC/MS . . . . .	22
2.3.2.1	Aspects of sample preparation . . . . .	23
2.3.2.2	Analytical pyrolysis . . . . .	24
2.3.2.3	Gas chromatography . . . . .	24
2.3.2.4	Mass spectrometry . . . . .	25
2.3.3	Multivariate data analysis . . . . .	26
2.3.3.1	Principal component analysis . . . . .	27
2.3.3.2	Partial least squares regression . . . . .	27
2.3.4	Applications of analytical pyrolysis . . . . .	28
<b>3</b>	<b>Materials and Methods</b>	<b>32</b>
3.1	Alkaline Sulfite Anthraquinone Pulping . . . . .	32
3.2	Analytical methods . . . . .	33

## CONTENTS

---

3.2.1	Standard analytical methods . . . . .	33
3.2.2	Analytical Pyrolysis . . . . .	34
3.2.2.1	Sample pretreatment and preparation . . . . .	34
3.2.2.2	Measuring conditions . . . . .	35
3.2.2.3	Data processing . . . . .	35
<b>4</b>	<b>Discussion of Results</b>	<b>37</b>
4.1	AS/AQ pulping process . . . . .	37
4.1.1	Composition of raw material . . . . .	38
4.1.2	Determination of favourable cooking conditions . . . . .	38
4.1.2.1	NaOH splitting ratio . . . . .	39
4.1.2.2	Cooking temperature . . . . .	39
4.1.2.3	Time of second NaOH charge . . . . .	39
4.1.3	Effects of NaOH splitting on pulps . . . . .	42
4.1.3.1	Effect on viscosity and brightness . . . . .	52
4.1.3.2	Effect on sulfonation . . . . .	53
4.1.3.3	Reference and replicate cooks . . . . .	56
4.2	Pyrolysis of ASA pulps . . . . .	58
4.2.1	Sample preparation . . . . .	59
4.2.2	Data pre-processing . . . . .	59
4.2.2.1	Smoothing and baseline correction . . . . .	63
4.2.2.2	Peak detection and deconvolution . . . . .	67
4.2.2.3	Ion extraction and integration . . . . .	74
4.2.2.4	Selection of extracted ions . . . . .	76
4.2.2.5	Normalization . . . . .	80
4.2.2.6	Removal of insignificant peaks . . . . .	90
4.2.2.7	Centering and scaling prior to MVA . . . . .	94
4.2.3	Exploratory data analysis . . . . .	97
4.2.3.1	External interferences . . . . .	97
4.2.3.2	Variable selection . . . . .	102
4.2.3.3	Identification of pyrolysis products . . . . .	104
4.2.3.4	Comparison of different pulping processes . . . . .	105
4.2.3.5	Comparison of samples A210 and B210 . . . . .	110
4.2.3.6	Comparison of the two delignification series . . . . .	117
4.2.4	Quantitative data analysis . . . . .	125
4.2.4.1	Quantification of sulfonic acid groups . . . . .	125
4.2.4.2	Quantification of pulp constituents . . . . .	127
<b>5</b>	<b>Summary</b>	<b>129</b>



# Chapter 1

## Introduction

Amongst the world-wide developed pulping technologies the kraft process is by far the most dominant process for the production of bleachable pulp grades. Because of the high strength properties of the produced pulps and the ability to pulp basically all hard- and softwoods the kraft process has outperformed the former leading acid sulfite process. However, pulping processes based on sulfite have also distinct advantages. Compared to the strongly alkaline kraft process, sulfite pulping is highly adjustable since it can be applied over a wide pH range and allows the production of various pulp grades. For example, the ASAM process developed by the work group of Professor Patt at the University of Hamburg received considerable attention in the 1980s - 90s due to the outstanding properties of the resultant pulps. Additionally the AS/AQ (alkaline sulfite anthraquinone) process was considered by some authors as a promising alternative to kraft pulping. But for several reasons, which shall not be discussed here, none of these processes attained commercial importance. Owing to the poor market acceptance of the AS/AQ process, only a handful of studies have been published on this sulfite based process, with few extending beyond process optimization coupled with standard analytical methods.

In a later work it was found that a modification of the AS/AQ process leads to a significant improvement, yielding pulps comparable with kraft pulps, particularly when softwood was used as feedstock (Rose 2003). The main modification was the reduction of the NaOH charge in the initial stage, while raising the NaOH concentration after the heating-up phase by addition of a second charge.

In the presented work the pulps generated by the aforementioned modified AS/AQ process were studied in detail by means of pyrolysis - gas chro-

matography/mass spectrometry (Py-GC/MS). The starting point was the execution of two delignification series, one without and the other with modification. One objective was to find the compositional differences responsible for the superior properties of the pulps produced by the modified process. Although standard analytical methods including the quantification of sulfonic acid groups (Katz *et al.* 1984) revealed important differences between the two delignification series, further details in particular about structural features of lignin were of interest.

Py-GC/MS was initially only intended to be tested as a novel rapid method to quantify sulfonic acid groups in pulp. But it was soon realized that Py-GC/MS had the potential to provide chemical fingerprints containing far more details on the samples, especially in combination with chemometric analyses. Previous studies have shown that the constituents of lignocellulosic materials could be distinguished and quantified with the aid of chemometrics (Bremer 1991, Kleen *et al.* 1993). However, in almost all studies only the major or well identified pyrolysis products were taken into account even though some of the several hundreds of further minor products contained in the pyrolysis fingerprints may provide valuable information. Nowadays, the computational advancement enables the processing of high amounts of data. In this work the focus was on the task of capturing as much information from the pyrolysis fingerprints of the AS/AQ pulps as possible. Within this scope much effort has been put on the pre-processing of data in a semi-automated manner to cope with the high complexity and to avoid error-prone manual evaluation. Eventually the pre-processed data was successfully evaluated by exploratory chemometric approaches revealing details of the residual lignin composition in AS/AQ pulps.

# Chapter 2

## Literature review

### 2.1 Wood and pulp chemistry

The basic purpose of wood pulping processes is the disintegration of the wood matrix to yield liberated fibers known as pulp which is not only utilized for papermaking but also as the raw material for various cellulose derivatives like cellophane and rayon silk (Sjöström 1993). Depending on the required end product, environmental and commercial constraints, and available expertise a suitable pulping process is selected. For most applications an extensive and selective removal of lignin from the wood matrix is desired which is referred to as chemical pulping. With respect to the established pulping technologies this target is only met by utilizing strong acidic or strong alkaline cooking conditions. As lignin is substantially responsible for the cohesion between the wood fibers its removal results in the desired defibration. But because of the close association with cellulose and hemicelluloses high chemical charges as well as fairly high temperatures have to be applied. This leads to some undesired degradation and dissolution of the polysaccharides accounting for losses in pulp yield and strength.

Regarding its chemical composition wood consists mainly of the three macromolecules cellulose, hemicelluloses and lignin which are all composed of the three elements carbon, oxygen and hydrogen. The components are closely associated with each other, the cellulose forming the skeleton of the wood cell and the hemicelluloses functioning as a matrix material and as a 'mediator' between lignin and cellulose. Lignin is viewed as an encrusting and cementing component being responsible for the rigidity of wood and the cohesion of adjacent cells. The relative proportions of these three polymeric constituents may vary depending on the wood species, tree age, habitat, cell type and even the cell wall type. In table 2.1 typical values for the overall composition of

common soft- and hardwoods are displayed according to Sjöström and Westermarck (1998). The two major hemicelluloses found in soft- and hardwood, glucomannan and xylan, are stated instead of the overall hemicelluloses content. All values refer to 'normal' wood, compression and tension wood found in soft- and hardwoods, respectively, have highly deviating values.

Table 2.1: Relative chemical composition of typical soft- and hardwoods used for pulping (adopted from Sjöström and Westermarck (1998))

Constituent	Softwoods [%]	Hardwoods [%]
Cellulose	37 - 43	39 - 45
Hemicelluloses		
Glucomannan <sup>a</sup>	15 - 20	2 - 5
Xylan <sup>b</sup>	5 - 10	15 - 30
Lignin	25 - 33	20 - 25
Extractives	2 - 5	2 - 4

a) Galactoglucomannans in softwood

b) Arabinoglucoronoxylan in softwood and Glucoronoxylan in hardwood

Opposed to cellulose exhibiting the same chemical composition in all wood species, the hemicelluloses and the lignin can show considerable variation e.g. between softwoods and hardwoods. In addition to the three polymers low molecular-weight substances summarized as extractives and inorganic compounds are found in wood (Sixta 2006, Sjöström 1993).

## 2.1.1 Polysaccharides

### 2.1.1.1 Cellulose

Cellulose is the most abundant biopolymer of the biosphere. In most wood species it is the main constituent with a relative proportion of approximately 37 - 45 % of the dry matter. Cellulose is a strictly linear homopolysaccharide consisting solely of  $\beta$ -1-4 linked anhydroglucose molecules with cellobiose being the smallest repeating unit (figure 2.1). The average degree of polymerisation (DP) of wood cellulose is quoted with about 10000. Due to their long-chained and unbranched character cellulose molecules tend to be subject to intra- and intermolecular forces leading to the aggregation to polymer bundles interlinked by hydrogen-bonds. These bundles again aggregate to

micro fibrils which show highly ordered crystalline regions alternating with less ordered amorphous regions (Sixta 2006, Sjöström 1993). The high degree of order in its ultrastructure accounts for the good mechanic durability of cellulose fibers in the direction of the polymer-orientation and is the basis for various applications of 'industrial' cellulose. Another important physical property is its insolubility in water and most organic solvents.

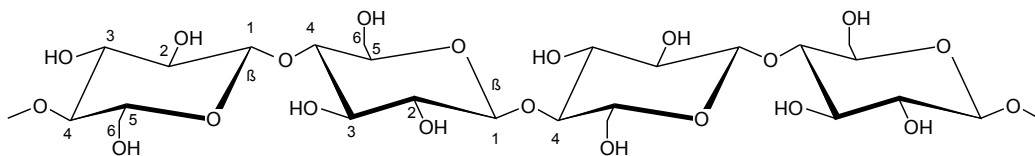


Figure 2.1: Cellulose structure

### 2.1.1.2 Hemicelluloses

Hemicelluloses include an assortment of different amorphous heteropolysaccharides consisting of monomeric units of D-glucose, D-xylose, D-mannose, D-galactose, L-arabinose, D-glucuronic acid, 4-O-methylglucuronic acid, D-galacturonic acid or in few cases L-rhamnose. These polysaccharides are branched and have a much lower DP (approx. 50 to 300) than cellulose contributing approximately 20-30% to the dry matter of wood (Sixta 2006, Sjöström 1993).

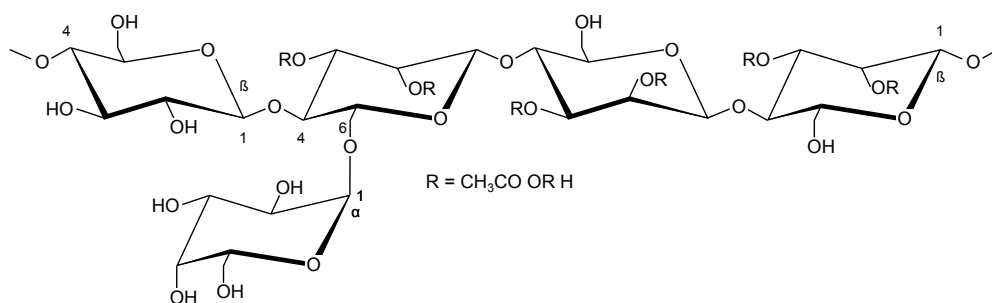


Figure 2.2: Softwood glucomannan structure

The predominant hemicelluloses found in softwood are glucomannans, galactoglucomannan and arabinoglucuronoxylans. The backbone of glucomannans consists of a slightly branched or linear chain of  $\beta$ -1-4 linked D-mannopyranose and D-glucopyranose units. Depending on the frequency of single units of D-galactopyranose being linked by  $\alpha$ -(1-6)-bonds to D-mannopyranose

units these hemicelluloses are referred to as glucomannan or galactoglucomannan. The C2- or C3-hydroxyl groups of the backbone are partly substituted by O-acetyl groups (figure 2.2) (Fengel and Wegener 1984, Sjöström 1993).

The backbone of arabinoglucoronoxylan, often referred to as xylan, consists of  $\beta$ -(1-4)-linked xylopyranose units. 4-O-methyl-D-glucuronic acid and L-arabinose are linked as single-unit side chains by  $\alpha$ -(1-2)- and  $\alpha$ -(1-3)-bonds, respectively. Substitutions by acetyl groups are not found ((figure 2.3)).

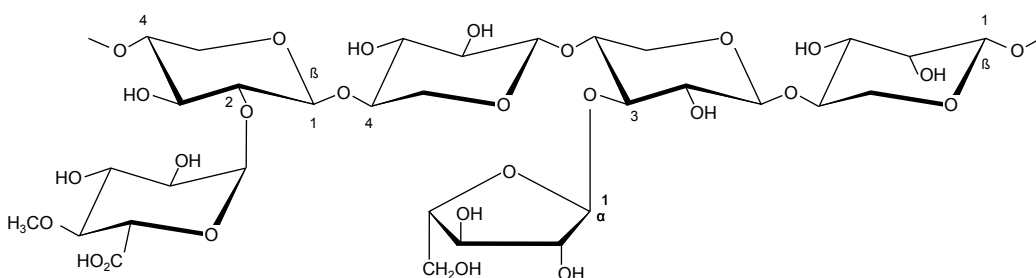


Figure 2.3: Softwood xylan structure

The major hemicellulose found in hardwoods is O-acetyl-4-O-methylglucurono- $\beta$ -D-xylan. Opposed to softwood xylan the backbone shows a high degree of substitution of the hydroxyl groups by acetyl groups at the C2 and C3 positions. Side chains consist of single units of 4-O-methylglucuronic acid. The second most abundant hemicellulose is glucomannan which has no side chains.

### 2.1.1.3 Dissolution and degradation of polysaccharides

Undesired losses of the polysaccharides can be considered the limiting factor in chemical pulping affecting pulp yield and strength properties. The high alkalinity and the high temperatures of 150 to 180°C applied in kraft, soda and AS/AQ pulping have several effects. Already in the heating-up period low-molecular hemicelluloses are dissolved and hemicellulosic acetyl groups are cleaved consuming considerable amounts of alkali. With increasing temperature also major parts of the higher-molecular amorphous hemicelluloses dissolve and both, hemicelluloses and cellulose are subjected to alkali-induced 'primary peeling' reactions, i.e. starting from the reducing end stepwise elimination reactions of monomeric units occur. At high temperatures further degradation of the polysaccharides involves alkali-induced hydrolysis leading

to random cleavage of the glycosidic linkages. Thus, 'secondary peeling' reactions are enabled starting from the new end groups formed. The peeling reactions continue until a competing 'stopping reaction' occurs stabilizing the end groups by the formation of an aldonic acid (Sjöström 1993).

In the last two decades considerable interest has been focused on the hex-enuronic acids (HexA) generated by alkali-induced demethoxylation reactions of the glucuronic acid residues present in xylan side chains. It has been shown that HexA consume permanganate during the essential Kappa tests leading to biased results. Furthermore, HexA are associated with paper yellowing, if not removed in bleaching, and may consume substantial amounts of bleaching chemicals, when e.g. a chlorine dioxide (D)-stage is employed (Buchert *et al.* 1995, Teleman *et al.* 1995, Li and Gellerstedt 1998, Jiang *et al.* 2000, Gustavsson and Al-dajani 2000, Sevastyanova *et al.* 2006, Sjöström 2006).

In alkaline sulfite processes reactions between  $\text{Na}_2\text{SO}_3$  and the polysaccharides may occur but do not play a major role. Yamazaki and Nakano (1972) have shown that sulfonation of holocellulose may take place with increasing tendency in alkaline environment. It is also assumed that the addition of  $\text{Na}_2\text{SO}_3$  may reduce the oxidative degradation of the polysaccharides (Ohi *et al.* 1989).

### 2.1.2 Lignin

#### 2.1.2.1 Native lignin

Lignin shows the most complex structure of the three major wood constituents. Although the detailed composition still remains unclear its major structural features have been elucidated. It is a hetero-polymer consisting of three-dimensionally interlinked monolignols which can derive from the three different phenylpropanoid precursors para-coumaryl, coniferyl and sinapyl alcohol. These monomeric building blocks incorporated in the polymer are commonly referred to as p-hydroxyphenyl, guaiacyl and syringyl lignin units (abbreviated with the acronyms H-, G- and S-units) which only differ in their degree of methoxylation of the phenolic residue. Lignins are found in all grasses, hard- and softwoods, but the overall amount and the ratio of the three different phenylpropane units vary greatly. Softwood lignin consists almost only of G-units, hardwood lignin of S- and G-units and only in grasses high amounts of H-units are found next to S- and G-units. A further characteristic adding to the complexity of lignin is the occurrence of various different bonding types between the monomers. The main linkages according

to Ralph *et al.* (2004) are shown in Figure 2.4. Table 2.2 displays experimentally determined values for the abundance of each of these linkages found in the literature. The arylglycerol- $\beta$ -arylether ( $\beta$ -O-4) linkage is by far the most abundant linkage with a proportion of up to 50 % in softwoods and around 60 % in hardwoods (Nimz 1974, Adler 1977, Brunow *et al.* 1998). Apart from the aryl ether linkages ( $\beta$ -O-4 and  $\alpha$ -O-4) a number of carbon-carbon bonds, referred to as *condensed* structures, are found. Due to the free C5 position at the phenolic residue particular linkages like the  $\beta$ -5 and the 5-5 bondings can only interlink G- or H-units. This implies that softwood lignin consisting mostly of G-units has higher proportions of these linkages and is more condensed than hardwood lignin.

Lignin also contains various functional groups. Next to methoxyl groups phenolic and aliphatic hydroxyl groups and a few terminal aldehyde groups are present. Since the majority of the phenolic hydroxyl groups are involved in the aryl ether linkages only 10 to 30% of the phenyl propane units have free phenolic hydroxyl groups (Brunow and Lundquist 2010).

The frequency of each bonding type and functional group is of great interest for chemical pulping because the reactivity and degradability of the lignin is directly influenced by these features. In pulping studies on hardwood the ratio of syringyl- to guaiacyl-units (S/G ratio) is a frequently studied structural feature (Guerra *et al.* 2008, Rutkowska *et al.* 2009, Santos *et al.* 2011, Silva *et al.* 2012). A high S/G ratio is attributed to a low amount of condensed lignin structures and hence a high proportion of  $\beta$ -O-4 linkages, which is stated to have a positive effect on alkaline delignification (Lapierre *et al.* 1999, Baucher *et al.* 2003).

Details on the biosynthesis and the structural features of lignin have been discussed and summarized, amongst others, by Sarkanen (1971), Ralph *et al.* (2004) and Brunow and Lundquist (2010).

### 2.1.2.2 Delignification chemistry

During chemical pulping delignification is basically reached by degradation and dissolution of lignin. Parts of the inter-unit linkages are cleaved and hydrophilic groups are introduced to render the resulting fragments soluble. Since the initially added pulping chemicals are gradually consumed and lignin fractions are gradually degraded and dissolved according to their reactivity the rate of delignification changes over the course of pulping. In this context the delignification process is described by dividing it into three phases. The *initial phase* is characterized by a rapid dissolution of *extractable* lignin already at temperatures below 140°C which may account for a removal of



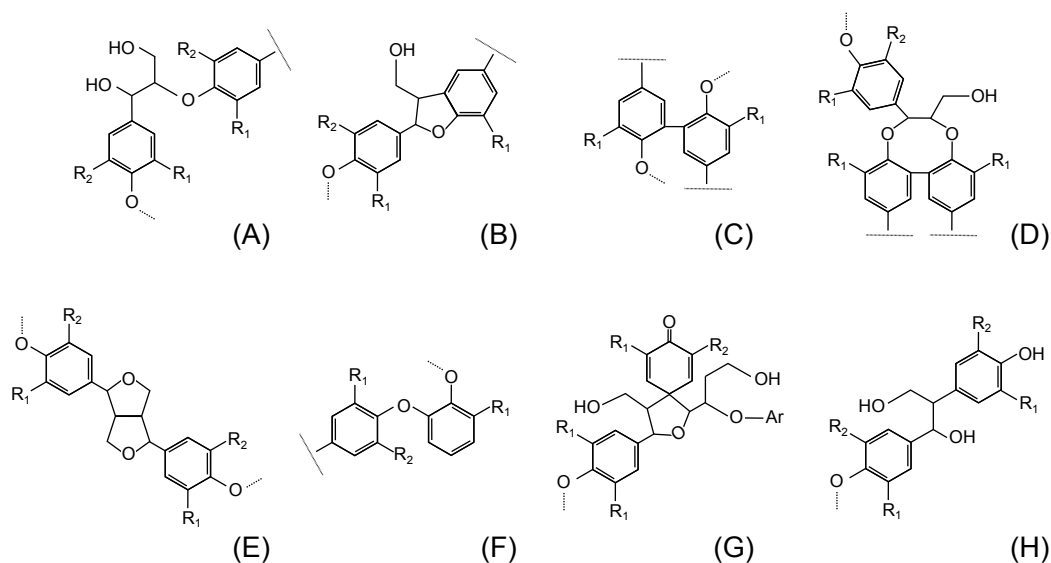


Figure 2.4: Major linkage structures of native lignins (p-hydroxyphenyl units:  $R_1 = R_2 = H$ ; guaiacyl units:  $R_1 = OMe$ ,  $R_2 = H$ , syringyl units:  $R_1 = R_2 = OMe$ ); adopted from Ralph *et al.* (2004).

20% of softwood lignin and 30% of hardwood lignin. In the *bulk phase* the major part of the lignin is selectively removed from the raw material. In kraft cooks approximately only 10% of the lignin remains in the pulp after the bulk phase. The *residual phase* refers to the final stage where the reactivity of the so-called *residual phase lignin* is low and the selectivity towards lignin degradation is very poor. At the transition to this stage it is usually recommended to terminate the cooking process to avoid high losses of polysaccharides (Gellerstedt 2009, Brännvall 2009).

In neutral and alkaline sulfite processes the active delignifying species are sulfite ( $SO_3^{2-}$ ), bisulfite ( $HSO_3^-$ ) and hydroxide ions ( $OH^-$ ) and hydrophilic groups are introduced by sulfonation via nucleophilic attack. A key reaction is the sulfonation of the  $C_\alpha$  of the propane side chain of aryl-ether units which may lead to subsequent sulfidolytic cleavage of the adjacent  $\beta$ -O-4 linkage (nucleophilic displacement). The delignification chemistry of the neutral sulfite pulping process has been studied by Gellerstedt (1976) and Chen *et al.* (1994a) with the aid of various lignin dimers representing typical structures in native lignin. It has been shown that at a pH range of 7 - 10  $\beta$ -O-4 cleavage was mainly restricted to dimers with free phenolic groups. The reaction path proceeded via the formation of a quinone methide intermediate which is also a typical intermediate in kraft pulping. Only non-phenolic  $\beta$ -aryl ether

## CHAPTER 2. LITERATURE REVIEW

---

Table 2.2: Linkages found in soft- and hardwoods

Structure	Linkage Type	Norway spruce [%]	Beech [%]
A	$\beta$ -O-4	36 <sup>a</sup> (48 <sup>b</sup> )	65 <sup>c</sup>
B	$\alpha$ -O-4	6-8 <sup>b</sup>	
B	$\beta$ -5	12 <sup>a</sup>	6 <sup>c</sup>
H	$\beta$ -1	2 <sup>a</sup>	15 <sup>c</sup>
E	$\beta$ - $\beta$	2.5 <sup>a</sup>	5 <sup>c</sup>
D	5-5-O-4	5 <sup>a</sup>	
F	4-O-5	4	1.5 <sup>c</sup>
G	Spirodienone	2 <sup>a</sup>	
C	5-5	4	2.3 <sup>c</sup>

a) Zhang and Gellerstedt (2000)

b) Erickson *et al.* (1973)

c) Nimz (1974)

structures with an  $\alpha$ -carbonyl group were also cleaved under these conditions (Gellerstedt 1976).

Further sulfonation of the side chain may lead to di- or trisulfonic acids but also sulfomethylation of the aromatic residue has been observed. Secondary reactions also involved are the subsequent elimination of sulfonic groups, cleavage of methylene from the methoxy groups and elimination of the terminal hydroxymethyl groups of the propane side chain to form enol ether structures liberating formaldehyde. Detailed reaction paths are depicted by Gellerstedt (1976) and Chen *et al.* (1994a).

The delignification chemistry of alkaline sulfite pulping with a pH greater 10 has not been studied in the same detail as the neutral sulfite process. But as the alkaline pulping process is capable to generate highly delignified pulps - with poor strength properties, though - it has been concluded that at high pH even non-phenolic  $\beta$ -aryl ether structures are cleaved (Gellerstedt 1976). The cleavage mechanism was suggested to follow the 'epoxide pathway' involving nucleophilic attack by the ionized neighbouring group in analogy to other alkaline processes (Gierer 1985). Due to the high alkalinity  $\text{OH}^-$  may

compete with  $\text{SO}_3^{2-}$  for the nucleophilic cleavage of phenolic  $\beta$ -aryl ether structures. The cleavage of the relatively stable condensed structures plays only a minor role in alkaline pulping (Gierer 1985).

### 2.1.2.3 Residual lignin

The lignin remaining in the pulp after the pulping process is termed *residual lignin*. The structure of the residual lignin differs from native lignin in several aspects. Considering sulfite pulp lignin the first major difference is the presence of sulfonated lignin structures since not all sulfonated lignin fractions are cleaved and dissolved. Secondly, the proportion of  $\alpha$ - and  $\beta$ -aryl ether structures in the residual lignin is significantly lowered as a function of the severity and selectivity of the pulping process. Neutral sulfite pulp lignin can be expected to still contain considerable amounts of the fairly reactive non-phenolic  $\beta$ -aryl ether structures. But the residual lignin of alkaline sulfite pulps may be approximately as enriched with alkali-stable enol ether structures and unreactive condensed lignin as kraft pulp lignin. However, it can be anticipated that the sulfonation partially hinders condensation reactions of lignin involving quinone methide intermediates which are typical for kraft pulping. During neutral sulfite pulping condensation reactions are not apparent (Gellerstedt 1976, Gierer 1985).

## 2.2 Alkaline Sulfite Pulping

Though the acidic sulfite process was the predominant pulping process until the 1950s at present it only accounts for approximately 10% of the chemical pulp production. A number of significant disadvantages have lead to the preference of the predominant alkaline kraft process for chemical pulp production. Foremost the inferior strength properties of the sulfite pulps, the long cooking time and a lower recovery yield of the cooking chemicals have to be noted in comparison to kraft pulping. Further disadvantages are its sensitivity towards bark, softwoods containing considerable amounts of resins (Rydholm 1965, Sixta 1998). Still, there are some advantages which explain the continuous interest in the process. To mention is the excellent bleachability of sulfite chemical pulp and the near-odorless process as opposed to the malodorous gases generated in kraft cooks. But in particular, its exceptional flexibility makes the sulfite process suitable for various niche-products (Patt and Kordsachia 1991). The conventional acidic sulfite process is conducted with aqueous solutions of calcium or magnesium hydrogen sulfite and sulfur dioxide at a pH below 2. The strong acidity leading to extensive hydrolytic

reactions on the polysaccharides is the main cause for the poor strength properties of the produced pulps. But the introduction of so-called soluble bases in the 1950s extended the applicable pH range for sulfite pulping. The substitution of calcium with magnesium, sodium or ammonium allows a higher flexibility in the adjustment of the pulping conditions. Particularly sodium as the base is utilized for sulfite pulping with neutral or alkaline aqueous solutions allowing the process to be conducted in a range between pH 7 and almost pH 13 (Ingruber 1985). The pH is set by choosing an appropriate ratio of the cooking chemicals sodium sulfite, sodium hydroxide and sodium carbonate. Along with the total chemical charge (based on wood) the ratio of the aforementioned chemicals permits an adjustment of the process in terms of severity and selectivity. Depending on the adjusted pH range the alkaline sulfite processes are divided into *neutral sulfite semi chemical* (NSSC) and *alkaline sulfite* (AS) pulping.

In the NSSC process  $\text{Na}_2\text{SO}_3$  or a mixture of  $\text{Na}_2\text{SO}_3$  and  $\text{NaHSO}_3$  is utilized as primary reactant.  $\text{NaOH}$  or  $\text{NaCO}_3$  are added to adjust the initial pH ranging between 7 and 10. Due to the weak alkalinity of the cooking chemicals the delignification reactions are slow and only minor amounts of lignin (25-50%) and hemicelluloses (30-45%) are degraded. In a second process step a mechanical defibration of the weakened wood matrix has to be applied. Mainly hardwoods and non-wood plants are utilized for the NSSC process with pulp yields ranging between 65% and 85% (McGovern 1952, Masura 1998).

The AS process is conducted with an initial pH ranging between 10 and 13 which is achieved by increasing the  $\text{NaOH}$  concentration. With  $\text{NaOH}$  as main reactant a further delignification can be accomplished, but extensive losses of yield and strength properties of the pulp have to be accepted. In order to receive pulps with acceptable strength properties and yield cooks have to be stopped at kappa numbers between 90 and 100 and only subsequent chlorine bleaching may yield pulp with sufficient brightness. Pulps with properties comparable to kraft pulp can hardly ever be attained (Ingruber 1985, Patt and Kordsachia 1991).

### 2.2.1 AS/AQ process

The discovery of the positive effect of anthraquinone (AQ) on alkaline pulping has lead to ongoing studies on alkaline sulfite processes. AQ causes stabilization of the polysaccharides and an observable improvement of the delignification kinetics in all alkaline pulping processes, including soda and

kraft pulping, but the enhancement on the alkaline sulfite process is much more pronounced. Only in the presence of sulfite and bisulfite AQ remains highly effective down to nearly pH 7, otherwise a pH range between 12 and 13 is necessary (Blain 1993, Chen *et al.* 1994b).

In a number of studies alkaline sulfite anthraquinone (AS/AQ) pulping has been considered as a promising alternative to conventional kraft pulping. Particularly in the late 1970s and throughout the 1980s works from Kettunen *et al.* (1979), Ingruber *et al.* (1982), McDonough *et al.* (1985) and Biasca (1989) have focused on a better understanding of the reaction kinetics and on possible improvements of AS/AQ pulping to receive pulps being competitive with kraft pulps. The process may generate pulps with strength properties similar to kraft pulps and comparably better bleachability and higher yield. These advantages diminish rapidly, however, when cooks are conducted to lower kappa numbers than 50 due to a significant decline in the delignification selectivity. But the lack of an appropriate and affordable chemical recovery system and the comparably long cooking time are considered as the main obstacles for an industrial application (Gellerstedt 1976, Biasca 1989).

### 2.2.2 ASAM process

The ASAM process refers to an AS/AQ process supplemented by methanol. The addition of methanol enhances the delignification selectivity significantly, even down to kappa numbers below 30, and enables the production of pulps with exceptionally high strength properties, high yields, facile bleachability and extensive lignin removal. The ASAM pulps have shown to be superior to kraft pulps in basically all important properties (Patt and Kordsachia 1991, Sixta 1998).

Depending on the wood species and the target properties of the pulp ASAM cooks are mostly conducted with  $\text{Na}_2\text{SO}_3$  to NaOH ratios ranging between 70/30 and 80/20, a total chemical charge of 20 - 25 %<sub>*o.d.wood*</sub> and methanol amounting to 10 to 35 %<sub>*liquor*</sub>. The process may also be conducted with  $\text{Na}_2\text{CO}_3$  replacing parts or all of the NaOH which lowers the alkalinity and hence the rate of delignification (Kordsachia and Patt 1987).

Because of its outstanding delignification performance the ASAM process has received a lot of attention in the pulping literature. In addition to the unfavourable chemical recovery system needed for sulfite processes the industrial implementation of the ASAM process failed because of the methanol demanding explosion proof equipment.

Details on the process can be found in various publications (Patt and Kordsachia 1986, Patt *et al.* 1987, Kordsachia and Patt 1987, Patt *et al.* 1991).

### 2.2.3 ASA process

To overcome the shortcomings of the AS/AQ process and to aim for pulp qualities close to ASAM chemical pulps without the use of an organic solvent Rose (2003) examined various cooking parameters of AS/AQ pulping of spruce and beech wood. The two key features which improved the AS/AQ process remarkably towards the aforementioned purpose were a shift of the  $\text{Na}_2\text{SO}_3$  to NaOH ratio towards NaOH and a segmentation of the added NaOH into two separate charges, termed NaOH splitting.

The favoured conditions for the modified AS/AQ pulping of spruce included an adjustment of the  $\text{Na}_2\text{SO}_3$  to NaOH ratio to 60/40, a fairly high total chemical charge of 27.5%/ o.d wood and a cooking time of 150 min at the maximum temperature of 175°C. 25% of the NaOH was added to the initial cooking liquor and the remaining 75% was added directly after the heating-up period of 90 min when the maximum temperature was reached (Rose 2003).

Even without NaOH splitting an increase of the NaOH charge improved the delignification resulting in kappa numbers well below 30. But on the downside the viscosity, as an indicator for pulp strength was comparably low which pointed to an extensive damage of the cellulose (Patt *et al.* 2002). The application of NaOH splitting showed a very pronounced positive effect, as shown in table 2.3. The kappa number could be reduced by 6.5 down to almost 20, the viscosity could be increased by 100 mL/g and the brightness of the pulps could be improved. The modified AS/AQ process was termed ASA process.

Table 2.3: Influence of NaOH splitting on AS/AQ pulping of spruce according to Rose (2003); total chemical charge: 27.5%,  $\text{Na}_2\text{SO}_3$ /NaOH ratio: 60/40, cooking temperature: 175°C, cooking time at  $T_{max}$ : 150 min

NaOH splitting [%]	Kappa no. [%]	Viscosity [ml/g]	brightness [ISO %]	yield [%]	shives [%]
100/0	26.7	1125	25.1	47.8	2.1
25/75 <sup>a</sup>	20.2	1228	32.6	47.7	2.3

a) 75% of NaOH added after 90 min when  $T_{max}$  was reached

## 2.3 Chemical Characterization

For the chemical characterization of lignocellulosic biomass a vast number of different methods are available and detailed descriptions can be found in literature. Distinctions between the various methods may be drawn with respect to the analytical technique or with respect to the level or depth of characterization. The most basic level is the qualitative and quantitative determination of the main components cellulose, hemicelluloses, lignin, extractives and inorganics. In most studies on pulping and bleaching performance the quantification of wood and pulp components plays an essential part. A set of standardized procedures designed for the pulp and paper industry allows the determination of each component separately (TAPPI and SCAN test methods). The inorganics are determined via the ash content, the extractives by a soxhlet extraction procedure, the lignin by *Klason lignin* or *kappa number* determination and the assessment of polysaccharides by extraction of lignin with sodium chlorite and subsequent *alkali dissolution* of the hemicelluloses. The relevant test methods can also be adapted to a smaller scale (Ona *et al.* 1995).

The compositional analysis of each component can be considered the next higher level of characterization. The methods are more time-consuming and also demand higher expertise. In particular hemicelluloses and lignin, showing high variation in composition, have been subject to multiple studies. Most methods involve several experimental steps including isolation and depolymerization of the wood component under study. Polysaccharides are effectively depolymerized by hydrolysis with aqueous acids or by methanolysis which was reviewed by Chambers and Clamp (1971), amongst others. As the final step, the quantification of the monomers is carried out with chromatographic techniques such as high performance anion exchange chromatography with pulsed amperometric detection (HPAEC-PAD) and gas chromatography/mass spectrometry (GC/MS) (Rocklin and Pohl 1983, Sullivan and Douek 1994, Sundberg *et al.* 1996).

For the analysis of lignin composition well-established degradative methods such as *nitrobenzene oxidation* (Sarkanen 1971), *thioacidolysis* (Lapierre *et al.* 1985) and *derivatization followed by reductive cleavage* (DFRC) (Lu and Ralph 1997) are applied. These procedures mainly lead to the cleavage of the highly abundant  $\beta$ -O-4 linkages without any undesired condensation reactions. The dissolved monomers are finally analysed by GC/MS, gas chromatography coupled with a flame ionization detector (GC/FID) or liquid chromatography (LC) giving close estimates of the ratio between the different

phenyl propane units (S/G/H ratio) and allow the quantitative determination of  $\beta$ -O-4 structures. With particular modifications of both procedures also C-C bonded dimers or even oligomers can be determined (Peng *et al.* 1998, Lapierre *et al.* 1991).

All degradative methods are unable to reveal the actual sequence and structure of the wood polymers in the sample under study and the degradation procedures may even lead to alterations obscuring some structural details. The highest level of characterization so far can be achieved by solution-state 2D nuclear magnetic resonance (NMR) methods which enable the elucidation of lignin subunit composition, lignin interunit linkage distribution and polysaccharide profiling without prior isolation of the components (Lu and Ralph 2011, Mansfield *et al.* 2012).

To supplement the structural analysis of lignocellulosic material there are also numerous methods available for the quantification of the various functional groups and, in case of pulps, methods for the determination of physical properties (e.g. fiber strength, brightness and viscosity) have high significance. Most studies on pulping and bleaching performance, however, concentrate only on a few particular structural and physical features to avoid dispensable and time-consuming analyses (O’Connell *et al.* 2002, Guerra *et al.* 2008, Rutkowska *et al.* 2009, Santos *et al.* 2011, Silva *et al.* 2012).

Regarding studies on sulfite pulping and sulfite pre- or post-treatment of wood or thermomechanical pulp, respectively, the determination of sulfonic acid groups incorporated into lignin may be of interest. The sulfonation is often a rate-determining step in the delignification (Rydholm 1965) and particularly for high-yield pulps the degree of sulfonation has an impact on papermaking properties (Atack *et al.* 1980, Zhang *et al.* 1994). Difficulties in developing an appropriate direct method for the determination of sulfonic acid groups arise from the presence of other anionic groups which make it necessary to distinguish between weak and strong acids. The review of Beatson (1992) has thoroughly covered a few direct methods (Sjöström and Enström 1966, Cappelen and Schöön 1966, Katz *et al.* 1984) and the indirect determination of sulfonic acid groups via the sulphur content (Douek and Ing 1989) up until the 1980s. The conductometric titration proposed by Katz *et al.* (1984) has been established as the reference method as it has proven as highly accurate and enables to distinguish between carboxylic and sulfonic acids. The method of Sjöström and Enström (1966) based on the selective ion-exchange interaction between sulfonic acids and benzidine ions and the potentiometric titration method proposed by Cappelen and Schöön (1966)



both lack complete selectivity (Katz *et al.* 1984). Westermarck and Samuelsson (1993) proposed a method similar to the one of Sjöström and Enström (1966) using quinoline hydrochloride as an alternative to benzidin. At a pH of 2.5 quinoline is selectively bond to the sulfonic groups and can be eluted again by 0.5 M HCl. The released quinoline is finally determined by UV-spectrophotometry. Results showed a very good agreement with the results using conductometric titration. Applications involving analytical pyrolysis for the sulfonic acid group determination is discussed in section 2.3.4.

### 2.3.1 Benefits of instrumental chemistry

The detailed characterization of wood and other lignocellulosic biomass has advanced quickly in the last decades. Because of the development and refinement of various spectroscopic and chromatographic applications and significant enhancement of the measuring devices good alternatives to a number of wet-chemical standard procedures have emerged. Though, wet-chemical procedures still play an important role, they are mostly time-consuming and often only allow the characterization of one or two features of the analyte at the time, e.g. kappa number. At present nearly any available chromatographic and spectroscopic technique has been tested for its suitability to substitute or complement traditional wet-chemistry. Techniques such as nuclear magnetic resonance (NMR), infrared (IR) or Raman spectroscopy and pyrolysis coupled with gas chromatography (Py-GC) and/or mass spectrometry (Py-GC/MS, Py-MS) (see section 2.3.2) have gained great interest, since they are capable of providing information on several structural features simultaneously and hence can be used as effective screening tools for large-scale sample sets. Because of the multivariate nature of the resulting analytical data the evaluation can be greatly improved by chemometric approaches (see section 2.3.3).

### 2.3.2 Py-GC/MS

Analytical pyrolysis enables the study of solid and liquid organic macromolecules. By applying enough thermal energy cleavage of covalent bonds occurs. The analysis of the resulting fragments by gas or liquid chromatography, mass spectrometry, or infrared spectroscopy may lead to qualitative, quantitative or structural information about the macromolecular analyte (Wampler 1995, Moldoveanu 1998). The most common analytical technique hyphenated with pyrolysis is gas chromatography (Py-GC) which allows the separation of the volatile fragments. For the detection and quantification of these volatiles mostly FID or MS are coupled with the GC. But also direct hyphen-

ation of the pyrolysis with mass spectrometry is a well-established technique (Moldoveanu 1998). Applications of analytical pyrolysis include the analysis of natural or synthetic polymers, fuel sources, micro-organisms, surfactants, composites, complex industrial, forensic and various environmental materials (Wampler 1995).

### 2.3.2.1 Aspects of sample preparation

In many cases analytical pyrolysis only demands very little sample preparation. Apart from reasonable drying solid samples do not have to be milled, extracted or subjected to other pretreatment as long as they fit into the device-specific sample holder. In particular, if only overall qualitative structural information is required this advantage makes pyrolysis a rapid screening tool.

Though, for the purpose of (semi-)quantitative analyses or detailed comparison of highly similar samples reasonable sample preparation becomes necessary. Because of very small sample sizes (well below 1 mg) being usually advantageous in analytical pyrolysis thorough milling helps to homogenize the samples and improve reproducibility significantly. Bremer (1991) also recommended a thorough desiccation of lignocellulosic samples since a noticeable influence of residual water on the pyrolysis fingerprints was observed. In addition, sample contamination has to be avoided as it can have high impact on the analysis results (Wampler 1995).

Further sample pretreatment may be necessary if certain inorganic species are present in the analyte. It has been reported by several authors that inorganic compounds may have a strong catalytic effect on the pyrolysis of lignocellulosic biomass altering the product pattern (van Loon *et al.* 1991, Kleen and Gellerstedt 1995, Muller-Hagedorn *et al.* 2003, Fu *et al.* 2008). Higher amounts of e.g. sodium or magnesium ions may even lead to the absence of any valuable chemical information in the data as it was observed for freeze-dried pulping liquors (in-house). In this case prior removal of the inorganic species is advisable.

For the well-established approach of using the pyrolysis apparatus for the simultaneous thermal decomposition and derivatization of analytes the manner of application of the additional reactant has to be considered. As an example tetramethylammonium hydroxide (TMAH) is widely used as a derivatizing agent for the analysis of lignocellulosic material. Mostly, the TMAH is added in excess as a diluted solution to achieve a thorough contact between sample and reactant. To remove the solvent and avoid undesired oxidation reactions the pretreated samples are dried under nitrogen or vacuum (Hardell and Nilvebrant 1996, Vane *et al.* 2001).

### 2.3.2.2 Analytical pyrolysis

By definition, pyrolysis refers to chemical degradation reactions caused by thermal energy in the absence of oxygen. In most analytical settings pyrolysis is utilized to transform macromolecular organic substances into volatile fragments which can subsequently be analysed by MS or GC/MS. If sufficient thermal energy is provided cleavage of covalent bonds by different degradation mechanisms is achieved and stable fragments are generated. For most applications pyrolytic reactions take place at temperatures well above 300°C (Moldoveanu 1998). Typical temperatures applied to lignocellulosic samples lie between 450 and 650°C (Alves *et al.* 2006, Rodrigues *et al.* 1999, Choi *et al.* 2001, Ucar *et al.* 2005, Yokoi *et al.* 2001, Gerber *et al.* 2012, Faix *et al.* 1991, Nunes *et al.* 2010, Kleen and Lindstrom 1994). Temperatures beyond 800°C lead to unspecific low molecular fragments which often lack any informative value. Apart from the temperature also other measurement parameters, e.g. heating rate, heating time and pyrolyzer design have a high impact on the resulting product distribution. Due to the significant improvement of pyrolysis instrumentation in the last two decades the measurement parameters can be controlled in a reproducible way. As a result the repeated pyrolytic degradation of an analyte under the same conditions ideally yields a similar characteristic "fingerprint" (Wampler 1995). Nowadays analytical pyrolysis is utilized for qualitative and quantitative applications and even minor differences between samples may be traceable by this technique. Wampler (1995), Moldoveanu (1998) and Irwin (1982) offer detailed descriptions of the history, reaction mechanisms and applications of analytical pyrolysis.

### 2.3.2.3 Gas chromatography

Gas chromatography enables the separation and analysis of vaporizable compounds without decomposition and, hence, the composition of complex mixtures may be elucidated. The separation mechanisms are based on the temperature-dependent different interactions between the inner coating of the separating column (stationary phase) and each component of a mixture (mobile phase) because of their molecular size and polarity. The quality of separation is influenced by a number of parameters, e.g. the choice of column length, column coating, carrier gas and temperature program. Well adjusted parameters allow a reproducible time-resolved detection of the separated components eluting at the end of the column (Hübschmann 1996). Although a slow temperature rise time can be expected to improve separation there is a trend towards short temperature programs with steep temperature ramps to increase the analysis throughput. This technique, termed "fast

GC", utilizes shorter columns and demands sophisticated data-evaluation due to inferior separation. It is best realized by hyphenation with the new generation of mass spectrometers (Time-of-Flight(TOF)-MS) which offer a high rate of data acquisition.

Today gas chromatography can be considered an indispensable workhorse technique in most analytical laboratories. The ability to detect and quantify trace amounts of various volatile substances present in complex mixtures and the development of various other analytical techniques hyphenated with GC results in a broad field of applications. Hyphenated with analytical pyrolysis sample-specific fingerprints can be obtained which may be used for classification or other multivariate approaches.

### 2.3.2.4 Mass spectrometry

For the detection and quantification of the GC separated molecules mainly flame ionization detectors and mass spectrometers are utilized. The major advantage of mass spectrometry is the additional ability to identify the eluting components. After entering the MS via a transfer line connecting the GC with the MS the GC separated molecules are ionized under high-vacuum. The most commonly used ionization method in mass spectrometers is electron ionization (EI). Here, each molecule is bombarded by electrons generating a radical cation which initiates an instant further fragmentation depending on its stability. All charged fragments are recorded by a mass selective detector resulting in a distinct and highly reproducible molecular fragmentation pattern called mass spectrum. Various commercial libraries are available containing extensive collections of mass spectra of identified compounds.

Instead of recording a broad range of mass fragments to receive comprehensive mass spectra, called full scan, the data collection may be reduced to a small number of certain ion fragments, called selected ion monitoring (SIM), to improve the detection limit. The selected ions serve as representatives of the associated molecules. For evaluation purposes it is also common practice to extract representative ions for each compound of interest from full scan measurements. The peak areas of extracted ions or ions collected in SIM mode are proportional to the corresponding full scan peaks (Hübschmann 1996). Reale *et al.* (2004) has thoroughly reviewed various analytical techniques utilizing mass spectrometry for lignin analysis.

### 2.3.3 Multivariate data analysis

For many years now multivariate approaches have been recognized as invaluable tools for the evaluation of extensive amounts of data. The early application of these statistical and mathematical methods to measured chemical data is strongly related to the increasing access to computers and go back to the 1970s (Kessler 2007, Otto 2007). Svante Wold and Bruce R. Kowalski introduced the term chemometrics which may be defined as follows: *'How to get chemically relevant information out of measured chemical data, how to represent and display this information, and how to get such information into data'* (Wold 1995). Chemometric techniques not only include exploratory multivariate approaches (pattern recognition, classification, discriminant analysis) and multivariate calibration methods (e.g. Partial least squares regression (PLSR)) but also quantitative structure-activity relationships (QSAR) studies, multivariate curve resolution (MCR) and design of experiments (DOE).

The benefit of *multivariate* analysis (MVA) of spectroscopic and chromatographic data can be explained by the nature of the acquired data. Most wet-chemical methods in wood and pulping science (e.g. kappa number determination, ash content) yield a single numerical result per sample. Also spectroscopic methods are often utilized for single responses, e.g. UV spectroscopic determination of dissolved lignin content may be measured at a wavelength of 280 nm (Sjöström 1999). These *univariate* data sets are typically evaluated by univariate analysis including statistics (e.g. arithmetic mean, standard deviation, analysis of variance (ANOVA)), univariate calibration (e.g. simple linear regression) and *bivariate* analysis, i.e. a relationship between two different univariate data sets at a time is explored (e.g. kappa number as a function of pulp yield).

In contrast, infrared spectroscopic and gas chromatographic measurements both yield signal profiles consisting of up to several hundred or thousand scans and each scan may be regarded as a variable. In chromatographic profiles, though, it is also common practice to treat the eluting peaks (consisting of several scans) as variables instead. Although by far not every scan holds valuable information, infrared spectroscopy and chromatographic devices serve the purpose of providing several details of a complex sample or sample mixture simultaneously. Provided that the amount of measured samples is sufficient in a statistical sense multivariate analysis enables to extract all the meaningful information from this kind of multivariate data.

Conventional univariate or bivariate data analysis is still routinely used for spectroscopic and chromatographic data but the advantages of MVA have made it a very popular alternative or even the method of choice.

In the following sections 2.3.3.1 and 2.3.3.2 short descriptions of the two MVA techniques principal component analysis (PCA) and partial least squares regression (PLSR) are given. Details on these and various other techniques can be found in multiple publications (Massart *et al.* 1997, Brereton 2003, Kessler 2007).

### 2.3.3.1 Principal component analysis

Principal component analysis (PCA) is a chemometric procedure which may be applied when a high number of variables, attributes or properties are measured on a large-scale data set and it is aimed at reducing the extensive data to a few meaningful and independent factors. PCA enables to reduce a large  $N$ -dimensional space into a small  $M$ -dimensional space ( $M \ll N$ ). An outstanding feature of this procedure is that most of the information contained in the data is retained and in most cases it actually will be displayed in a clearer way. PCA merges strongly intercorrelated variables into new *latent* variables which are also termed factors or principal components (PC). These principal components are determined with respect to their importance for the data set. The explained variance of each PC defines the sorting order. The first PC is always showing in the direction of the maximal variance within the data. The second PC has to be perpendicular to the first as the PCs construct a new coordinate system. In addition it has to explain the next highest variance in the data. It is proposed to extract as many PCs as necessary to gather all important information contained in the examined data set. The random noise, e.g. caused by fluctuations of the measuring device or sampling variation, should be excluded. Hence, PCA separates meaningful patterns from random noise. In certain cases PCA may be susceptible to errors. If the model contains too few PCs the data is not described sufficiently (*underfitting*) and if parts of the random noise is included into the model (*overfitting*), unpredictable negative effects can arise when the model is applied on new data (Massart *et al.* 1997, Kessler and Kessler 2010).

### 2.3.3.2 Partial least squares regression

Partial least squares regression has gained considerable importance in the last decades to describe dependencies between multiple, sometimes highly intercorrelated variables. In chemistry PLSR has emerged by far as the most popular multivariate regression algorithm. In particular in spectroscopy sam-

ple properties (termed y-variables), tedious to measure by other means, are calibrated by PLSR from rapidly determined spectra (termed x-variables). The popularity of this regression method can be reasoned by particular advantages: Opposed to other multivariate approaches PLSR still performs well when x-variables are highly correlated and/or intercorrelated and the number of scans or peaks (variables) is much higher than the number of samples (objects). Both is usually the case in IR spectra and Py-GC/MS data. In analogy to PCA the PLSR procedure extracts principal components but for this purpose the calculations include the known sample properties (y-variables) of the calibrants. As a result the PLS components are more associated with the target values than it is the case if the y-variables were excluded. The risk of over- or underfitting persists. With the aid of the resulting calibration models the properties of unknown samples can be calculated on basis of their measured spectra or chromatograms (Brereton 2003, Kessler and Kessler 2010).

### 2.3.4 Applications of analytical pyrolysis

Analytical pyrolysis has been extensively applied for the characterization of lignocellulosic material. Utilized techniques include **Py-MS** (Evans *et al.* 1986, Pouwels and Boon 1990, Tuskan *et al.* 1999, Labbe *et al.* 2005, Mann *et al.* 2009), **Py-GC/FID** (Bremer 1991, Marques *et al.* 1994, Yokoi *et al.* 1999, Ucar *et al.* 2005, Alves *et al.* 2006), **Py-GC/MS** (Faix *et al.* 1988, Kleen *et al.* 1993, Sjöberg *et al.* 2002, Ucar *et al.* 2005) and pyrolysis coupled with simultaneous derivatization primarily with TMAH, often named **THM-GC/MS** (Hatcher *et al.* 1995, Hardell and Nilvebrant 1996, Filley *et al.* 2002), but also other derivatizing agents were applied (Kuroda 2000, Fabbri *et al.* 2002). Also derivatization prior to the pyrolysis has been investigated. Camarero *et al.* (1999) employed diazomethane methylation to various isolated lignins and concluded that pyrolysis may be used for the determination of free phenolic groups.

Apart from studies focusing primarily on analytical pyrolysis (Galletti *et al.* 1995, Camarero *et al.* 1999), there are numerous publications comparing or correlating pyrolysis results with other analytical techniques (Backa *et al.* 2001, Lima *et al.* 2008, Nunes *et al.* 2010) or describing in-depth characterization of lignocellulosic biomass with analytical pyrolysis supplementing the fleet of analytical techniques applied (Ibarra *et al.* 2007, Rencoret *et al.* 2008). Most studies concentrate on lignin because of its distinct and highly reproducible degradation pattern providing straight forward details on the samples (Galletti and Bocchini 1995). The numerous volatile degradation

products mainly include derivatives of monomeric phenylpropane units characteristic for the lignin polymer (Faix *et al.* 1990). Apart from cleavage of the comparably weak  $\alpha$ - and  $\beta$ -O-4 linkages yielding the monomers the propanoid sidechain of the lignin fragments is partly or completely degraded. In addition pyrolytic dehydrogenation reactions lead to double bonds in the side chain. The chemistry of decomposition becomes even more complex as secondary reactions take place which may result in e.g. the conversion of guaiacols to catechols (Faix *et al.* 1987). It is still not clearly answered which lignin substructure each of these pyrolysis products derive from (Dorrestijn *et al.* 2000). To get a better insight into the cleavage mechanisms of the various chemical bonds of lignin structures numerous studies have been conducted on model compounds (Brezny *et al.* 1983, Klein and Virk 1983, Evans *et al.* 1986, Faix *et al.* 1988, Masuku *et al.* 1988, Bredenberg *et al.* 1989, Britt *et al.* 1995, Kuroda *et al.* 2007, Kawamoto and Saka 2007, Watanabe *et al.* 2009).

Analytical pyrolysis has gained considerable popularity for the assessment of changes in ratio of the p-hydroxyphenyl (H), guaiacyl (G) and syringyl (S) units of lignin. Although several alternative methods like thioacidolysis, NMR or FTIR are also applicable analytical pyrolysis may be the quickest and most straightforward technique besides FTIR. In particular the S/G ratios of hardwoods are used as an important indicator for the degradability of lignin and hence has significance in studies dealing with forest breeding (Rodrigues *et al.* 1999), genetic engineering of wood properties (Baucher *et al.* 2003), the comparison of pulp wood species (Rencoret *et al.* 2007) or the changes in the course of delignification (Ibarra *et al.* 2005, Rovio *et al.* 2011). Owing to the higher reactivity of syringyl type lignin all degradation methods including analytical pyrolysis tend to overestimate the syringyl moiety (Sarkanen and Hergert 1971, Genuit *et al.* 1987). In most studies the S/G ratio has been determined by calculating the ratio either between the sums of all syringyl-type and all guaiacyl-type phenols, respectively (Rodrigues *et al.* 1999, Choi *et al.* 2001), or only between the sums of defined selections of syringyl-type and guaiacyl-type phenols (Lima *et al.* 2008, Nunes *et al.* 2010). To determine appropriate correction factors for the overestimation of the syringyl-type lignin several studies have correlated the results of analytical pyrolysis with other methods (Böttcher 1993, Lima *et al.* 2008, Nunes *et al.* 2010).

PCA was used by several authors to perform discriminative analyses on the basis of analytical pyrolysis. In a study on *Eucalyptus camaldulensis* Yokoi *et al.* (1999) showed that within-tree variations of lignin composition can well



be traced by utilising Py-GC/FID data for a multivariate approach. And also a discrimination of trees of the same species with different origins succeeded (Yokoi *et al.* 2001). Eleven different *E. camaldulensis* trees were distinguished using 13 G- and 13 S-lignin derived products as the variables. The products deriving from polysaccharides were not considered. Also the S/G ratios were determined simply by taking the ratio of the respectively summed up S- and G-lignin derived products. But a discrimination by means of the S/G ratios was insufficient.

Backa *et al.* (2001) compared FTIR and Py-GC/FID for the characterization of fungal degraded birch wood by means of PCA and PLS. They concluded that both analytical techniques could be utilized to give detailed information on structural changes and to predict the weight losses (from 0 to 45%) due to fungal degradation. But Py-GC/FID was somewhat superior for the assessment of the different degradation patterns with respect to the type of fungus under study (brown-rot versus white-rot fungus).

Sjöberg *et al.* (2002) employed Py-GC/MS along with a combination of enzymatic hydrolysis and capillary electrophoresis for the analysis of the composition of the surface and inner layers of softwood pulp fibers obtained from various alkaline pulping processes. The evaluation of the Py-GC/MS data by PCA enabled a clear discrimination between surface and inner layer samples but also between kraft and soda-type pulps. In addition, the surface layer samples could be associated with relatively higher abundances of lignin-derived products with shortened aliphatic side-chains indicating a higher degree of lignin degradation. The higher lignin content on the surface layer as compared to the inner layers was also revealed by the pyrolysis data. The calculations of the respective lignin contents, though, were not performed by a multivariate approach. For each sample the peak areas of lignin-derived products were summed up and simply related to the respective sum of all peak areas. This simple method of lignin quantification has also been investigated by Alves *et al.* (2006) and Fahmi *et al.* (2007) on some softwoods and grasses respectively. They correlated the sum of area normalized lignin-derived peaks to results obtained from the Klason method and built simple linear regression models with correlation coefficient of  $R^2=0.93$  and  $R^2=0.88$  respectively. Fahmi *et al.* (2007) used PCA to preselect the best correlating lignin-derived products for quantification.

For the quantification of lignin and the polysaccharides also the potential of multivariate linear regression has been investigated. Bremer (1991) compared several methods for the quantification of the main constituents by

Py-GC/FID. More than 50 lignocellulosic samples, mainly comprising various wood species, and 114 identified peaks were used as basis for the study. Next to the comparison of simple linear regressions using various area sums of meaningful subselections of peaks multivariate PLS regressions were conducted. Although some of the simple regression models were acceptable it could be shown that PLS regression yielded the best results. PLS models with correlation coefficients  $R^2 \geq 0.99$  were obtained for lignin, the sum of hexoses, sum of pentoses, glucose and xylose. Only for mannose, galactose and arabinose  $R^2$  was below 0.9.

In the study of Kleen *et al.* (1993) PCA and PLS were conducted on the Py-GC/MS data obtained from 32 softwood kraft pulps with kappa numbers ranging from 85 to 25 and pulp yields lying between 59.7 and 43.1%. PCA enabled a clear grouping of the pulps in dependence of the cooking time mainly caused by the decreasing lignin content over time by using only 23 pyrolysis products. Various further details were concluded from the PCA results presented by the score and loading plot which were in accordance with the prior knowledge of the authors about kraft pulping. From the obtained PLS regression results the authors concluded a high potential of Py-GC/MS for the quantitative analysis of the main constituents of softwood kraft pulps. Various further studies dealing with the analysis of lignocellulosic material by means of analytical pyrolysis combined with multivariate data evaluation can be found in literature (Sjöberg *et al.* 2004, Labbe *et al.* 2005, Meier *et al.* 2005, Vinciguerra *et al.* 2007, Alves *et al.* 2009, Gerber *et al.* 2012).

The feasibility of employing analytical pyrolysis for the quantification of sulfonic acid groups in lignosulfonic acids has been illustrated by van Loon *et al.* (1993). A selective and quantitative procedure based on Py-MS was applied on a number of reference lignosulfonates and effluent samples from sulfite pulp mills. In previous studies it was already demonstrated that the pyrolysis of sulfonic acids yields  $\text{SO}_2$  and the capability of using this pyrolysis product for quantification was suggested (van de Meent *et al.* 1982, van Loon *et al.* 1991). As the Py-MS technique is lacking appropriate separation of the pyrolysis products the quantification has to be done by selectively integrating peaks of marker ions unique to the respective analyte. In case of  $\text{SO}_2$   $m/z$  64 is used as the representative. Best results were achieved with the standard addition method.

# Chapter 3

## Materials and Methods

### 3.1 Alkaline Sulfite Anthraquinone Pulping

**Samples** analysed in this work were obtained from cookings with wood chips of spruce (*Picea abies*). The wood chips were supplied by the sawmill Ruser in Bornhöved (Schleswig-Holstein). The wood chips were sorted by a vibrating screen with a slotted sieve of 8 mm and a wire mesh with mesh size of 6 mm. Afterwards wood chips exceeding the length of approx. 40 mm, as well as bark and branch particles were manually removed. The dry content of the screened wood chips was determined by taking five samples of the thoroughly mixed chips drying them to constant weight at 105°C. After gravimetrical determination of the dry content, portions of 600 g<sub>o.d.wood</sub> were sealed in airtight PE bags. The wood was stored prior and after screening at -18°C.

Prior to the cooks 600 g<sub>o.d.wood</sub> of wood chips were **steamed** in a wire basket insert for 30 min. The water uptake after steaming was gravimetrically determined and taken into account for the adjustment of the liquor to wood ratio.

**Cookings** were conducted in two identical batch digesters (M/K-Systems Inc.) each with a volumetric capacity of 7 l and equipped with liquor-circulation. The wire basket insert containing the wood chips was placed into the digester and the cooking liquor and anthraquinone (0.1%<sub>o.d.wood</sub>) was added. When a sufficient flow of the circulation pump (approx. 2 l/min) was ensured the digester was sealed and the cook started. A perforated steel-plate placed on top of each cooking batch ensured an even distribution of the circulated cooking liquor. The installed JUMO-controller allowed temperature and time controlled cooks.

After **termination** of the cook the sealed digester was quickly cooled down to as low as 60°C with the aid of a water cooling system (water temperature approx. 0°C) to minimize losses of matter due to evaporation. Care was taken to have a similar rate of cooling down in each cook. The degas and drain valves were opened, all free flowing spent sulfite liquor collected and stored at -18°C. The chips in the basket insert were rinsed for 10 min under a flow of tap water and left to drain for another 10 min. In a PE-bucket the batch was covered with 14 l of deionised water and left for 24 h overnight. After the chips were transferred into a strainer and left to drain for 5 min they were centrifuged in a spin drier for another 5 min. The weight of the batch was determined and a sample taken and stored in a PE-bag at -18°C. Depending on the degree of delignification the batch was washed and pulped in a laboratory pulper. The shives were separated in a screen slot and the dry content of pulp and shives was gravimetrically determined (at 105°C). If the the degree of delignification was low samples for dry content determination were taken after spin-drying and the remaining batch stored in a PE-bag at -18°C.

The reference kraft and ASAM cooks were conducted in a rotary digester with a volumetric capacity of 7 l was used. Due to lack of a cooling system the cooling down period exceeded 90 min. The work-up procedure was similar to the AS/AQ cooks.

## 3.2 Analytical methods

### 3.2.1 Standard analytical methods

- **Lignin content:** The lignin content was assessed according to Klamason (TAPPI T 222 om-88). The acid-soluble fraction was determined according to TAPPI T 250 (1976).
- **Extractives:** The content of extractives was determined by successive hot-water and cyclohexane/ethanol extraction (Soxhlet apparatus) on the basis of TAPPI T 204 cm-97.
- **Ash content:** The ash content was determined according to TAPPI T 211 om-93 and TAPPI T 413 om-93.
- **Dry content:** The dry content was determined gravimetrically according to the Zellcheming specification IV/42/67.

- **Kappa number:** The determination of the kappa number was conducted according to the Zellcheming specification IV/37/80 using a titrator device (SCHOTT) based on temperature compensation.
- **Brightness:** The preparation of the samples for the determination of brightnesses was conducted according to the Zellcheming specification V/19/63. The ISO brightness was assessed with an Elrepho 2000 according to SCAN C 11:75.
- **Intrinsic viscosity:** The intrinsic viscosities (termed simply *viscosity* in the discussion) were determined according to the Zellcheming specification IV/36/61 by means of a capillary viscometer using a copper ethylenediamine solution. The pulp viscosity can be utilized as an estimate for the mean degree of polymerization of the polysaccharides. The viscosity may also be used as an estimate for strength potential of pulps.
- **Carbohydrate composition:** The carbohydrate composition was determined on acid-hydrolysed pulps according to Sinner *et al.* (1975), Sinner and Puls (1978).
- **Determination of sulfonic and carboxylic acid groups:** The contents of sulfonic and carboxylic acid groups were determined by the conductometric titration method (Katz *et al.* 1984).
- **Hexenuronic acids:** The contents of HexA was determined on 4 pulp samples at the Royal Institute of Technology, KTH / Wood Chemistry and Pulp Technology (Stockholm, Sweden) by the method of Gellerstedt and Li (1996).

### 3.2.2 Analytical Pyrolysis

#### 3.2.2.1 Sample pretreatment and preparation

Prior to analysis the pulp samples were acid-washed according to the pretreatment in the method of Katz *et al.* (1984) to remove  $\text{Na}^+$  and milled in a ball-mill cooled by liquid nitrogen. Due to incomplete defibration the samples of the short cookings ( $A_{30}$  -  $A_{90}$  and  $B_{30}$  -  $A_{150}$ ) had to be defibrated before acid-washing. A bleached chemi-mechanical spruce pulp (BCTMP spruce) was provided by Åbo Akademi, Turku, Finland. Samples were accurately weighed ranging from 120 - 150  $\mu\text{g}$  and the weights recorded.

### 3.2.2.2 Measuring conditions

The pyrolysis system consisted of a Frontier Lab Micro furnace Double-shot Pyrolyzer (Py-2020iD) equipped with an Autosampler (AS-1020 E). The interface of the pyrolyzer was kept at a temperature of 360°C and was purged with a continuous helium flow for 10 s prior to pyrolysis. After pyrolysis the products were transferred (split 1:50) into the capillary column (ZB-1701 (Phenomenex) 60 m x 0.25 mm, 0.25  $\mu$ m) via the directly connected GC-injector. The injection port of the Agilent 6890 GC System was kept at 280°C. The gas chromatography (Agilent 6890) was performed with helium as the carrier gas at a flow rate of 1 ml/min. The oven program started off with 4 min of isothermal condition at 45°C, then was raised at a rate of 5 °C/min to 280 °C and was finally kept at this temperature for 15 min. For mass spectral detection an Agilent 5973N MSD was used with an electron impact ionisation energy of 70 eV. The scan range was 15 - 600 m/z. All measurements were performed in TIC mode. If not stated otherwise, at least duplicate analyses were performed.

### 3.2.2.3 Data processing

Identification of the products was carried out using an in-house library, NIST MS library (02) and literature comparison. For baseline and smoothing the software *metAlign* (Lommen 2009) was utilized. The procedure was conducted in Nominal Mass Mode with the following settings: "Retention Begin" 1, "Retention End" 11500, "Maximum Amplitude" 12000000, "Peak Slope Factor" 1.0, "Peak Threshold Factor" 2.0, "Peak Threshold" 0, "Average Peak Width at Half Height" 7. "Keep Peak Shape" was activated. Details on the parameters are found in the manual or have been described by Lommen (2009). Peak detection and deconvolution was performed with AMDIS (Stein 1999) with the aid of the implemented *Batch Job* mode. The following filter settings were used: "Min. Model Peaks" 5, "Weights" 1, "Minimum S/N" 20.0, "Weights" 1, "Min. Certain Peaks" 0.95, "Weights" 1, "Min. Abundance" 1.0, "Weights" 1, "Min. Signal Strength" 0, "Weights" 0. The following deconvolution settings were employed: "Component width" 32, "Omit m/z" 0 15 17 18 19 29 32 44, "Adjacent peak subtraction" one, "Resolution" high, "Sensitivity" medium, "Shape requirements" medium.

Extraction of the AMDIS results, data filtering to compile the global peak list and statistical calculations were conducted with the aid of self-written scripts in MATLAB (The MathWorks, Natick, MA) using implemented functions. In addition, chromatograms were exported from the ChemStation (Agilent Technologies) as *netCDF* files and imported into MATLAB utilizing the

### CHAPTER 3. MATERIALS AND METHODS

---

freely available iCDF function published by Skov and Bro (2008). For integration of peak areas of extracted ions MS-SIM-Tools (in-house software) was employed. Multivariate analyses were performed with the aid of the PLS Toolbox for MATLAB v. 7.02 (Eigenvector Research, Inc., Wenatchee, WA). For calculations of Fisher's discriminant ratios a free MATLAB code supplied by Will Dwinnell ([predictr@bellatlantic.net](mailto:predictr@bellatlantic.net)) was implemented.

# Chapter 4

## Discussion of Results

### 4.1 AS/AQ pulping process

In the course of previous in-house studies conducted on alkaline sulfite anthraquinone pulping, the influence of important process parameters on the yield and quality of the generated pulp was investigated (Rose (2003), (see chapter 2.2.1)). The focus was on the generation of bleachable grade pulps with strength properties comparable with kraft pulps. The effect of variation of the total chemical charge, duration of the cook and the ratio of cooking chemicals, sodium sulfite to sodium hydroxide, was verified. A vital finding was that a time-based proportionate addition of sodium hydroxide to the AS/AQ cooking process can lead to an enhanced delignification of softwoods. This approach was termed *NaOH splitting* (see chapter 2.2.1). In comparison with AS/AQ cooks, where all cooking chemicals were added to the initial impregnation liquor, similar cooks with NaOH splitting yielded pulps with lower kappa numbers as well as higher viscosities, brightnesses and strength properties. The positive effect of keeping the concentration of sodium hydroxide low at the beginning of the cook is also known for the kraft process. Due to a lower pH at the beginning the pH-dependent degradation of carbohydrates is reduced and the sulfide sorption enhanced at the same time. It is referred to as one of the principles of so-called *extended delignification*. To get a closer understanding of the enhancement achieved by NaOH splitting in the AS/AQ process, two delignification series were performed. Two series of ten cooks, each terminated at different times, were conducted. The first series was performed with all chemicals added at the beginning (series A). For the second series the conditions of the NaOH splitting approach were applied (series B). Beforehand approx. 30 cooks were performed to determine



the cooking parameters for the delignification series. In addition some cooks of the delignification series were repeated.

### 4.1.1 Composition of raw material

For all softwood cooks and the subsequent analyses conducted industrial wood chips of *Picea abies* were used. Apart from being one of the most important softwoods for pulping spruce wood is the most thoroughly studied species in terms of its ultrastructure, chemical composition and behaviour in pulping processes. The composition of the raw material was determined and is listed in 4.1. The results are in good agreement with values stated in the literature (Fengel and Wegener (1984)).

Table 4.1: Composition of *Picea abies* raw material.

Constituent	<i>Picea abies</i> [% <sub><i>o.d.w.</i></sub> ]
KLASON-lignin	27.32
Acid-soluble lignin	0.3
Extractives Cyclohexane-Ethanol	1.64
Extractives Water	1.57
Glucose	47.4
Xylose	5.2
Mannose	12.4
Galactose	1.9
Arabinose	0.8
Rhamnose	-
Ash content	0.239

### 4.1.2 Determination of favourable cooking conditions

Before the delignification series were performed the desirable process conditions had to be assessed. Although most pulping conditions could be adopted from the results of the previous work (Rose (2003)), some minor alterations were done. The total chemical charge of 27.5%<sub>*o.d.wood*</sub> (calculated as NaOH), the ratio of cooking chemicals, sodium sulfite to sodium hydroxide of 60:40,

and the heating-up period of 90 min were kept unaltered. For all cooking trials the wood chips were presteamed to remove enclosed air and to enhance impregnation.

#### 4.1.2.1 NaOH splitting ratio

For the delignification series with NaOH splitting the proportion of NaOH to be added with the initial pulping liquor had to be defined. For spruce, under the previously described cooking conditions, it was verified that NaOH splitting ratios between 50/50 and 25/75 may be favourable. The produced pulps had kappa numbers well below 25 and exceptionally good viscosities (Patt *et al.* (2002), Rose (2003)). A main goal of this study was to gather details particularly on the delignification performance of AS/AQ cooks with and without NaOH splitting. Therefore it seemed appropriate to choose a splitting ratio for the NaOH of 25/75 for the series B as it resulted in pulps with the lowest kappa number.

#### 4.1.2.2 Cooking temperature

Most of the cooks of the previous work were performed at cooking temperatures  $T_{max}$  of 180 and 175°C. For the present study it was decided to lower  $T_{max}$  to 170°C as it allowed a slightly more gentle pulping (Patt *et al.* (2002)) and was more viable in terms of industrial applicability. In first cooking trials performed with NaOH splitting (25/75) at 170°C it became apparent that the cooking time had to be prolonged by 30 min to reach a kappa number well below 30. But lowering  $T_{max}$  from 180 to 170 °C resulted in an improvement of viscosities by approx. 200 ml/g at the expense of an increase of the kappa number from approx. 20 to 27.

#### 4.1.2.3 Time of second NaOH charge

The preferable time for the second NaOH addition was investigated by Rose (2003) for cooks conducted at 175°C with pine wood and a NaOH splitting ratio of 50/50. The results suggested an addition of 75% of the total NaOH straight after the heating-up period of 90 min when  $T_{max}$  is reached. In the present study the influence of the time for the second NaOH addition was investigated again for the cooks conducted at 170°C with spruce wood and a NaOH splitting ratio of 25/75. In table 4.1.2.3 the results are summarized.

Table 4.2: Influence of time  $t_2$  of second NaOH addition on pulp yield, kappa number, viscosity, brightness, rejects and final pH of the AS/AQ pulps.

Cook <sup>a)</sup>	NaOH splitting	$t_2^b)$ [min]	Total yield [% <sub>o.d.wood</sub> ]	Kappa number	Viscosity [ml/g]	Bright- ness [%ISO]	Rejects [% <sub>o.d.wood</sub> ]	Final pH <sup>c)</sup>
ASAsp22	100/0	-	49.5	30.2	1135	22.4	2.1	11.7
ASAsp23	100/0	-	49.1	30.4	1131	22.1	2.1	12.1
ASAsp20	25/75	90	50.5	27.0	1228	25.4	2.6	11.6
ASAsp24	25/75	90	50.3	27.1	1248	25.6	2.9	11.9
ASAsp19	25/75	120	50.4	25.1	1279	28.9	1.8	11.9
ASAsp21	25/75	150	49.7	24.6	1333	30.3	1.7	12.0
ASAsp26	25/75	150	49.5	24.2	1303	29.9	1.5	12.3
ASAsp27	25/75	180	50.5	23.6	1317	31.2	1.5	12.4
ASAsp31	25/75	180	49.7	26.5	1326	29.8	1.6	12.3
ASAsp28	25/75	210	49.5	27.6	1375	31.4	1.7	12.4
ASAsp29	25/75	240	50.8	28.7	1384	32.7	2.6	12.6
ASAsp30	25/75	270	51.0	34.2	1382	32.1	2.7	12.8

a) Total chemical charge: 27.5%<sub>o.d.wood</sub>, ratio Na<sub>2</sub>SO<sub>3</sub>/NaOH: 60/40, T<sub>max</sub>: 170°C, heating-up time: 90 min, AQ: 0.1%<sub>o.d.wood</sub>

b) The second charge of NaOH was added with 600 ml of water. The liquor/wood ratio increased from 4.3 to 5.38

c) The end pH refers to the pH measured on sulfite spent liquor at 20°C

## CHAPTER 4. DISCUSSION OF RESULTS

---

Apart from ASAsp22 and ASAsp23 all cooks displayed in table 4.1.2.3 were performed with a NaOH splitting ratio of 25/75. The time  $t_2$  of the second NaOH addition was varied between 90 and 270 min with respect to the cooking time of 300 min including the heating-up period of 90 min. The duplicate cooks performed without NaOH splitting (ASAsp22 and ASAsp23) serve as reference cooks.

The yields of all cooks ranged within narrow limits of 49 and 51% implying that the variation of  $t_2$  only had marginal effect on the yield. Overall, the cooks with NaOH splitting (except ASAsp30) yielded pulps with lower kappa numbers and higher viscosities than the two reference cooks. This confirmed the observations of Rose (2003) with respect to the general improvements achieved with NaOH splitting. But also the influence of the time of the second NaOH addition became apparent. Opposed to the results of the former work (Rose (2003)) the lowest kappa number was achieved when  $t_2$  was 150 or 180 min. Presumably the reduction of  $T_{max}$  from 175 to 170°C, resulting in a decreased rate of reaction, and the lower amount of NaOH in the first stage of the cook lead to a discrepancy with respect to former results (Rose (2003)).

In the case of cook ASAsp30 the high final kappa number of 34.2 may be explained by the late addition of the second load of NaOH. Added only 30 min before termination of the cook the remaining time may not have been sufficient for the NaOH to accomplish the slow alkaline cleavage reactions and dissolution of the unreactive residual phase lignin.

Other effects achieved by NaOH splitting are higher brightnesses and viscosities of the unbleached pulps. The brightness of 22.4 %ISO and the viscosity of 1135 ml/g, as measured for the reference pulp of cook ASAsp22, could be raised by up to 10 %ISO and 250 ml/g, respectively (ASAsp29). The later the second NaOH charge was added the higher was the viscosity and the brightness of the pulp.

Figure 4.1 illustrates the influence of  $t_2$  on the kappa number and viscosity of the generated pulp for the cooking conditions described above. For the delignification series with NaOH splitting (series B) it was decided to set the time  $t_2$  of the second NaOH charge at 180 min, where the lowest kappa number and yield of rejects were achieved, and the viscosity and brightness were reasonably high (table 4.1.2.3).

A further alteration was the introduction of a water cooling system. In this context it has to be noted that in table 4.1.2.3 only the cook ASAsp31 was

## CHAPTER 4. DISCUSSION OF RESULTS

performed with water cooling and may explain the higher kappa number and viscosity of the pulp as compared to cook ASAsp27.

Since the series of cooks were intended to yield pulps and sulfite spent liquors for analytical studies, biased results may arise due to continuous reactions occurring at a long cooling-down phase and losses of volatile components when degassing the digester. For a temperature drop from 170 to 100°C the cooling system enabled to shorten the duration of cooling from 90 to 30 min keeping the digester sealed. Because of the rapid cooling and the lower cooking temperature, as mentioned above, the cooking time at  $T_{max}$  was finally prolonged to 240 min with respect to the results shown in table 4.1.2.3.

It can be anticipated that cooks employed with a different charge of spruce raw material may demand another optimal time of addition of the second NaOH charge.

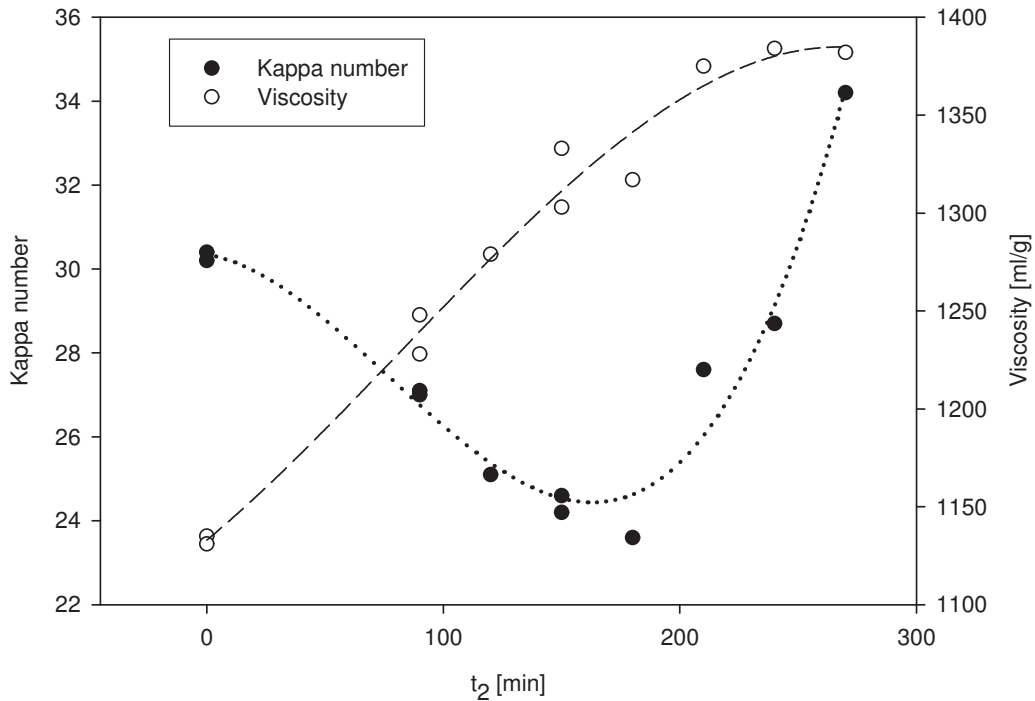


Figure 4.1: Effect of time  $t_2$  (including heating-up period) of second NaOH charge on the kappa number and viscosity.

### 4.1.3 Effects of NaOH splitting on pulps

For the two delignification series 10 cooks were performed for each series. It was anticipated that the most significant differences between the two series would be observable before  $t_2$  (time of second NaOH addition). Hence, for the period of the first 180 min the AS/AQ cooks were terminated at relatively short time intervals after 30, 60, 90, 120, 150 and 180 min, respectively. The time intervals between each of the last three cooks in the sequence were 60 min, at 210, 270 and 330 min. An additional cook was terminated at 190 min, ten minutes after the second alkali charge, to monitor any rapid effect hereof. In the following discussion the delignification series without NaOH splitting is referred to as series A and the series with NaOH splitting as series B, respectively.

Table 4.3: Chemical composition of pulping liquor.

	Series A	Series B
Chemical charges, as NaOH, % <sub>o.d.wood</sub>		
Total charge	27.5	27.5
Initial charge	27.5	19.25
Na <sub>2</sub> SO <sub>3</sub>	16.5	16.5
NaOH, initial charge	11	2.75
Anthraquinone charge, % <sub>o.d.wood</sub>	0.1	0.1
Liquor/wood ratio		
Initial	4.38	4.3
at 2nd charge	-	5.38

Although the chemical charge (in %<sub>o.d.wood</sub>) in both series was identical with respect to a complete cooking cycle, it has to be kept in mind that the composition of the initial cooking liquors of series A and series B differ fundamentally from each other (table 4.2). Only 25% of the NaOH charged in series A was present in the initial liquors of series B. Also after addition of the second NaOH charge in series B the difference in liquor to wood ratio between the two series increased. Hence, comparisons of results from each series had to be made carefully, in particular regarding the cooks covering the first 180 min of the cooking time.

## CHAPTER 4. DISCUSSION OF RESULTS

Table 4.3 summarizes some of the results of the analyses conducted according to the standard analytical methods described in section 3.2.1 for the delignification series which will be discussed in the following sections. To simplify the discussion the time of termination (30 - 330 min) and the ratio of the NaOH splitting (100/0 or 25/75) are referred to as A and B series subscripted with the termination time of the respective cook (e.g. A<sub>30</sub> or B<sub>210</sub>).

Table 4.4: Comparison of results on total yield, kappa number, carbohydrate yield, viscosity, brightness and rejects of series A and B.

	Cook	Total yield [% <sub><i>o.d.w.</i></sub> ]	Kappa number	Yield $\sum$ CH [% <sub><i>o.d.w.</i></sub> ]	Visco- sity [ml/g]	Bright- ness [% iso]	Rejects [%]
<i>series A</i>	A <sub>30</sub>	94.8	173.1 <sup>a)</sup>	62.9	-	-	-
	A <sub>60</sub>	83.5	176.5 <sup>a)</sup>	59.5	-	-	-
	A <sub>90</sub>	67.9	125.9 <sup>a)</sup>	49.6	-	-	-
	A <sub>120</sub>	58.0	73.4	48.6	727	19.4	37.2
	A <sub>150</sub>	54.8	54.7	47.3	1084	20.4	12.4
	A <sub>180</sub>	52.9	50.6	48.3	1173	22.0	5.3
	A <sub>190</sub>	51.5	42.4	45.9	1183	21.8	3.4
	A <sub>210</sub>	51.7	40.3	-	1158	22.0	3
	A <sub>270</sub>	50.5	35.9	45.7	1108	22.3	1.8
	A <sub>330</sub>	50.3	28.6	46.5	1066	23.1	1.1
<i>series B</i>	B <sub>30</sub>	95.4	167.9 <sup>a)</sup>	63.9	-	-	-
	B <sub>60</sub>	91.5	168.3 <sup>a)</sup>	60.2	-	-	-
	B <sub>90</sub>	84.5	130.8 <sup>a)</sup>	61.1	-	-	-
	B <sub>120</sub>	72.8	101.2 <sup>a)</sup>	58.0	-	-	-
	B <sub>150</sub>	67.6	78.8 <sup>a)</sup>	53.8	-	-	-
	B <sub>180</sub>	64.8	70.4	55.5	673	36.1	36.8
	B <sub>190</sub>	54.0	48.9	47.2	921	31.2	10.9
	B <sub>210</sub>	53.3	40.0	48.6	1251	30.5	5.1
	B <sub>270</sub>	51.8	30.1	48.8	1326	31.6	2.4
	B <sub>330</sub>	48.7	23.3	44.5	1221	30.6	1.4

a) kappa numbers were estimated on basis of KLASON and acid-soluble lignin fractions and a kappa factor of 0.165

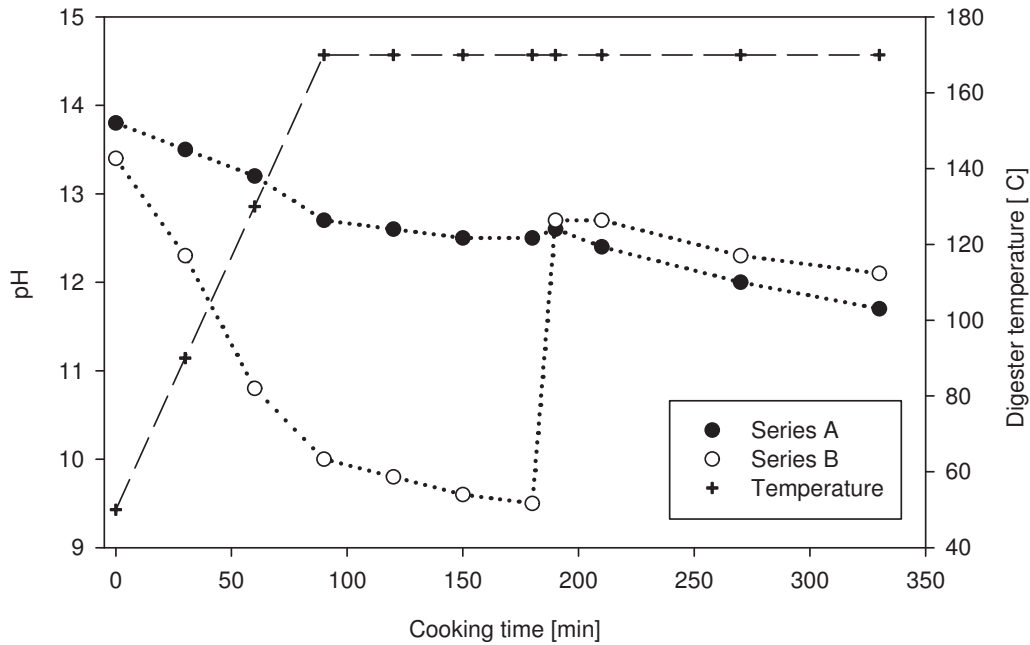


Figure 4.2: PH profile over the course of the two delignification series.

When the pH values of the sulfite spent liquors after each cook are plotted against the cooking time (figure 4.2) the aforementioned differences in cooking liquor composition become apparent. The pH values plotted were measured on cooled liquors (20°C) and were not corrected to account for the actual pH at the corresponding cooking temperature (temperature compensation). But even with these biased values the difference between the pH profiles of series A and series B can be noticed. For both series the initial pH was between 13.5 and 14 which is also a typical initial pH range of white liquors in kraft cooks. Due to the higher initial NaOH charge the initial pH of the cooking liquor of series A was slightly higher than for series B. For series A a steady and slow decrease of the pH can be observed with a final pH of 11.7. The decline in the initial phase is slightly steeper and if temperature compensation was considered the decline would be even more pronounced. The steeper decline in the heating-up period was most likely mainly due to deacetylation of the glucomannans and dissolution of low molecular hemicelluloses converted to sugar acids which is also typical for kraft cooks. Compared to series A the pH profile of series B is highly deviating between 0 - 180 min of the cooking time. The much more pronounced decline of pH from 13.5 to 10 in the heating-up period may be explained by the stronger



neutralising effect induced by the liberated acetyl groups and low molecular hemicelluloses as the initial NaOH charge was much lower. The overall low pH between 9 and 10 in the subsequent cooking time between 90 and 180 min could be assumed to have severe effects on the course of sulfonation and delignification. After addition of the second NaOH charge the pH leaped up to a pH just below 13 showing a similar trend to the A series for the final 150 min but at an overall higher level (approx. pH difference of 0.35).

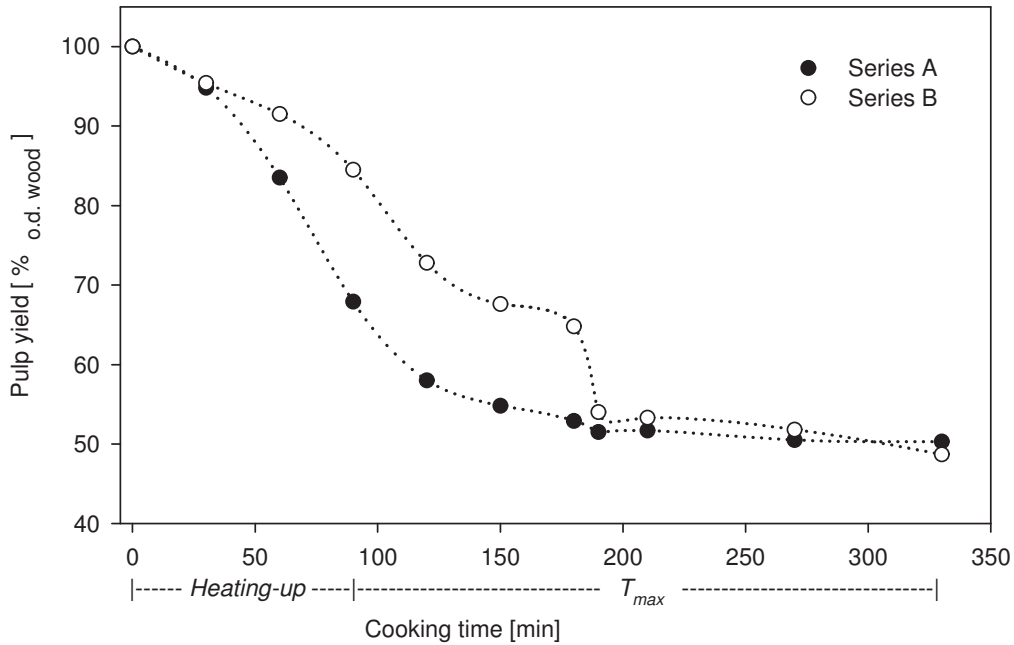


Figure 4.3: Pulp yields of series A and B as a function of cooking time.

When the pulp yield is plotted against the cooking time (figure 4.3) a good overview on the quality of the two delignification series is obtained. For both series no apparent outlier should be present to assure reasonable evaluation of the course of delignification. Knowing the cooking conditions the displayed courses of yield loss are in line with the expectations and match well with the courses of delignification for both series depicted in figure 4.4.

The concept of dividing the pulping process into three distinct kinetic phases of delignification was initially elaborated for kraft pulping. Particularly the plot for series A in fig. 4.3, with its three clearly separable stages of yield loss,

indicates that this concept may also apply for AS/AQ pulping. The initial phase characterised by only minor degradation is followed by the bulk phase which is the core delignification stage consequently leading to a rapid yield loss. In the residual phase the rate of delignification is notably diminished and the proportion of undesirable carbohydrate degradation is elevated which finally demands a termination of the cook.

In the early heating-up period (after 30 min at 90°C) only minor yield loss with respect to the native wood before pre-steaming was observable (approx. 5%<sub>o.d.wood</sub>) and was almost identical for both series. This minor loss is believed to be mainly due to the release of NaOH-soluble extractives and of acetyl moieties of the glucomannans hydrolysed during pre-steaming and by NaOH. But also dissolution of some hemicelluloses and lignin fractions may have taken place.

Alterations caused by pre-steaming were not evaluated here. The almost exhaustive cleavage and removal of the acetyl groups during pre-steaming and the first 30 min of the heating-up period was verified by pyrolysis-GC/MS

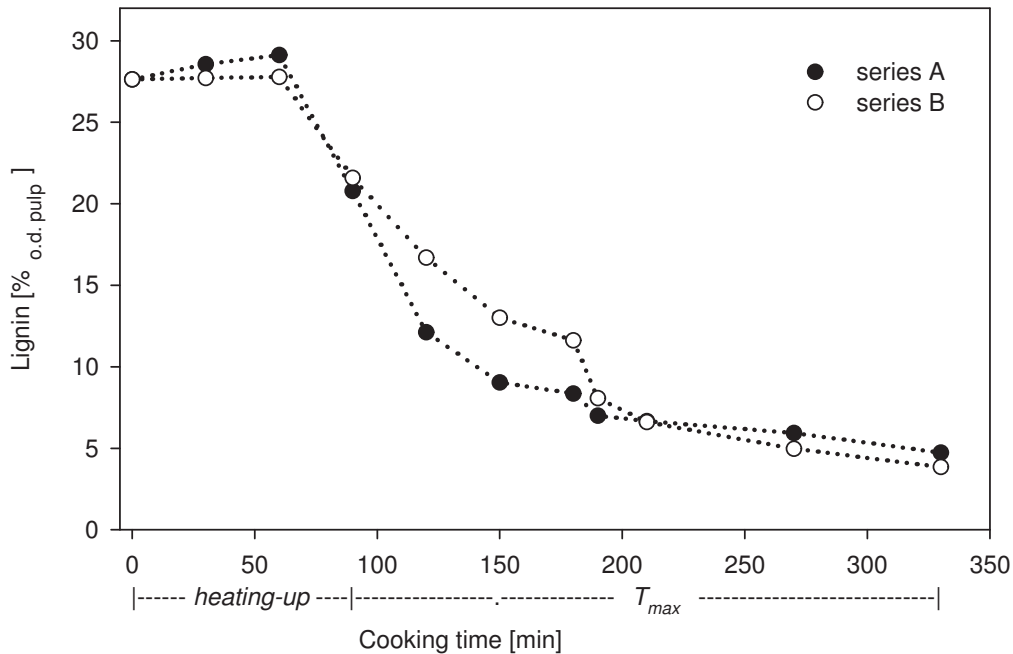


Figure 4.4: Lignin content of pulps as a function of cooking time.

## CHAPTER 4. DISCUSSION OF RESULTS

---

(section 4.2.3.6). Only approx. 10% of the initial acetyl groups were found in samples A<sub>30</sub> and B<sub>30</sub>.

The first 30 min may be considered as the impregnation phase where primarily penetration of cooking liquor into the wood voids and subsequent diffusion of the reactants into the wood matrix take place. The high alkalinity of the cooking liquor and the steadily increasing temperature promoted the swelling of the wood matrix enhancing hereby gradually the accessibility for the chemicals (Sixta 2006).

Within the subsequent 90 min the course of the series A showed a rapid yield loss of almost 40%<sub>o.d.wood</sub>. The impregnation process may not have been complete after 60 min, but the onset of extensive delignification and carbohydrate degradation reactions was apparently responsible for the considerable yield loss already after 60 min at 130°C, when  $T_{max}$  has not yet been reached. Comparing the yield loss and the change in lignin content of series A within the first 60 min (figure 4.3 and 4.4) it can be seen that the lignin content slightly increases even when considerable yield loss between 30 and 60 min was observed. This implies an unfavourable higher degradation and dissolution of polysaccharides as compared to the delignification.

After 120 min at a yield of 58%<sub>o.d.wood</sub> the yield loss and the rate of delignification within series A slowed markedly down. After 150 min the bulk phase was completed indicated by the subsequently slow rate of delignification. For the cooks covering the last 210 min of series A a slow and almost linear decline in pulp yield and lignin content was observed.

The yield loss and delignification rate within series B show different trends, particularly in the period between 30 and 190 min, which can be explained by the NaOH splitting. The initial chemical charge was substantially lower. The neutralising effect of released acids rapidly reduced the pH as already shown in figure 4.2 resulting in a less extensive swelling of the fibers, a slower penetration of chemicals and a less severe degradation. The period of the initial phase associated with the impregnation phase with only minor yield losses was apparently prolonged. In series B the steep decline in yield began 30 min later than in series A (at 60 min). The gradient of the decline in this phase was slightly smaller and, analogous to series A, after 150 min the degradation eventually slowed down marking the end of the bulk phase at a much higher yield (67.6%) and kappa number (79%) than in series A. As a kappa number of 73.4 was already reached in series A after 120 min, hence only after 30 min at  $T_{max}$ , it took an hour longer for the pulp of series B to reach a similar kappa number.

## CHAPTER 4. DISCUSSION OF RESULTS

---

The major impact of the alkalinity on the delignification in the AS/AQ process was already described in former works (Ingruber *et al.* 1982, Kettunen *et al.* 1979, McDonough *et al.* 1985, Patt *et al.* 2002). Without the second NaOH addition the course of degradation would be expected to continue more or less in parallel to series A with a final pulp yield of approx. 60% and a kappa number of approx. 50 after 330 min.

As soon as the second NaOH charge was added in series B the delignification process was instantly accelerated. Within 10 min, between the cooks B<sub>180</sub> and B<sub>190</sub>, the kappa number decreases by more than 20 units. Also an instant loss of yield attributed to lignin and polysaccharide degradation could be observed. As an effect the difference in yield and the degree of delignification between series B and series A diminished. The positive key effect of NaOH splitting could eventually be demonstrated on the pulps of the terminal cooks. The pulp B<sub>330</sub> was superior to the pulp A<sub>330</sub> with respect the kappa number, viscosity and brightness. The final kappa number of 23.3 reached with the final cook of series B was significantly lower than the respective kappa number of series A (see table 4.3). However, in comparison of the pulps A<sub>330</sub> and B<sub>330</sub> the yield of B<sub>330</sub> was slightly lower. Though, retrials of the full-length cook with NaOH splitting indicated that the yield of B<sub>330</sub> was unusually low. As the aforementioned results in table 4.1.2.3 illustrate the yield could not be improved by NaOH splitting.

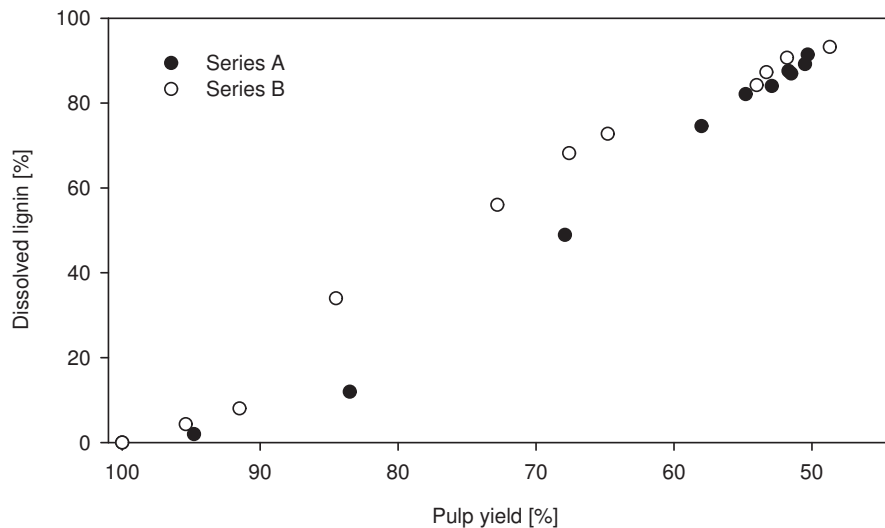


Figure 4.5: Dissolved lignin as a function of pulp yield.

## CHAPTER 4. DISCUSSION OF RESULTS

---

If the dissolved lignin is plotted against the pulp yield the higher selectivity of the cooks with NaOH splitting can be visualized (figure 4.5). 15-20% more of the lignin is dissolved at yields between 65 and 85% in series B. This difference diminishes as soon as the second NaOH charge is added, but a minor advantage in selectivity remains for series B.

Next to the delignification a considerable degradation of the polysaccharides has to be accepted for all alkaline pulping processes. Not only the close association between the components and intensely cross-linked nature of the lignin-carbohydrate-complexes is hindering the selective removal of lignin, but also the harsh conditions applied in most pulping processes and the use of chemicals with limited selectivity result in unwanted carbohydrate degradation. Depending on the chemical and structural features of the various carbohydrates they are known to show vital differences in sensitivity towards degradation (Sixta 2006, Sjöström 1993). Particularly alkaline peeling reactions lead to an extensive degradation of hemicelluloses.

Comparing the progression of carbohydrate degradation between series A and series B again a considerable influence of NaOH splitting was apparent (figure 4.6). The significant difference in pH between the two delignification series for the first 180 min of the series may explain the major differences. In series A 30% of the polysaccharides were degraded after 180 min and only further 3% are decomposed in the remaining 150 min of the series. As for the slower yield loss and delignification the weak alkalinity in series B also caused a preservation of the polysaccharides in the first 180 min. Only 20% are lost here. After addition of the second alkali charge, though, an instant dissolution of 10% of carbohydrates took place. At the end of the series at 330 min 65% of the initial carbohydrate content remained in the pulp, slightly less than in pulp A<sub>330</sub>.

Known for its alkali-instability particularly the glucomannans were prone to a rapid degradation within the first 90 min of series A, already after 60 min, when  $T_{max}$  was not yet reached, the mannose content was more than halved. After 90 min the mannose content stayed at a more or less constant level. In series B the lower pH in the first 180 min caused a higher preservation of the cellulose and glucomannans. The xylans are more alkali-stable which is reflected in the results of the carbohydrate analysis in table 4.4. The proportion of xylose with respect to the total carbohydrate content increased gradually in the course of delignification in both series. Regarding the last cooks of each series where the yield differences between the two series are

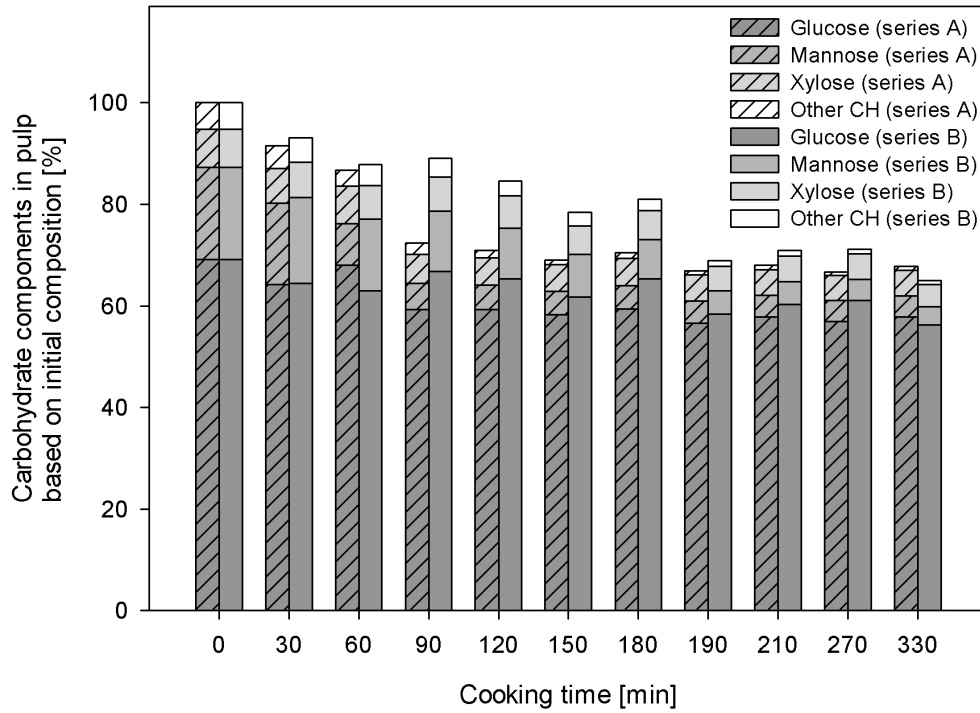


Figure 4.6: Carbohydrate composition as a function of cooking time for series A and series B. Carbohydrate compositions displayed are based on initial composition of native spruce wood.

only marginal the xylose content of pulps of series A was actually slightly higher.

---

## CHAPTER 4. DISCUSSION OF RESULTS

---

Table 4.5: Carbohydrate composition of the pulps of series A and B.

	Cook	R	$\sum$ CH	Glu	Man	Xyl	other CH
		[%]	[%]	[%]	[%]	[%]	[%]
<i>series A</i>	A <sub>30</sub>	27.1	66.4	46.5	11.6	4.9	3.3
	A <sub>60</sub>	28.5	71.2	55.6	6.7	6.0	2.6
	A <sub>90</sub>	20.5	73.0	59.9	5.1	5.8	2.3
	A <sub>120</sub>	11.3	83.8	70.0	5.8	6.4	1.7
	A <sub>150</sub>	7.3	86.4	72.8	5.8	6.6	1.2
	A <sub>180</sub>	6.8	91.3	77.0	5.9	7.0	1.4
	A <sub>190</sub>	5.5	89.0	75.4	5.8	6.8	1.0
	A <sub>210</sub>	-	-	-	-	-	-
	A <sub>270</sub>	5.0	90.5	77.2	5.7	6.7	1.0
	A <sub>330</sub>	3.9	92.4	78.8	5.6	7.0	1.0
<i>series B</i>	B <sub>30</sub>	27.1	66.9	46.3	12.1	5.0	3.5
	B <sub>60</sub>	26.7	65.8	47.2	10.6	5.0	3.0
	B <sub>90</sub>	21.1	72.3	54.2	9.6	5.5	3.0
	B <sub>120</sub>	16.7	79.6	61.5	9.4	6.0	2.8
	B <sub>150</sub>	12.8	79.5	62.7	8.5	5.7	2.8
	B <sub>180</sub>	9.8	85.6	69.2	8.1	6.1	2.3
	B <sub>190</sub>	7.3	87.4	74.2	5.8	6.1	1.3
	B <sub>210</sub>	5.8	91.1	77.6	5.8	6.4	1.4
	B <sub>270</sub>	3.9	94.2	80.8	5.5	6.6	1.2
	B <sub>330</sub>	2.9	91.4	79.2	5.1	6.2	1.0

#### 4.1.3.1 Effect on viscosity and brightness

Already in chapter 4.1.2 it was pointed out that the application of NaOH splitting enhanced the viscosity and the brightness of the pulp under cooking conditions stated. Though, regarding the results in table 4.1.2.3 a comparison of the effect of NaOH splitting can only be made on basis of equal cooking time.

For the different cooking conditions used in the two delignification series (see section 4.1.3) basically the same effects were observable. Table 4.3 displays the kappa numbers, viscosities, yields and brightnesses of the pulps at the progressing stages of the two series. The viscosity and brightness of the terminal pulp generated with NaOH splitting ( $B_{330}$ ) were significantly higher than the pulp  $A_{330}$ . But the kappa number and yield were lower for the pulp  $B_{330}$  as compared to  $A_{330}$ . On this basis alone the results may be misleading as it could be assumed that a cook without NaOH splitting to the same yield or kappa number as the pulp  $B_{330}$  might eventually result in a similar viscosity and brightness. Continuous removal of lignin and hemicelluloses may enrich cellulose and hereby improve viscosity and brightness.

Following the trend of viscosities and brightness throughout the progression of the cooks, though, leads to other conclusions. In series A already after 190 min the highest viscosity was reached which slowly decreased towards the final cook at 330 min. Any extension of the cooking time is very likely to further decrease the viscosities of the generated pulps. Regarding the last three cooks the viscosities were all approx. 100-200 ml/g lower than the respective viscosities of series B.

Just as the yield is decreasing slower for series B the point of defibration was reached later in the course of the cooks than in series A. The low viscosities for  $B_{180}$  and  $B_{190}$  were due to high amounts of lignin and hemicelluloses and incomplete defibration and are not representative for comparison. The viscosities of the last three pulps  $B_{210}$ ,  $B_{270}$  and  $B_{330}$  reflect the high viscosity level reached by NaOH splitting and the applied cooking conditions.

The brightness of the pulps of series A increased slightly from the first measurement of 19.4 %ISO at 120 min to 23.1 %ISO for the final pulp. For the respective pulps of series B a significantly higher brightness was observed throughout. At a kappa number of around 70 the pulp had more than 15 %ISO higher brightness than the pulp with a similar kappa number cooked without NaOH splitting. The addition of NaOH at 180 min may explain the brightness loss from 36.1 to 31.2 %ISO of  $B_{190}$ . But the pulps of the subsequent cooks maintained the brightness at around 30 %ISO.



Both, higher viscosities and higher brightnesses of the unbleached pulps can be considered as main benefits of NaOH splitting.

#### 4.1.3.2 Effect on sulfonation

As it is one of the key reactions in the AS/AQ-process the degree of sulfonation of the lignin was of particular interest for this thesis. Although the sulfite charge was identical in both delignification series it was anticipated that differences in the extent of sulfonation reactions between the two series existed. In previous studies it has been shown that different ratios of  $\text{Na}_2\text{SO}_3$  to NaOH applied in AS/AQ-cooks vitally affect the kinetics of the process.

Table 4.6: Sulfonic and carboxylic acid groups content in pulps of series A and B.

	Cook	Lignin	$\text{SO}_3\text{H}$	$\text{SO}_3\text{H}$ per lignin	$\text{COOH}$
		[%]	$[\mu\text{mol/g}]$	$[\mu\text{mol/g}]$	$[\mu\text{mol/g}]$
<i>A series</i>	A <sub>30</sub>	28.6	41.3	145	180
	A <sub>60</sub>	29.1	55.2	190	187
	A <sub>90</sub>	20.8	50.6	244	189
	A <sub>120</sub>	12.1	39.1	323	138
	A <sub>150</sub>	9.0	31.2	345	123
	A <sub>180</sub>	8.4	23.4	280	115
	A <sub>190</sub>	7.0	26.7	382	99
	A <sub>210</sub>	6.7	23.0	346	104
	A <sub>270</sub>	5.9	18.7	315	94
	A <sub>330</sub>	4.7	13.3	282	87
<i>B series</i>	B <sub>30</sub>	27.7	50.2	181	153
	B <sub>60</sub>	27.8	100.0	360	161
	B <sub>90</sub>	21.6	149.7	694	148
	B <sub>120</sub>	16.7	132.2	792	146
	B <sub>150</sub>	13.0	109.4	842	135
	B <sub>180</sub>	11.6	79.5	685	112
	B <sub>190</sub>	8.1	40.1	497	96
	B <sub>210</sub>	6.6	22.9	347	91
	B <sub>270</sub>	5.0	19.9	400	85
	B <sub>330</sub>	3.9	16.0	417	86

## CHAPTER 4. DISCUSSION OF RESULTS

The amount of sulfonic acid groups in the pulps was determined by conductometric titration according to Katz *et al.* (1984). The results received directly for the samples (table 4.5, col. 3) are based on pulp. Already within the heating-up period sulfonic acid groups were found in the fibers. In series A the pulp received after 60 min had the highest amount of sulfonic acid groups ( $55.2 \mu\text{mol/g}$ ). In the further course of the series the amount decreased steadily. The results for series B showed clear differences. The maximum amount of sulfonic acid groups was reached later, after 90 min when  $T_{max}$  was reached, and its abundance was almost three times as high as in series A. Again, it gradually decreased and the pulps of the final cooks of both series were almost equally low. Hence, by comparison of the sulfonic acid group content of the terminal pulps no hint is given towards the apparent differences between pulps produced with NaOH splitting and those produced conventionally.

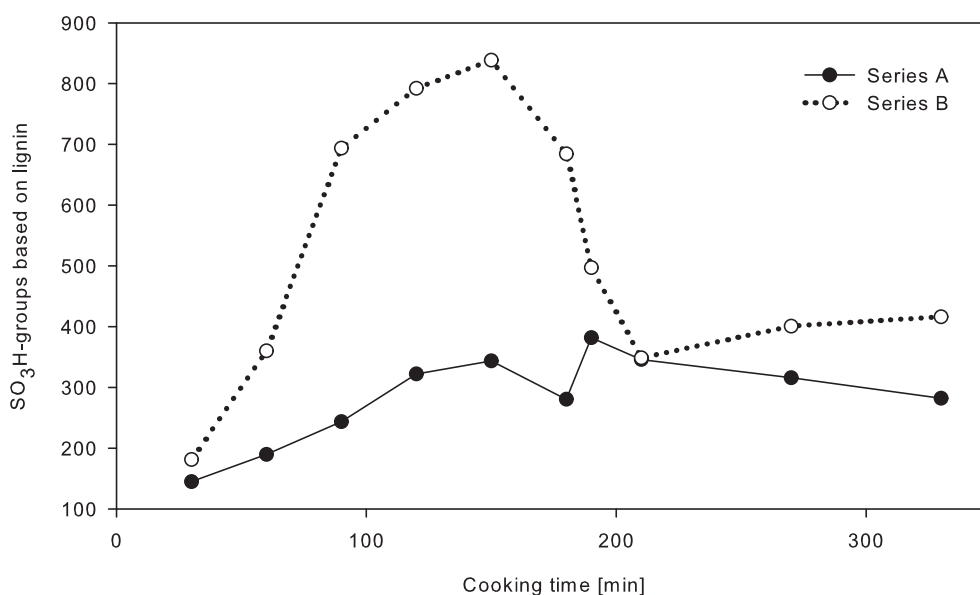


Figure 4.7: Degree of sulfonation in pulps of series A and B.

The conductometrically determined values of sulfonic acid groups are based on pulp. To draw meaningful conclusions about the kinetics of sulfonation it is more appropriate to review the sulfonic acid group content on the basis of the lignin content of each pulp as almost exclusively the lignin is sulfonated. The values of sulfonic acid groups based on lignin are displayed in table 4.5,

## CHAPTER 4. DISCUSSION OF RESULTS

---

column 4. Again clear differences in the course of delignification of the two series could be described. When plotted against the cooking time (figure 4.7) the degree of sulfonation of the lignin in series A shows a moderate, almost linear increase towards the cook terminated at 190 min. For the pulp A<sub>190</sub> the highest degree of sulfonation of series A was estimated with  $382\mu\text{mol/g}_{\text{lignin}}$ . Also the subsequent decline is slow and almost linear. Here it may be assumed that until the cooking time of 190 min the rate of sulfonation was slightly higher than the lignin dissolution. The pulp A<sub>180</sub> showed an unexpectedly low value. It is believed that the cook was not conducted appropriately, e.g. the liquor circulation was possibly too low. This assumption was supported by the other analytical results also showing unexpectedly diverging values.

The degree of sulfonation of series B increased immediately and much steeper than for the corresponding pulps of series A. The peak value was measured for the pulp generated after 150 min (B<sub>150</sub>). Apparently it was not the second NaOH charge alone causing a steep decline of the degree of sulfonation in the further course of series B. A change in the reaction kinetics already within the 30 min before the second NaOH charge is likely to explain the decline between the pulps B<sub>150</sub> and B<sub>210</sub>. Until a cooking time of 150 min the speed of sulfonation reactions was notably higher than the speed of the dissolution of cleaved lignin fragments. The lower degree of sulfonation of pulp B<sub>180</sub> thereafter may only be attributed to a somewhat abrupt slowing down of sulfonation. A sudden increase in the rate of lignin dissolution is not reasonable without the second NaOH charge being added. The drastically decreasing values for the pulps B<sub>190</sub> and B<sub>210</sub> may well be explained by the immediate promotion of lignin dissolution due to the second NaOH addition.

### 4.1.3.3 Reference and replicate cooks

Table 4.7: Degree of sulfonation of 4 pulps with kappa numbers of approx. 30.

Pulp	Kappa No.	SO <sub>3</sub> H <sup>a)</sup> μmol/g	S/C <sub>9</sub> <sup>b)</sup>
Acid sulfite	29.3	1365	0.259
ASAM	28.4	921	0.175
B <sub>270</sub>	30.1	401	0.076
A <sub>330</sub>	28.6	282	0.054

a) based on lignin content

b) molar ratio based on lignin monomer of 190 g/mol

The degrees of sulfonation of the pulps A<sub>330</sub> and B<sub>270</sub> were compared with those of two reference pulps, one generated by an acid Na-sulfite and the other by an ASAM process. All 4 pulps compared had a kappa number of approx. 30. A molar ratio was calculated assuming a molar mass of a lignin monomer to be 190 g/mol. The results displayed in table 4.6 indicate that the degree of sulfonation is highest in the acid sulfite pulp with 25% of the lignin monomers being sulfonated. The residual lignin of the ASAM pulp also showed a considerable degree of sulfonation with 17.5 %. For the two AS/AQ pulps the degree of sulfonation was far below 10%. The slightly higher degree of sulfonation of the pulp B<sub>270</sub> was anticipated upon the aforementioned results.

At this point it has to be highlighted, that the pulps A<sub>210</sub> and B<sub>210</sub> had almost the same pulp yield, kappa number, carbohydrate composition and degree of sulfonation. All other cooks of series A and series B, compared on basis of cooking time, yielded pulps with clear differences either in pulp yield or kappa number or both. The viscosities and brightnesses though were different. It was decided to take a closer look at this particular cooking stage. For this purpose additional cooks with the same conditions, two for each delignification series, were performed. The results are shown in table 4.7. It can be noticed that the chemical compositions of the pulps from the replicate cooks show some variation. Unfortunately results from the carbohydrate analysis of sample A<sub>210</sub> are missing. Hence only the B<sub>210</sub> pulp could be compared with the replicate pulps with respect to carbohydrate composition. The glucose content only showed little variation, but the amount of mannose was apparently higher and of xylose lower in the replicate pulps. In addition the

## CHAPTER 4. DISCUSSION OF RESULTS

Table 4.8: Analysis results for pulps generated by replicate cooks with a cooking time of 210 min. The corresponding results for A<sub>210</sub> and B<sub>210</sub> are included for reference.

Cook	SO <sub>3</sub> H*	Kappa No.	HexA	$\sum$ CH	Glu	Man	Xyl	other CH
	[ $\mu$ mol/g]		[ $\mu$ mol/g]	[%]	[%]	[%]	[%]	[%]
A <sub>210</sub>	346	40.3	-	-	-	-	-	-
R1A <sub>210</sub>	481	42.1	31.5	90.0	77.2	6.3	5.6	1.0
R2A <sub>210</sub>	496	40.2	35.2	93.7	79.9	6.4	6.2	1.2
B <sub>210</sub>	348	40	-	91.1	77.6	5.8	6.4	1.4
R1B <sub>210</sub>	594	41	21.1	90.7	77.5	6.3	5.4	1.5
R2B <sub>210</sub>	545	40.8	17.8	92.1	78.7	6.3	5.6	1.6

\*) based on lignin content

degrees of sulfonation were considerably higher in the replicate pulps. And when the replicate pulps from series A are compared to the corresponding pulps from the B series a clear difference in the degree of sulfonation could be noticed. However, the kappa numbers were around 40 for all pulps. The compositional differences, which may have also effected the gegree of sulfonation, are believed to be due to the different batch of spruce raw material used for the cooks.

The hexenuronic acid content was only determined for the 4 replicate pulps. The results (depicted in table 4.7) illustrate that the high NaOH concentration throughout the cooks of series A had a significant effect on HexA formation. It can be assumed that, in comparison to series B, also the pulps from the other cooking stages of series A contained higher amounts of HexA. The higher HexA content may be partly responsible for the lower degrees of brightness of the pulps from the A series.

## 4.2 Pyrolysis of ASA pulps

For the analysis of the sulfite pulps pyrolysis-GC/MS was chosen to reveal details on structural features which would confirm or supplement the results gathered by the other analytical methods discussed in section 4.1. For the discrimination of the pulps generated in the two AS/AQ delignification time series, series A and series B, Principal Component Analysis (PCA) was employed. PCA is also able to extract the most significant pyrolysis products if a successful discrimination is achieved. To confirm the detected differences between the time series isolated evaluation of the meaningful pyrolysis products was conducted.

The second objective was to assess whether and which wood components of the studied samples could be quantified employing multivariate calibration with the Partial Least Squares regression (PLS) method on the Py-GC/MS data. PLS was already successfully applied to Py-GC/FID data of various woods and grasses (Bremer 1991) and on Py-GC/MS data of kraft pulps (Kleen *et al.* 1993). Opposed to the approaches of Bremer (1991) and Kleen *et al.* (1993) which used the peak areas of 114 pyrolysis products of the FID signals and the peak areas of only 26 peaks of the total ion current (TIC) respectively, in the presented work the calibrations were based on peak areas of extracted ions as representatives. Furthermore the number of peaks considered for the multivariate calibrations was considerably higher than in the aforementioned studies. The reasons for this approach will be discussed in the respective sections.

The quantification of sulfonic acid groups was of particular interest as they represent a unique structural feature of sulfite pulps and lignosulfonates. Pyrolysis-GC/MS was tested as a rapid alternative to the time-consuming conductometric method of Katz *et al.* (1984). Apart from using multivariate calibration also the applicability of straight-forward univariate linear regression using external standards was assessed. Multivariate calibrations generally demand a considerable amount of calibrants, therefore univariate linear regression with a small set of calibration samples was believed to be easier and quicker to perform. Moreover the pyrolysis of sulfonic acids only yields one major product.

A further objective was to conduct appropriate preprocessing procedures on the gathered Py-GC/MS raw data. There are many pitfalls and problems arising when Py-GC/MS data is to be processed by multivariate analysis. All of these are discussed extensively in various publications. In this study only

one of many possible approaches was worked out which largely depended on the available software tools and expertise.

### 4.2.1 Sample preparation

As it holds true for most analytical techniques care had to be taken on an appropriate sample preparation. Milling in a ball-mill cooled by liquid nitrogen ensured a sufficient homogeneity of the samples. Prior to ball-milling pulps were acid-washed according to the pretreatment conducted in the conductometric method of Katz *et al.* (1984) to remove  $\text{Na}^+$ . It was already described by other authors (Kleen *et al.* 1993) that  $\text{Na}^+$  vitally affects the pyrolysis resulting in a different pyrolysis fingerprint. It would not be helpful to find differences between samples without knowing whether they are caused by differences in structural features or caused by variations of the  $\text{Na}^+$  content.

### 4.2.2 Data pre-processing

Many GC/MS applications including Py-GC/MS are well suited for large-scale analyses because of rapid and fairly simple sample preparation and a relatively high repeatability. But several hindrances can make evaluation of large data sets difficult. Foremost the long-term reproducibility of the GC separation conditions is of concern (Windig *et al.* 1979). Instrument fluctuations result in variations in the overall signal intensity and gradual column degradation causes retention time drifts, alterations in the product patterns and background noise due to column bleed and artefacts. Data pre-processing may not yield any analytical results of interest, but is critically significant and can decide between failure and success (Pierce *et al.* 2012).

Before qualitative or quantitative evaluation of Py-GC/MS data is to be employed it is recommended to assess whether and which data pre-processing steps may be necessary to yield reliable results. The purpose of pre-processing is the minimization or removal of unwanted and irrelevant systematic variation, e.g. caused by uncontrolled external factors, scatter or baseline shifts (Gabrielsson and Trygg 2006). The necessary pre-processing steps highly depend on the complexity of the chromatographic data and the aim and method of evaluation. If only a small set of well separated, prominent peaks is used for analysis the pre-processing steps may be marginal which is often the case in standard GC/MS applications. Using single ion monitoring would even further reduce the number of peaks and a straightforward integration and normalization of the resulting peak areas by sample weight, sample concen-

tration or internal standard leads to the desired results. Another important intention of pre-processing is to prepare a unified format of the analytical data. In particular when statistical analysis and the application of MVA methods are intended, the data is best evaluable when transformed into matrix format.

In terms of complexity Py-GC/MS fingerprints of lignocellulosic samples have much in common with GC/MS profiles in metabolomic studies (Jonsson *et al.* 2006, Dixon *et al.* 2007) or in studies on herbal medicines (Liang *et al.* 2010). Py-GC/MS of wood or pulp samples may also yield highly complex total ion current (TIC) signals which can contain far more than 300 pyrolysis products. Many of the products are coeluting or are near the detection limit. In figure 4.2.2 a pyrogram of sample B<sub>30</sub> is depicted. The retention time range between 3 and 45 min, which is depicted in graph A, contained almost all of the major pyrolysis products. Graph B shows an enlarged section of the retention time range between 20 and 30 min. This time interval alone contained more than 100 peaks when the minor peaks were included. Again, in many cases only the prominent and well separated peaks are chosen which reduces the effort on evaluation, e.g. Bremer (1991) used 114 and Kleen *et al.* (1993) only 26 peaks. When multivariate approaches are to be employed it can be advantageous to keep as much information as possible in the data set throughout the preprocessing procedures. Hence, ideally all peaks should be retained. Eventually, the multivariate analysis is supposed to extract the valuable information from the preprocessed data. In metabolomic studies it is quite common that amongst several hundred peaks only very few metabolites, maybe even of low intensity, are the sought-after biological markers (Jonsson *et al.* 2006). Likewise it was anticipated by the author that a thorough pre-processing would facilitate to find meaningful differences between the AS/AQ pulps of series A and series B. In particular the pulps of both series after the cooking time of 210 min were of interest. Regarding the results of the previous compositional analyses they showed very high resemblance.



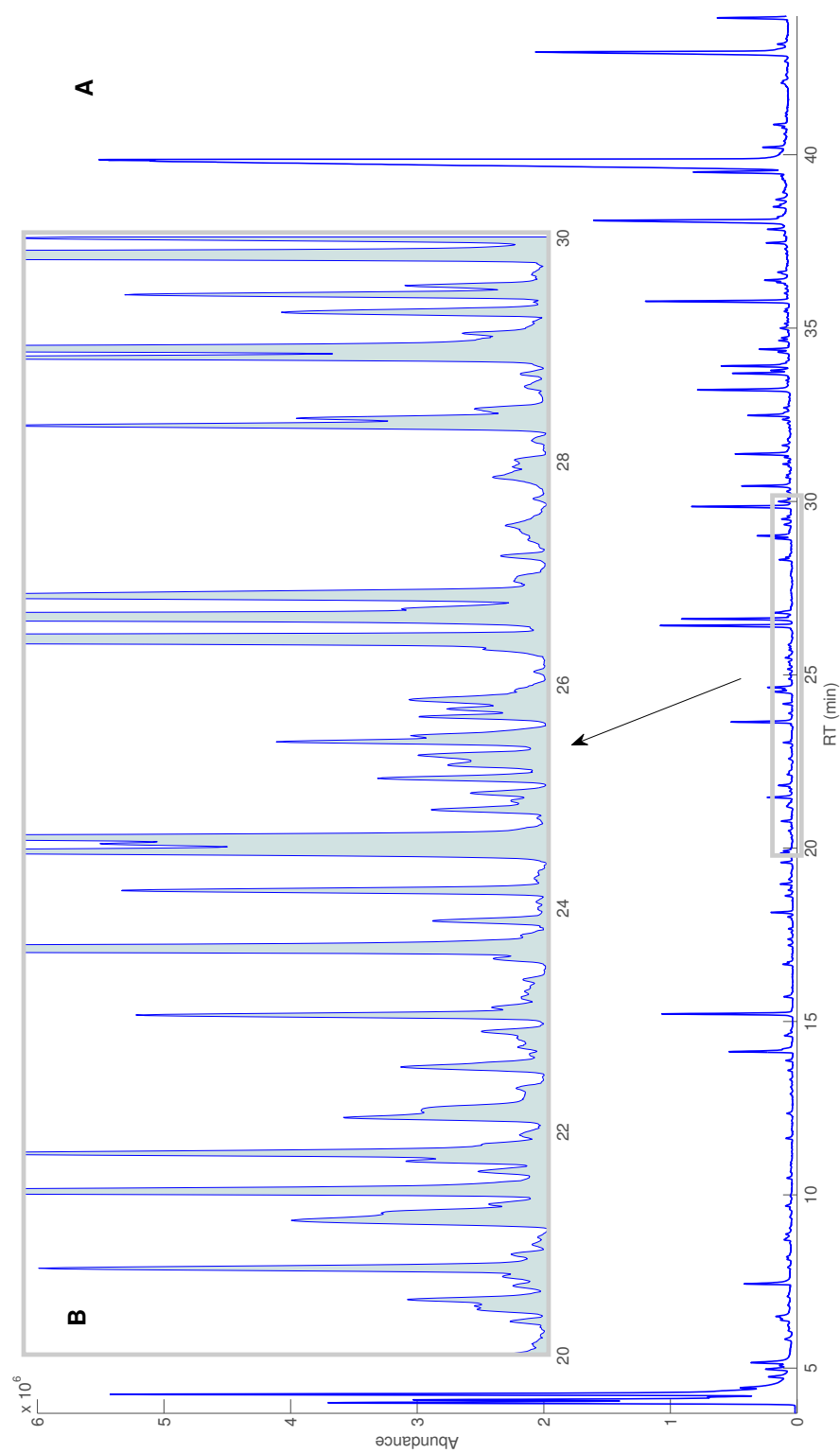


Figure 4.8: Pyrogram of an AS/AQ pulp sample. (A) Main region including most major and minor peaks; (B) enlargement of region of RT 20 - 30 min.

## CHAPTER 4. DISCUSSION OF RESULTS

---

The key measurement series conducted with Py-GC/MS amounted to 160 measurements which all had to be preprocessed in the same manner. Because none of the software tools available to the author was able to execute all desired pre-processing steps 5 different software tools were utilized. The chromatography software (*ChemStation*, Agilent Technologies) was responsible for the data acquisition. It is also commonly used for evaluation but the demand for a batch-wise or sequential processing of 160 measurements could not be met by the available software package. Sequential smoothing and background correction was conducted with *metAlign* (Lommen 2009), peak detection and deconvolution with *AMDIS* (Stein 1999). *MATLAB* (The MathWorks, Natick, MA) was utilized to build a global peak- and ionlist based on the deconvoluted peaks in all measurements. The sequential integration of the extracted ion peaks based on the ionlist was automated by the *MS-SIM-Tools* (in-house software) in connection with the *ChemStation*.

Although retention time drifts are commonly of major concern and have been addressed by various studies (Johnson *et al.* 2003, Clifford *et al.* 2009) it was not an issue in the aforementioned measurement series conducted. If measurements were to be compared over a longer time period retention time alignment or another preprocessing strategy would have been necessary.

The employed pre-processing steps are summarized in figure 4.8 including the main benefits and obstacles associated with each step. Details are described in the sections 4.2.2.1 and the following.

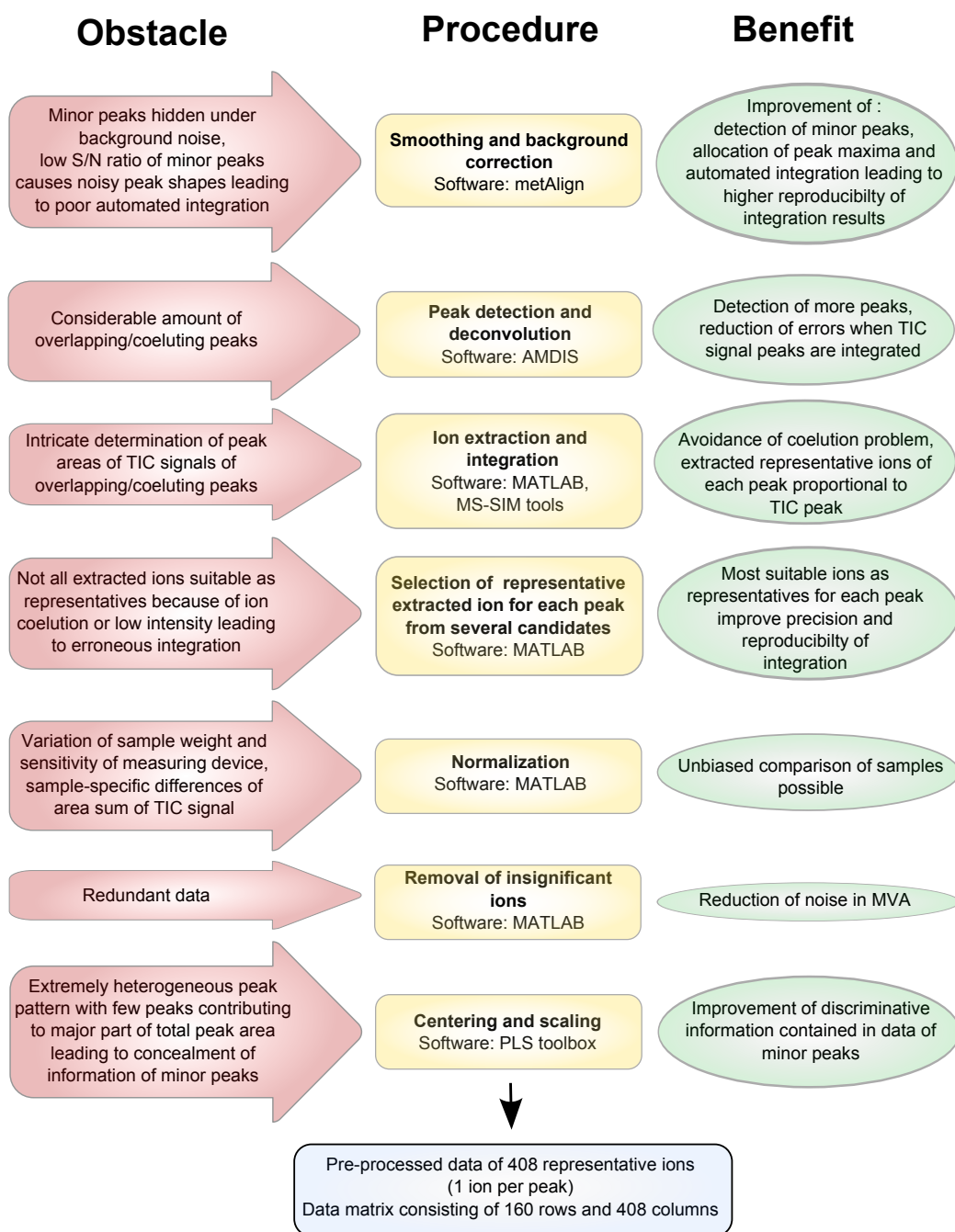


Figure 4.9: Flowchart summarizing the conducted pre-processing steps.

#### 4.2.2.1 Smoothing and baseline correction

Smoothing and baseline correction (BC) are the first steps in most pre-processing pipelines employed on GC/MS data. These two procedures improve the signal to noise ratio (S/N) by eliminating the chemical and detector noise from the signal and background respectively with a minimum of signal distortion (Vivó-Truyols and Schoenmakers 2006, Lommen 2009). Though, possible loss of chemical information has to be taken into account and be kept at a minimum by adjusting the processing parameters to the data.

In the presented work the most significant benefit from smoothing and baseline correction was the overall improvement of the automated integration of the peaks by the ChemStation integration algorithm. Because of the high number of measurements and peaks in each measurement a manual inspection of the 'quality' of peak integration was to be avoided as far as possible. For the two procedures, abbreviated in the following with BC, the free software metAlign was used. The details on the algorithms have been described by the author of the software (Lommen 2009).

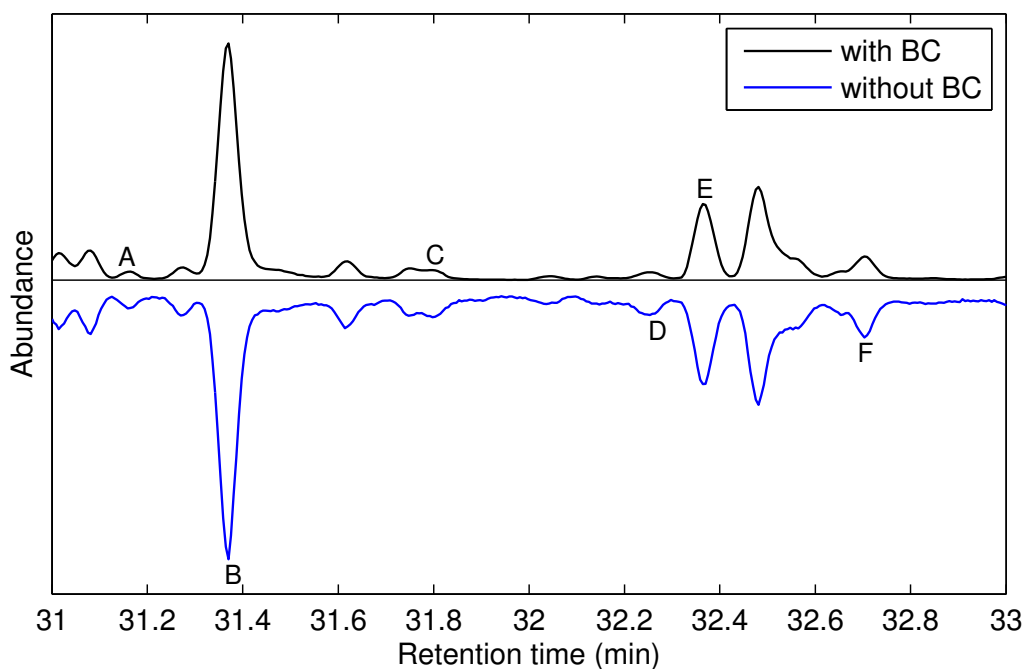


Figure 4.10: Effect of smoothing and baseline correction shown for a small section of a pyrogram. The peaks denoted with the letters A - F are picked as examples for the calculations of RSDs shown in table 4.8.

Regarding Py-GC/MS most of the fairly constant background noise is contributed by air which is easily identifiable in the pyrograms by the masses  $m/z$  18, 28, 32 and 44. At elevated temperatures the column bleed increases and exceeds the contribution by the air. In figure 4.9 a small section of a pyrogram after smoothing and baseline correction is compared to the unprocessed mirror-imaged correspondent (referred to in the following as raw *chromatogram*). Apart from peak B (medium sized peak) all peaks displayed are of low intensity compared to the main peaks of the pyrogram. At the illustrated level of magnification the effect of smoothing is not observable, but it can clearly be seen that the offset caused by the background has disappeared and some almost buried peaks (between C and D) show more articulate peak shapes. Because of an already high signal to noise ratio (S/N) in the raw chromatogram the BC processing for the more prominent peaks (e.g. peak B) is not really demanded. The effect is barely observable in the respective mass spectrum (figure 4.10).

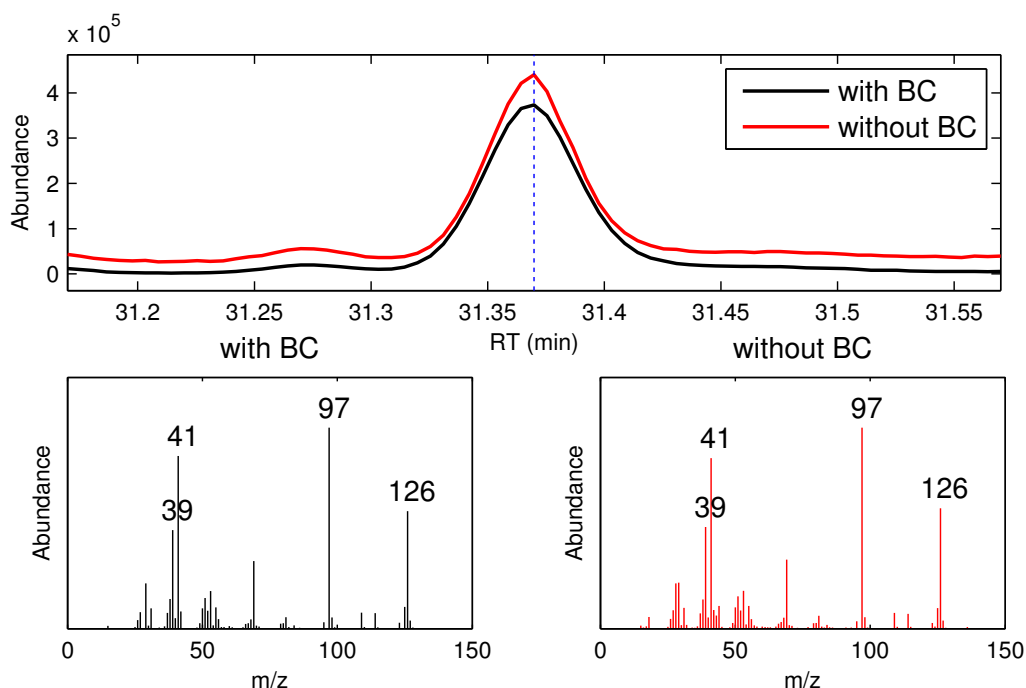


Figure 4.11: Effect of BC processing on TIC signal of peak B (upper plot) and the mass spectrum of peak B (lower left plot) in comparison with the unprocessed signal (lower right plot).

But in case of minor peaks the BC processing leads to a considerable improvement of the signal to noise ratio which can be visualized by comparison

of the mass spectra after and before BC. Depicted in the upper graph of figure 4.11 the contribution of the background to the total signal at the retention time of peak C (dotted line) can be observed. In the mass spectrum of peak C of the raw chromatogram (lower right in figure 4.11) the mass ions of  $N_2$  and  $CO_2$  ( $m/z$  28 and 44) show the highest intensity masking the mass spectral information of the minor peak C (lower left in figure 4.11).

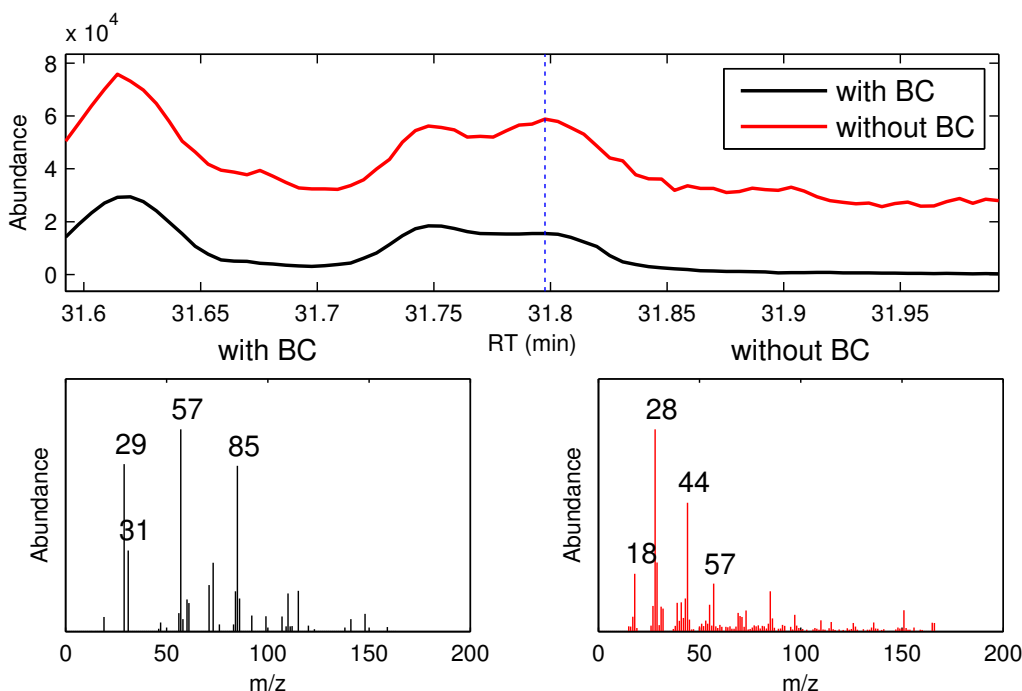


Figure 4.12: Effect of BC processing on TIC signal of peak C (upper plot) and the mass spectrum of peak C (lower left plot) in comparison with the unprocessed signal (lower right plot).

To assess the benefit of the BC preprocessing the relative standard deviations (RSD) of normalized peak areas were calculated on the basis of 17 replicate measurements. For each of the 6 peaks denoted in figure 4.9 with A - F a representative ion of their respective mass spectra was integrated. By these means erroneous integration because of overlapping peaks was avoided (see section 4.2.2.4). The RSDs of the peak areas before and after the BC step ( $RSD_{raw}$  and  $RSD_{BC}$ ) together with the respective retention times (RT) and selected ions are shown in table 4.8. The  $RSD_{raw}$  values lie all between approx. 9 and 22%. 5 out of the 6 RSDs were improved by the preprocessing, only one value slightly increased. 4 of the 5 improved  $RSD_{BC}$  values only

## CHAPTER 4. DISCUSSION OF RESULTS

Table 4.9: Results for the RSDs calculated for 6 normalized ion peak areas of 17 replicate measurements.  $RSD_{raw}$  refers to the raw and  $RSD_{BC}$  to the BC processed data basis. Peak areas were normalized by the total mass spectrum (sum of all mass spectra of entire pyrogram).

Peak	A	B	C	D	E	F
RT (min)	31.15	31.37	31.79	32.26	32.36	32.70
Ion	137	97	57	164	111	138
$RSD_{raw}$ (%)	7.38	22.13	16.17	9.47	10.22	8.67
$RSD_{BC}$ (%)	6.58	20.52	4.54	10.77	8.70	7.64

show a difference of 1-1.5% compared to the  $RSD_{raw}$  values. Though for peak C the improvement is highly significant decreasing from 16.17 to 4.54%.

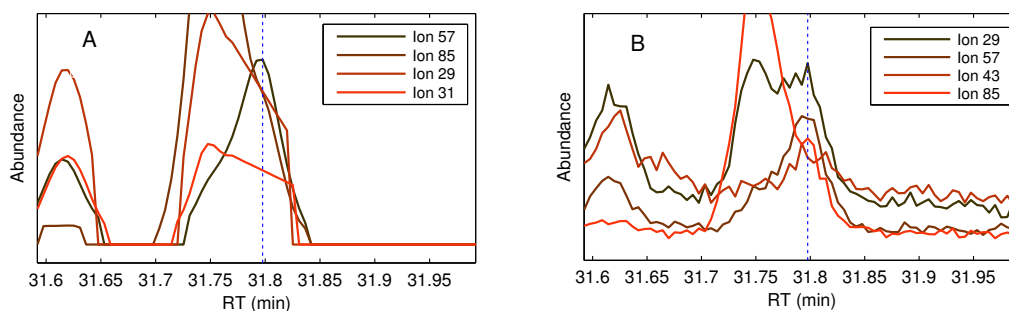


Figure 4.13: Effect of BC processing illustrated on extracted ions at the RT of peak C. Plot A shows the processed, plot B the raw signals.

In case of the conducted measurement series the effect of smoothing was only moderately perceivable when the TIC signals were inspected. When the corresponding extracted ion currents (EIC) were reviewed the effect of smoothing was clearly visible. Figure 4.12 displays the currents of the 4 biggest ions at the retention time of peak C for the BC processed (A) and raw data (B). The initially very noisy peak shape of the signal of ion 57 (B) was considerably smoothed by the BC processing (A) resulting in a much more reliable automated integration of the ion peak. This explained the significant improvement of the  $RSD_{BC}$  over the  $RSD_{raw}$  of peak C.

That the smoothed ion signals of  $m/z$  31, 57 and 85 are showing poor peak shapes (ideally a gaussian peak shape is achieved) indicates that the intensity of this particular peak is close to the detection limit and at the limit of the BC algorithm to work reliably.

#### 4.2.2.2 Peak detection and deconvolution

The purpose of chromatography - the best possible separation of the components in a sample mixture - is commonly tried to be met by optimizing the measuring conditions. Ideally this instrument optimization prior to the data acquisition would lead to a complete chromatographic separation of all sample components of interest resulting merely in gaussian shaped peaks. In this case the peak detection and the integration would be straightforward. But for the separation of complex samples containing various substance classes and yielding a high number of components complete separation of all components is hardly achievable. Some peak shapes are asymmetric and the quality of separation and peak shapes decrease due to the gradual column degradation. Considerable numbers of overlapping and even some truly coeluting peaks are the rule. The task of peak detection takes a central role in almost all evaluations of chromatographic data and hence detection algorithms are implemented in virtually every evaluation software for chromatography to enable automatized peak detection. The quality of the algorithms, though, can vary greatly.

For the Py-GC/MS data it was found that the peak detection performed by the ChemStation, even in combination with the MS-SIM-Tools, was incomplete and therefore unsatisfactory. Manual review of each processed measurement was necessary and for a large measurement series this was regarded as unacceptable. The visual inspection of the acquired pyrograms revealed a high number of overlapping peaks. Most of the overlapping peaks could be recognized visually because of typical double peak shapes or peak shoulders. Figure 4.13 illustrates the overlapping of two components, an unknown lignin derived product (A) and a further unknown component (B), leading to a barely perceivable peak shoulder in the TIC signal of the corresponding peak (blue dotted signal in plots A2 and B2). The ChemStation detected and integrated the two components as one peak ignoring the presence of the minor counterpart A. When marker ions, selected from the respective mass spectra of the two components (plots A1 and B1), are plotted (in this case 4 each, see plots A2 and B2) the components can easily be distinguished. A difference in retention time of 0.04 min can be observed.

Figure 4.14 depicts a further example of interference between two components, 5-hydroxymethylfurfural (A) and an unknown component (B). In this case neither the ChemStation nor the visual inspection revealed the two almost coeluting components with a retention time difference of 0.14 min. The TIC signal (blue dotted signal in plots A2 and B2) describes a perfectly



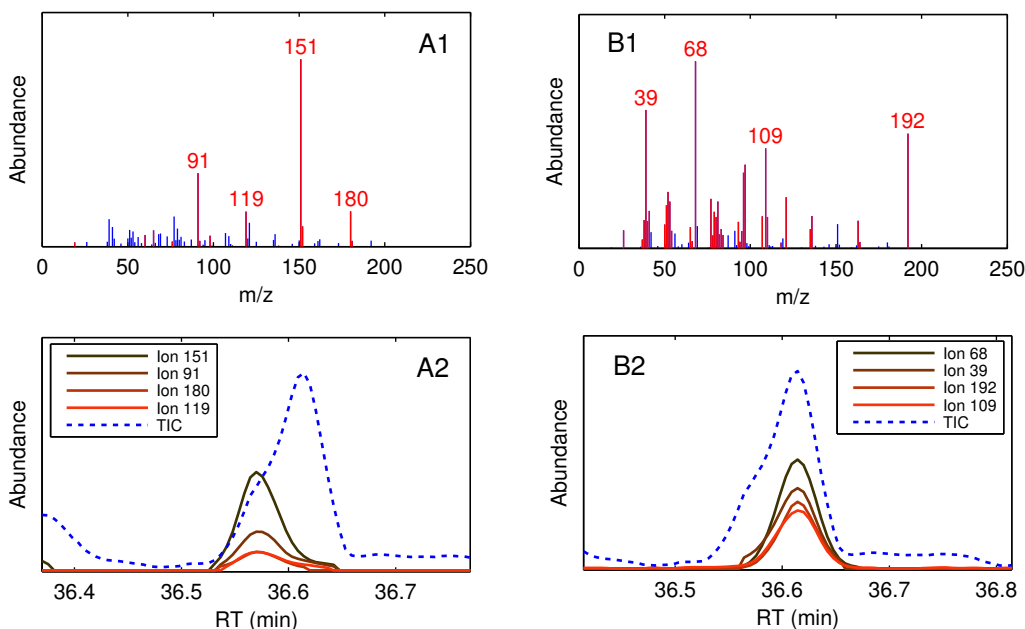


Figure 4.14: Effect of deconvolution. Deconvolution revealed the mass spectra of two overlapping components indicated by the mass traces marked red in plot A1 and plot B1 respectively. Plot A2 and B2 show the corresponding peaks of the 4 most prominent extracted ions for each component. The intensity of the TIC signal was lowered for display purpose.

shaped peak without any shoulder. The plotted marker ions (plots A2 and B2) show that the smaller component B is buried beneath component A.

To oppose the problem of overlapping and coelution several deconvolution strategies and algorithms were developed. Deconvolution enables the separation of overlapping signals into their individual contributions. Deconvolution is of major interest not only in chromatographic but also in spectroscopic applications (e.g. Infrared and Raman spectroscopy). The necessity of deconvolution in chromatography even increases with the ongoing trend towards time-saving, short measurements.

For the presented work the freely available and user-friendly software AMDIS was utilized for peak detection and deconvolution. The software allowed to process the data in a sequential mode, i.e. a high number of measurements could be processed with the same parameter settings so that for each measurement peaks were detected and deconvoluted. Although it is often referred to as *batch-processing* it may be more precisely termed *sequential processing*

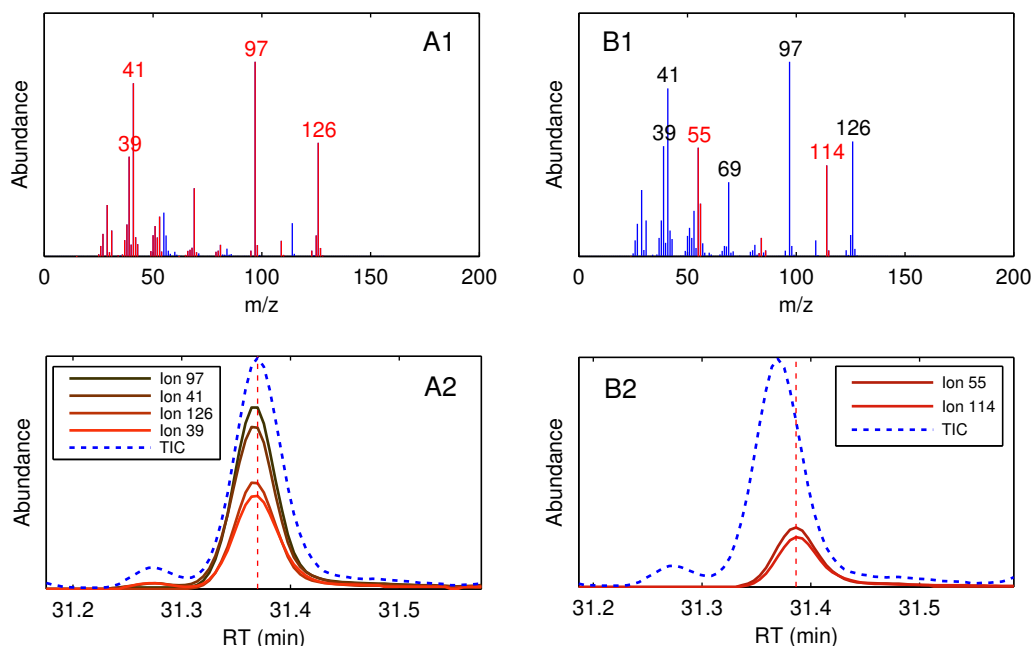


Figure 4.15: Effect of deconvolution. Two almost coeluting components (5-hydroxymethylfurfural with an unknown component) revealed by deconvolution. Plots A1 and B1 show the mass spectra (marked red) and A2 and B2 the corresponding peaks of the most prominent mass traces. The intensity of the TIC signal was lowered for display purpose.

in order to contrast the AMDIS procedure with the fairly recent approach of processing all or a subset of all measurements together by multivariate curve resolution (MCR), hence by a true *batch-processing* step (Jonsson *et al.* 2005, Thysell *et al.* 2007).

For the set aim of capturing as many peaks as possible in the chromatographic profiles AMDIS performed well in detecting many peaks which were missed out in the initial attempts using only the MS-SIM-Tools and the ChemStation. But by following the path of using AMDIS several new problems arose which had to be coped with. Firstly the deconvolution often resulted in two or even three results for the same peak with varying 'suggestions' for the possible nature of the extracted mass spectrum. This problem was reduced by optimization of the parameter settings but could not be completely resolved. Secondly, as the deconvolution was performed on each pyrogram separately the task of combining and matching the results of many measurements to build a global peak list had to be solved. The results of AMDIS are stored in

text-files. To tackle these problems some free software solutions are available which were made to process AMDIS results (Broeckling *et al.* 2006, Behrends *et al.* 2011). Although those options could have met the target the solution of Behrends *et al.* (2011) was too recent and the solution of Broeckling *et al.* (2006) not flexible enough to meet the desired demands. The novel deconvolution procedure based on MCR could have been a helpful alternative but was restrained by the lack of expertise in MCR and lack of a freely available software tool tailored for GC/MS data. The MCR method would have been advantageous as it processes all measurements together yielding a global peak list. Also the method is able to deconvolute truly coeluting peaks which is not possible with AMDIS where a small RT deviation of coeluting peaks is necessary.

It was decided to write own MATLAB scripts to perform the extraction and filtering of the AMDIS data to yield an appropriate global peak list. A global peak list served to give the data matrix necessary for subsequent analyses its dimension. For the 160 measurements a matrix was built consisting of 160 rows (one measurement per row) and one column for each peak found in at least two measurements (see description below). After peak integration each cell contained the peak area of the representative ion peak and if peaks were absent for some samples the corresponding entries would be set to zero (see also section 4.2.2.3).

Table 4.10: Path of generation of the global peak list for all 160 deconvoluted chromatograms.

Peak extraction process	No. of peaks
Peaks found by AMDIS in each pyrogram	243 - 444
Concatenation of all peaks	42475
Filter 1	17118
Filter 2	746
Filter 3	467
Manual removal of replicate entries	458

Table 4.9 summarizes the size of the peak list after each step performed for the generation of a global peak list. Deconvolution was employed on all 160 measurements resulting in quite varying amounts of detected peaks in each pyrogram (243 to 444 peaks), despite the same parameter settings. After importing the AMDIS results into MATLAB the individual peak lists

of the pyrograms were concatenated. To end up with a global peak list summarizing all occurring peaks in the data without multiple entries for the same peak the concatenated peak list had to be filtered. Several steps were chosen for this purpose starting from pre-filtering for removal of obvious replicate entries. This step (filter 1) reduced the peak list approx. by half through comparing mass spectral data with equal retention time on the basis of ordering the mass traces ( $m/z$ ) for each entry by intensity and matching the most significant ordered ions (in this case 4) against each other. In addition singular entries were removed assuming that these were non-optimal deconvoluted peaks or artefacts because all samples were at least measured as duplicates. For the next step (filter 2) small adjustable 'RT windows' were selected and all entries were merged with the same base ion. By this coarse filtering step coeluting components would disappear from the peak list if they have the same base ion (e.g. isomers). The step could have been fine-tuned by the application of more advanced algorithms (e.g. *Probability Based Matching* (McLafferty 1977) or *Weighted Dot Product* (Stein 1999)) but it has proven to work reasonably well for the analyzed data and reduced the peak list to 746 entries. Because of the aforementioned problem of AMDIS sometimes giving several suggestions for the same peak (missing the base ion) or because of inferior deconvolution of peaks near detection limit in some samples a further filtering step (filter 3) had to be applied. Like in the first step the most significant mass traces (in this case 4) were compared against each other but this time in 'RT windows' to account for small retention time shifts. The resulting peak list of 467 peaks was finally reviewed and some replicate entries of strongly time-shifting peaks of anhydrosugars (see figure 4.15, B) were removed manually. The three briefly described filters could be merged to one step but the adaptability would probably be lost.

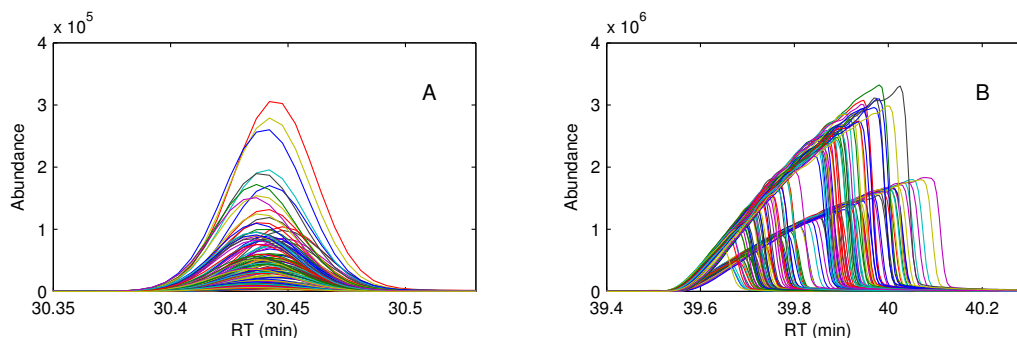


Figure 4.16: Overlay of the peak of 4-Vinylguaiacol (A) and Levoglucosan (B) for 160 measurements.

Figure 4.15 illustrates why several entries for levoglucosan (plot B) could be found after automated filtering of the data. As stated in the introduction of section 4.2.2 retention time shifts were not accounted for in the pre-processing procedures applied. Plot A shows the overlay of the symmetric peak of 4-Vinylguaiacol from 160 measurements. The retention time drift can be considered as reasonably small. Plot B gives a different picture. Levoglucosan, a major product from pyrolysis of pulp, shows a poor separation behaviour on the GC column resulting in highly asymmetric peak shapes which may be due to overload and high polarity. The elution of levoglucosan starts for all measurements within close proximity of 39.55 min. But because the highly varying abundances and the asymmetry the peak maxima are shifted within a range of 0.5 min (RT between 39.65 and 40.15 min) which can be considered a very high deviation in GC/MS applications. The RT windows selected for filter 3 were smaller than the deviation hence levoglucosan (and two other products) had multiple entries in the peak table.

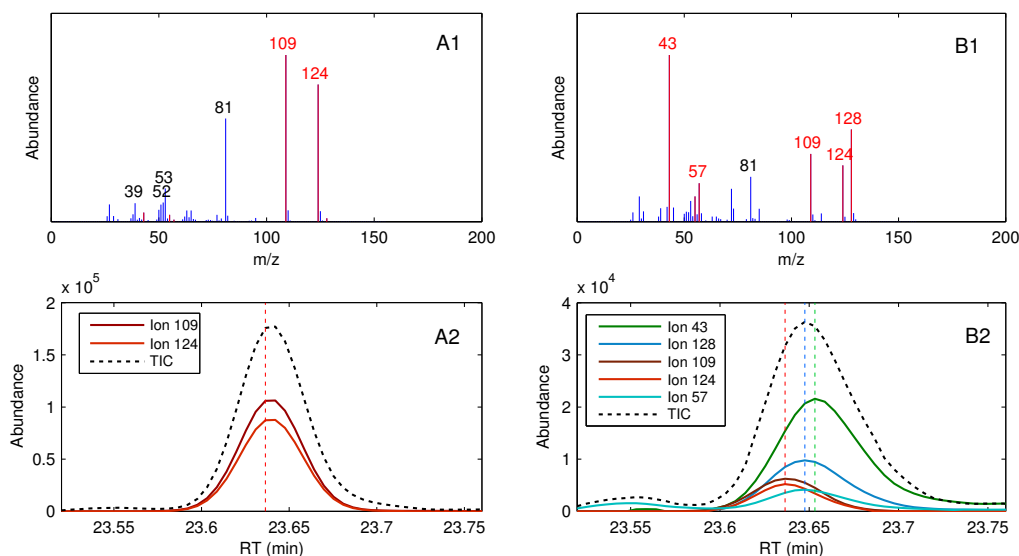


Figure 4.17: Comparison of coeluting peaks extracted from a pyrogram at the initial (A1, A2) and the terminal cooking stage (B1, B2). In the initial stage no coeluting peak was detectable.

It could have been considered to use only a subset of the measurements to construct the global peak list but as one wood and 28 different pulp samples were measured it was not straightforward to decide which samples to select. Moreover, the additional effort of evaluating 160 instead of 28 measurements

would have been marginal as the peak selection was eventually executed by the written MATLAB scripts. The simplest approach which was tested would have been to only use one measurement, e.g. from the center of the delignification time series. But in this case peaks were missed. In figure 4.16 an example is given where a pyrolysis product may have easily been overlooked. A1 shows the mass spectrum and A2 the TIC and ion profiles measured from a sample of the initial cooking stage at 30 min and B1 and B2 are from a sample of the final cooking stage at 330 min at the same retention time. On pyrolysis of the sample B<sub>30</sub> from the initial cooking stage basically only guaiacol was eluting with the ions  $m/z$  109 and 124 as the most prominent mass traces in the mass spectrum (A1 and A2). Measurements of the samples from the terminal cooking stage ( B<sub>330</sub>) revealed that one or two other components elute at the almost same retention time (difference of 0.01 min between red and blue dotted vertical lines) with the ions  $m/z$  43, 128 and 53 as most prominent mass traces (B1 and B2). It is not clear if the latter mentioned ions are of the same component or if actually two components ( $m/z$  128 and 57 of one and  $m/z$  43 of the other) coelute with Guaiacol with a retention time difference marked by the blue and green dotted vertical lines. AMDIS results suggest two components but ion  $m/z$  43 highly correlates with the ions  $m/z$  128 and 57. Regarding the B series the intensity of the second/third component starts increasing for the samples taken after a cooking time of 180 min. Hence if any sample from an earlier cooking stage was used as the only measurement for the deconvolution these procedure the coeluting components would have most likely been missed.

Although it was anticipated that the global peak list containing 458 peaks had many redundant entries marker ions for all peaks were extracted and integrated as described in the following section 4.2.2.3. With the aid of statistical methods on the integration results further reduction of the global peak list could be achieved.

#### 4.2.2.3 Ion extraction and integration

The most straightforward procedure of evaluating the chromatographic profiles would be to use the peak areas of the TIC chromatogram for each peak. But this approach is hindered by the numerous overlapping and coeluting peaks. When FID detectors are used instead of MS detectors the only remedies are to ignore the coeluting peaks, to try to resolve them by MCR methods or to prolong the chromatographic separation (using low temperature gradients, e.g. 3°C/min) to minimize the overlapping as far as possible as it was done e.g. by Bremer (1991). In case of wood or pulp analysis it is also common practice to only concentrate on the evaluation of the most prominent peaks where the error due to coelution is not regarded as significant (e.g. Rodrigues *et al.* 1999).

As discussed before when MS detectors are employed there is the additional option of using the mass spectral data to aid the separation of overlapping/-coeluting peaks. Kleen *et al.* (1993) and Sjöberg *et al.* (2004) used the peak areas of the TIC chromatogram for well separated peaks. For some overlapping/coeluting peaks they utilized the peak areas of extracted ions as representatives for the mass spectra of the corresponding components. Since the peak areas of extracted ions are proportional to the respective TIC peak areas they multiplied the peak areas of the extracted ions with prior determined factors to obtain the TIC peak areas. This step is necessary when the actual contribution of a component (only biased by the varying response factors) to the chromatogram is of interest.

In the presented work all data analyses are based on extracted ions as representatives for each peak, thus the extracted ion currents (EIC) are utilized rather than the TIC signals. At the initial stage of pyrolysis data evaluation the use of AMDIS was not considered. Instead the MS-SIM-Tools were in the focus as evaluation tool. The MS-SIM-Tools allow the extraction of one or even several representative ions for each peak and the integration of the respective peak areas. One of the main benefits was to yield more or less Gaussian peak-shaped and noise-free signals for the extracted ions facilitating the automated integration and helping when overlapping peaks were to be evaluated as illustrated in figures 4.13 and 4.14 of section 4.2.2.2. The downside of using the MS-SIM-Tools for peak detection was that many minor components in overlapping/coeluting peaks were not automatically detected because it relies on the peak detection algorithm of the ChemStation where no deconvolution is performed. As examples both peaks depicted in the aforementioned two figures were not detected when the MS-SIM-Tools were employed. The only remedy would have been to add missing representative

## CHAPTER 4. DISCUSSION OF RESULTS

---

ions manually to the extracted ion list generated by the MS-SIM-Tools. But this could only be done if the coeluting components were discovered by other means. Another possibility would have been to choose as many as 10 to 12 ions to be extracted for each peak with the hope that one of the numerous ions belongs to the coeluting peak but this would have generated a too extensive amount of data.



#### 4.2.2.4 Selection of extracted ions

When AMDIS is employed for peak detection and deconvolution the generated results also include extracted ions used as *model ions* for deconvolution. It could have been an option to use these ions as representatives for the peaks but it was found that in many cases these proposed model ions varied from measurement to measurement causing conflicts when the global peak list was set up. In other cases these were also not optimal to use for the analysis of the delignification time series because when ions of already low intensity in the corresponding mass spectra were proposed as model ions these ions disappeared completely in measurements where the analyzed components were near the detection limit. Particularly to monitor the changes of minor peaks/components in the course of pulping it seemed most appropriate to choose the most prominent ion in each mass spectrum. An example where this choice is appropriate can be reviewed in figure 4.14 in the previous section. The ion 97 for the major peak and ion 55 for the minor coeluting peak should preferably be picked.

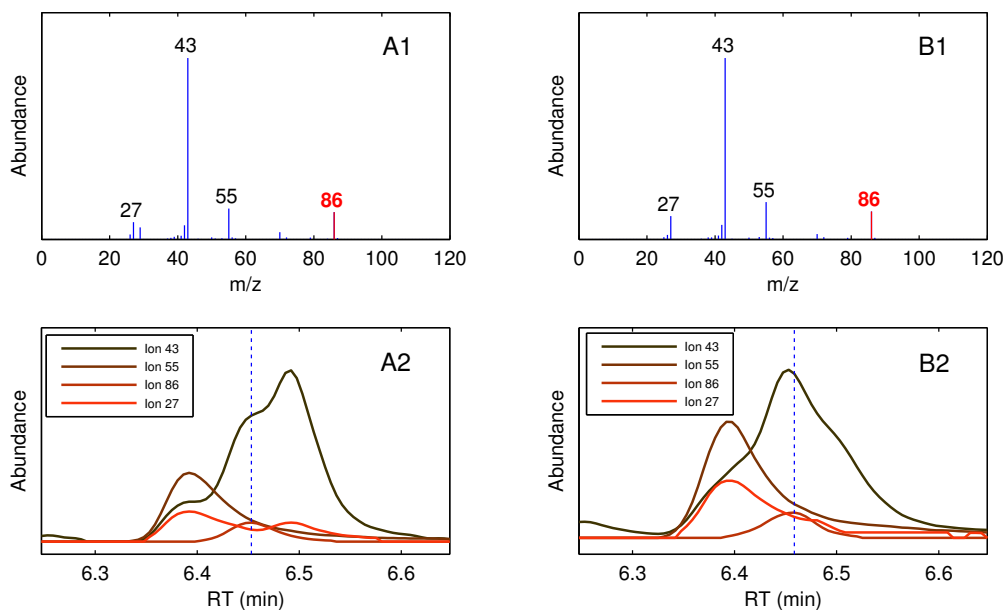


Figure 4.18: Selection of representative ions. The most prominent  $m/z$  43 is a major ion of 3 overlapping peaks.

Though several cases were found in the data where the most prominent ion would have been the wrong choice. In figure 4.17 a case of three overlapping

peaks at a retention time around 6.45 min is illustrated. Only the EIC signals for the 4 most prominent ions recorded at the retention time marked with the vertical dotted line are displayed (A2 and B2). A1 and A2 are the mass spectrum and the ion profiles respectively extracted from the pyrolysis data of a sample of the initial cooking stage at 30 min and B1 and B2 from a sample of the final cooking stage at 330 min.

Ion  $m/z$  43 is by far the most prominent ion for the middle peak but ion  $m/z$  43 is also present in the two other overlapping components. Proper integration of the signal of ion  $m/z$  43 is hindered and subject to errors. Instead of ion  $m/z$  43 the ion  $m/z$  86 with much lower intensity but much better peak shape is preferably chosen as the representative ion of the middle peak. When the initial and terminal stage samples are compared the change of the relative intensities of the 3 overlapping peaks to each other can be observed by the shape-change of the profile of ion  $m/z$  43.

The obstacle of selecting the most appropriate ions as peak representatives for each peak without manual review was tackled by extracting and integrating the 4 major ion peaks from the deconvoluted mass spectra of each pyrolysis product (in some cases only 1 to 3 ions were extractable). The selection of the presumed 4 major ions was carried out in MATLAB. The extraction and integration of the 1615 ion peaks was conducted with the MS-SIM-Tools. A subsequent selection procedure was applied to choose finally one ion per component. The selection procedure was based on Pearson's correlation coefficients calculated for the ion peak areas by the equation:

$$r_{xy} = \frac{\sum_{i=1}^I (x_i - \bar{x})(y_i - \bar{y})}{\sqrt{\sum_{i=1}^I (x_i - \bar{x})^2 \sum_{i=1}^I (y_i - \bar{y})^2}} \quad (4.1)$$

It was assumed that within replicate measurements nearly all peaks highly correlate with each other. Low correlation coefficients computed for a peak would indicate that the amount of random variation of the corresponding peak is higher than the systematic variation affecting all peaks equally. Hence if 4 ions of the same TIC peak are compared the ion with the highest average of 1615 correlation coefficients is presumed to have the most consistent integration results. To account for the changes in sample composition the calculations were performed for 9 sets of replicate measurements separately (with 6 to 17 replicate measurements each).

## CHAPTER 4. DISCUSSION OF RESULTS

Table 4.11: Two examples for the selection of the representative ion on basis of mean correlation coefficients.

Sample	No. replicates	4-Ethylguaiaicol				Methyl pyruvate			
		m/z	m/z	m/z	m/z	m/z	m/z	m/z	m/z
		137	152	98	39	43	31	102	45
B <sub>30</sub>	10	0.69	0.69	0.69	0.69	0.62	0.37	0.66	0.49
B <sub>60</sub>	17	0.74	0.74	0.73	0.73	0.69	0.65	0.68	-0.19
A <sub>90</sub>	11	0.75	0.74	0.73	0.74	0.55	0.48	0.60	0.57
B <sub>90</sub>	13	0.73	0.73	0.71	0.72	0.70	0.55	0.69	0.11
B <sub>120</sub>	6	0.72	0.71	0.71	0.71	0.64	0.71	0.71	0.11
B <sub>150</sub>	6	0.73	0.73	0.72	0.71	0.61	0.58	0.67	0.52
B <sub>270</sub>	6	0.65	0.62	0.66	-0.28	0.64	0.66	0.64	0.29
B <sub>330</sub>	8	0.62	0.60	0.62	0.60	0.50	0.35	0.49	-0.12
<i>S<sub>BCTMP</sub></i>	12	0.68	0.68	0.65	0.67	0.55	0.42	0.51	0.55
<b>sum</b>		<b>6.30</b>	6.24	6.24	5.29	5.49	4.77	<b>5.64</b>	2.33

In table 4.10 the ion selection is exemplified by the results for the 4 extracted ion peaks of two pyrolysis products, 4-ethylguaiaicol and methyl pyruvate. For 4-ethylguaiaicol the 4 ions m/z 137, 152, 98 and 39 and for methyl pyruvate the ions m/z 43, 31, 102 and 45 were extracted. The mean correlation coefficients range for most ions between 0.5 and 0.75. Only the fourth ion in case of both pyrolysis products shows strongly deviating results for some replicate sample sets.

The poor correlation for m/z 39 of sample set B<sub>270</sub> may be explained by the low intensity of that ion compared to m/z 137 and 152 (see figure 4.18, plot A1) hence in sample sets with low lignin content m/z 39 was in some measurements below the detection limit and set to zero. The same explanation may apply for m/z 45 of methyl pyruvate resulting in the overall poor mean correlations (m/z 45 is not displayed in figure 4.18, plot B1). The sum of the mean correlation coefficients was the selection criterion for the choice of the representative ion for each pyrolysis product. For 4-ethylguaiaicol the most prominent ion m/z 137 was selected but for methyl pyruvate m/z 102 was selected instead of m/z 43 despite the much lower intensity of m/z 102. Plot B2 in figure 4.18 may illustrate a likely explanation. The peak of ion m/z 43 shows a peak shoulder indicating that the ion is also found in the overlapping peak eluting before which easily leads to erroneous peak integration.

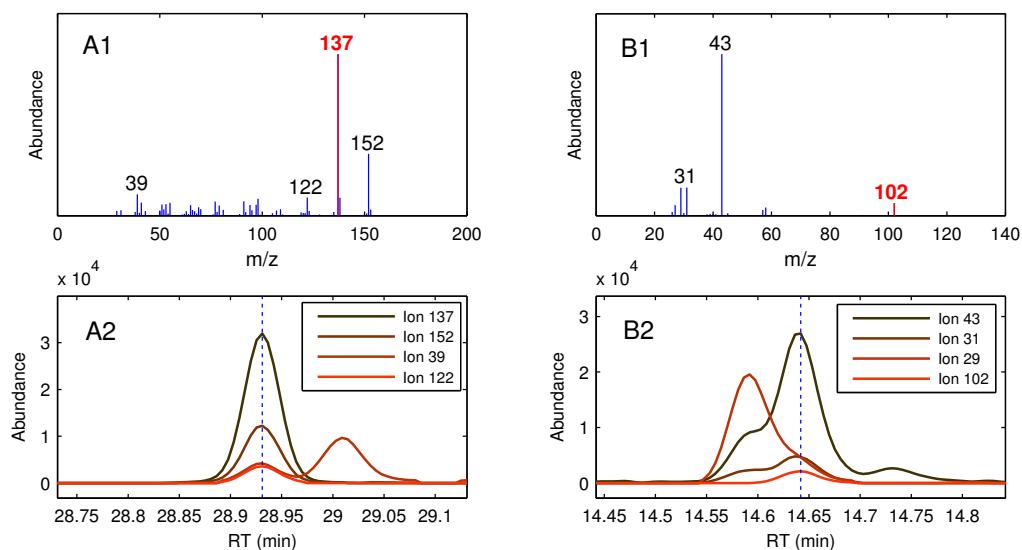


Figure 4.19: Selection of representative ions. The selected ions (highlighted red) for 4-ethylguaiaicol (A1, A2) and methyl pyruvate (B1, B2) on the basis of the results displayed in table 4.10.

Instead of using the mean correlation coefficient, which is in this case equivalent to the sum of correlation coefficients, for the selection of the best ion, some threshold value could be set and only correlation coefficients passing the threshold would be summed.

#### 4.2.2.5 Normalization

In Py-GC/MS applications between-sample variations are mainly introduced by differences in sample-weight but also by inhomogeneity due to insufficient milling. The measurement device is another source causing variations in the acquired data. Here sensitivity changes of the mass spectrometer between each measurement are of major concern. They may not be significant for short measurement series, but particularly when large-scale analyses are conducted unpredictable fluctuations have to be expected. If the mass spectrometer demands a 'tuning' procedure in between a series, as it was the case in the presented measurement series, an abrupt sensitivity leap can be observed. To compensate these and other between-measurement variations and to facilitate sample comparison chromatographic data is usually normalized.

The internal standard method is the most common normalization technique in GC applications (Lu and Ralph 1997, Sundberg and Holmbom 2004, Ekeberg *et al.* 2006) where the internal standard (IS) may be added to the sample stock solution before injection. Hereby sensitivity changes of the measuring device and deviations of injection volume can be compensated. It is also, but less frequently, utilized when analytical pyrolysis is hyphenated with GC (Bocchini *et al.* 1997, Odermatt *et al.* 2003, Becerra and Odermatt 2012). Because of the different sample introduction in pyrolysis (solid samples) additionally to the IS a sample-weight normalization is appropriate to compensate the sometimes considerable sample weight differences. A shortcoming of the IS method may be that the sample handling of the internal standard can introduce additional variation. It may also be a challenge to find an adequate IS for the samples to be measured as it should behave similar to the analyte, be inert towards interaction with the analyte and completely resolved from the latter. In all Py applications a potential volatility of the IS is of additional concern since all sample containers (e.g. sample cups) are open. This holds particularly true when autosamplers are used and hence each sample may be exposed to atmospheric environment for a different time period.

When internal standards are not utilized, as it is the case in most Py-GC/MS studies, other normalization techniques have to be applied. Especially when MVA methods are employed normalization to constant sum (also termed sum or area normalization) is most commonly used (Johansson *et al.* 1984). For each chromatogram all baseline corrected signals are summed up and the obtained total sum used as a normalization factor. Hence constant sum normalization results in the total sum of each normalized chromatogram to equal 1 (Pierce *et al.* 2012). Although the variations between replicate measure-

ments are minimized effectively some major problems can arise from constant sum normalization. Because of the fixed sum for all samples an unwanted interdependence between the variables is introduced. The increase of the intensity of major variables (i.e. peaks) automatically lowers the intensity of other peaks in the sample. This dependency may be true for compositional data but not for 'open' data acquired by Py-GC/MS where all or many components may increase in intensity resulting in an overall higher total signal (see figure 4.20). The consequences of this so called *closure effect* due to normalization can be the introduction of spurious correlations and the elimination of true correlations between variables (Johansson *et al.* 1984). An additional negative effect arising from constant sum normalization is related to the presence of heteroscedastic noise, i.e. increase of absolute noise with increasing signal intensity, in GC/MS data. By constant sum normalization the high absolute amount of noise present in large peaks is redistributed to the other peaks which can affect particularly the minor peaks obscuring relevant information (Kvalheim *et al.* 1994). The same problems arise for other common normalization methods like mean normalization where the mean signal of each chromatogram is forced to equal 1, or minimum-maximum normalization where the biggest peak is forced to equal 1. It has been recommended to use these normalization procedures only for measurements with overall high similarity which was not the case with the measured pulp samples.

The series of 160 measurements was conducted without internal standard. For the purpose of direct monitoring of changes in intensity of various single pyrolysis products as a function of the delignification progress constant sum normalization was not an option because of the aforementioned reasons. Therefore a different normalization strategy had to be applied. Although the sensitivity fluctuations showed to be moderate a major obstacle was the MS tuning procedure which was employed in the middle of the series after 80 measurements. In figure 4.19 the weight normalized *TIC signals* (sum of all signals across each chromatogram which can be regarded as equivalent to the total peak area) of the 17 replicate measurements ( $wn\ TIC_{BC}$ ) are plotted against the series of measurements. It can be noticed that the tuning induced a sensitivity leap resulting in an approx. two-fold increase of the weight normalized TIC signal. A further indicator for the sensitivity changes may be the background noise signal which can easily be monitored by the extracted ion current (EIC)  $m/z$  28 (base ion for  $N_2$ ) as air is always a major contributor to background noise in pyrolysis applications. In fact two different contributions of air to the TIC signal in a pyrogram can be observed. One air signal observed as a prominent peak at the beginning of the pyrogram is due to the brief opening of the device for the sample in-

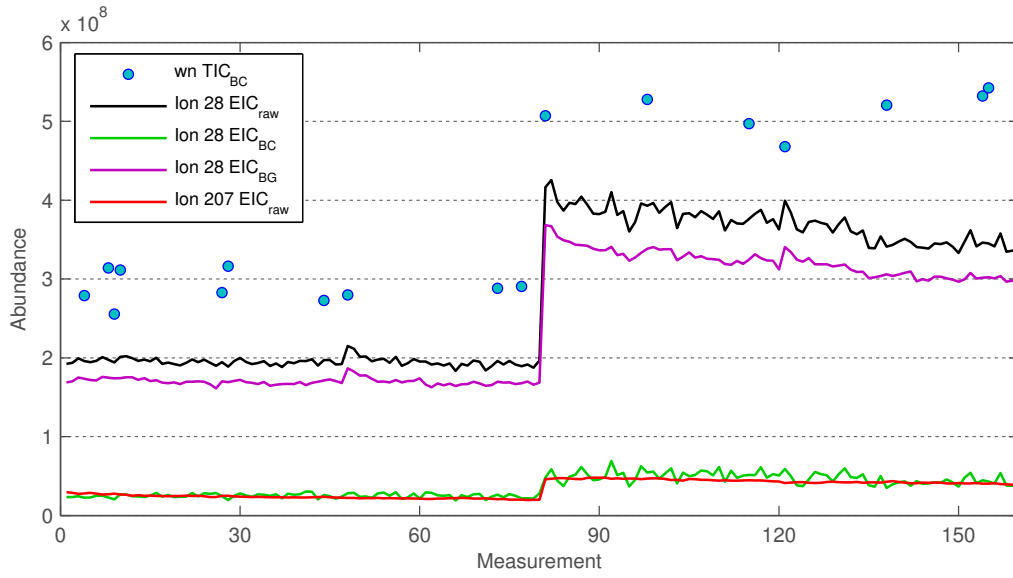


Figure 4.20: Comparison of 5 different signals across the 160 measurements conducted. The BC processed TIC signals of the 17 replicate measurements of sample B<sub>60</sub> were weight normalized (wn TIC<sub>BC</sub>). *Ion 28 EIC<sub>raw</sub>* and *Ion 28 EIC<sub>BC</sub>* refer to the summed up ion current of m/z 28 for each unprocessed and BC processed chromatograms respectively, *Ion 28 EIC<sub>BG</sub>* was calculated as the difference between *Ion 28 EIC<sub>raw</sub>* and *Ion 28 EIC<sub>BC</sub>*.

## CHAPTER 4. DISCUSSION OF RESULTS

---

troducton (ion  $m/z$  28  $EIC_{BC}$  in figure 4.19) and the second contribution is a constant noise signal (ion  $m/z$  28  $EIC_{BG}$ ) caused by minor leakage of the system which is never completely sealed. The black signal (ion  $m/z$  28  $EIC_{raw}$ ) amounts from the sum of these two contributions. A further marker ion for the background noise is  $m/z$  207 ( $SiO_4$  marker, ion  $m/z$  207  $EIC_{raw}$ ) mainly arising from column bleed which showed the least variation between measurements.

Table 4.12: RSDs of sample B<sub>60</sub> ( $wn\ TIC_{BC}$ ) calculated for 10 replicates within the first, 7 replicates within last 80 measurements and all 17 within the whole series. Additionally the RSDs calculated for  $Ion\ m/z\ 28\ EIC_{raw}$ ,  $Ion\ m/z\ 28\ EIC_{BC}$  and  $Ion\ m/z\ 28\ EIC_{BG}$  separately for the first and last 80 and for all 160 measurements.

	Measurements		
	1 - 80	81 - 160	1 - 160
$RSD_{wnTIC}$	6.80	4.92	30.39
$RSD_{28raw}$	2.50	5.92	31.48
$RSD_{28PK}$	10.72	15.52	35.28
$RSD_{28BG}$	2.4	5.35	31.28

As mentioned above apart from the sensitivity leap between measurement 80 and 81 the variation of the TIC signals within the 17 replicate measurements was moderate with an RSD of 6.8% for 10 weight normalized replicates ( $wn\ TIC_{BC}$ ) within the first 80 measurement series and 4.92% for 7 replicates within the second half (see  $RSD_{wnTIC}$  in table 4.11). When the RSDs for the marker ion ( $m/z$  28) of the background noise, the air peak and the combined signal are calculated separately for the first 80 and the last 80 measurements the RSDs for the background noise are the lowest with 2.4 and 5.35% respectively ( $RSD_{28BG}$ ). As expected the RSDs for all displayed signals over the complete measuring series are high due to the sensitivity leap.

It was decided to combine weight normalization for all samples with one of the 4 displayed signals as an additional normalization factor analogous to an IS method. The background noise signal (ion  $m/z$  28  $EIC_{BG}$ ) turned out to give the overall best results for the complete measurement series range with calculated RSDs for all but one replicate measurements well below 10% and the lowest mean RSD. The only exception were the four-fold replicates of sample A<sub>270</sub> which yielded an RSD slightly above 10%. In table 4.12 the RSDs ( $RSD_{wnTIC}$ ) for the replicates of 5 samples are displayed. Of these



## CHAPTER 4. DISCUSSION OF RESULTS

Table 4.13: RSDs of BC processed TIC signals for 5 different sets of sample replicates after weight-background normalization.

Sample	No. of replicates	$RSD_{wbnTIC}$
B <sub>30</sub>	10	7.49
B <sub>60</sub>	17	7.56
A <sub>90</sub>	11	3.45
B <sub>90</sub>	13	5
B <sub>330</sub>	8	2.65

5 displayed samples the RSD of sample B<sub>60</sub> with the 17 replicates actually showed the highest RSD.

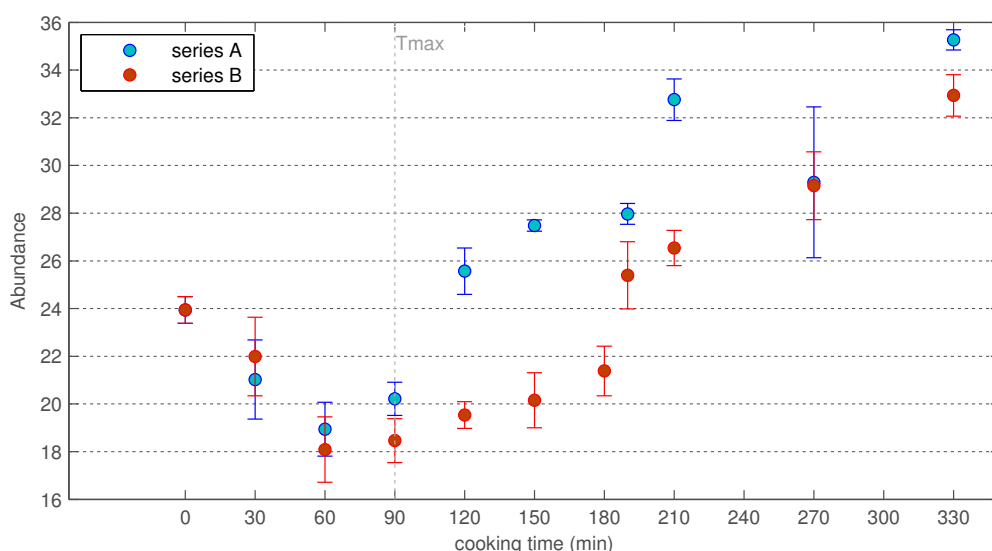


Figure 4.21: BC processed and weight-background normalized TIC signals acquired for samples of the delignification series as a function of cooking time. Errorbars/-standard deviations were calculated from 2 to 17 replicates for each sample. For display purposes all TIC signals were multiplied by the factor 1000.

The benefit of the elaborated normalization method, referred to from here on as weight-background normalization (wbn), was that it allowed to compare the measurements over the complete series rather than only separately within the first and last 80 measurements. This was of particular interest as not all samples of the two delignification series were measured either within the first or the last 80 measurements. When the *wb* normalized TIC signals

of the delignification series are plotted against cooking time, as depicted in figure 4.20, significant changes of the TIC signals can be observed. Comparing samples at a cooking time of 60 min and 330 min the TIC signal has almost doubled. The figure also illustrates that the variations in the TIC signal show a systematic pattern with an initial decrease followed by gradual increase over the cooking time. Only sample A<sub>270</sub>, which also had the highest RSD (as shown in table 4.12) illustrated by the large errorbars in the figure, shows an unexpected behaviour. The reasons for the strong divergence of the TIC signals is not straightforward but is most likely associated with the significant change of pulp composition in the course of pulping. The samples with the lowest TIC signal have the highest and the samples with highest TIC signals the lowest lignin content. One explanation could be different ratios of volatile products to char residues. But it may also be explained by the differences in relative detector response between the various pyrolysis products. Although response factors of the pyrolysis products were not determined on the employed measuring device, anhydrosugars like levoglucosan (main product from pyrolysis of lignocellulosic biomass) have significantly higher response factors than phenolic compounds. Hence the high carbohydrate content of the samples from the final stage of pulping should be expected to result in higher TIC signals.

Apart from the weight-background normalization another normalization procedure was elaborated for the data set. Johansson *et al.* (1984) suggested to use only the sum of a subset of the available variables (e.g. peaks) for normalization to minimize the closure effect caused by constant sum normalization and termed it *selective closure*. The recommended criteria for the selection of the variables was to choose as many variables as possible with the constraint that only variables with similar means and standard deviations are selected and the very large and very small variables are excluded. This normalization technique was applied by Kleen *et al.* (1993) and Sjöberg *et al.* (2002) on pyrolysis data of pulps.

Also in the presented work constant sum normalization on the pyrolysis data of the analyzed pulps was having strong biasing effects because the differences between the measurements were huge regarding comparison of samples from the initial and terminal cooking stage. In particular the levoglucosan peak amounted for some samples to a relative peak area of over 30% dominating the pyrogram and hence also normalization results when included as a variable for normalization.

Because of the particular problem of the autotune performed in the middle of the analyzed measurement series the approach suggested by Johansson *et al.*

(1984) for selecting peaks for normalization led to abnormally high standard deviations and biased calculated means for all peaks. It could have possibly been solved by applying the selection procedure for the first 80 and last 80 measurements separately and then merge the results.

But instead a different method for the determination of a suitable subset of peaks for normalization was elaborated. The scope of the procedure was to conserve the partially large differences between the TIC signals of different samples (as already shown in figure 4.20) and to minimize the deviations within replicate measurements. Although the weight-background normalization described above already gave reasonable results it was hoped to find an appropriate normalization independent of the background noise as the background noise could easily deteriorate the data if e.g. a small leakage of the measuring device abruptly or gradually increases.

Analogous to the selection of the representative ion for each peak described in section 4.2.2.4 this approach based on the correlation coefficients between the peak areas within the replicate measurements. The assumption was made that variables with the highest sum (or mean) of correlation coefficients within replicates were more likely suitable candidates for normalization. Since again 9 different replicate sets were utilized a ranking order of the ions was calculated by summing up, for each variable (peak) separately, the mean correlation coefficients of the 9 replicate sets. A further assumption made was that the TIC signal (area sum) trend yielded by the weight-background normalization (displayed in figure 4.20) closely represented the unbiased data. Hence a subset of peaks was to be selected for normalization, termed here selected-peaks normalization, which yielded a similar trend of the TIC signals as displayed in figure 4.20. Mathematically the convergence to the weight-background normalized data was assumed to be achieved with the highest correlation between the selected-peaks normalized and the weight-background normalized TIC signals. Following the aforementioned ranking order of the ions the peak areas were added up stepwise and each resulting sum was applied for normalization. For each step the correlation was calculated on one data set consisting of all replicate sets. It has to be mentioned that prior to the described stepwise summation of the peak areas each ion peak area was multiplied by a previously determined respective factor to estimate the corresponding TIC peak area for each component.

In figure 4.21 it can be seen that the iteratively calculated correlation coefficient gradually increases reaching values beyond 0.95 when more than 280 peaks are included. After the inclusion of the 305th peak the correlation coefficient abruptly declines and stays constant at around 0.75. From the 458 peaks eventually 285 peaks were selected when a correlation coefficient of 0.974 was reached. It may appear that the normalization factor amounting

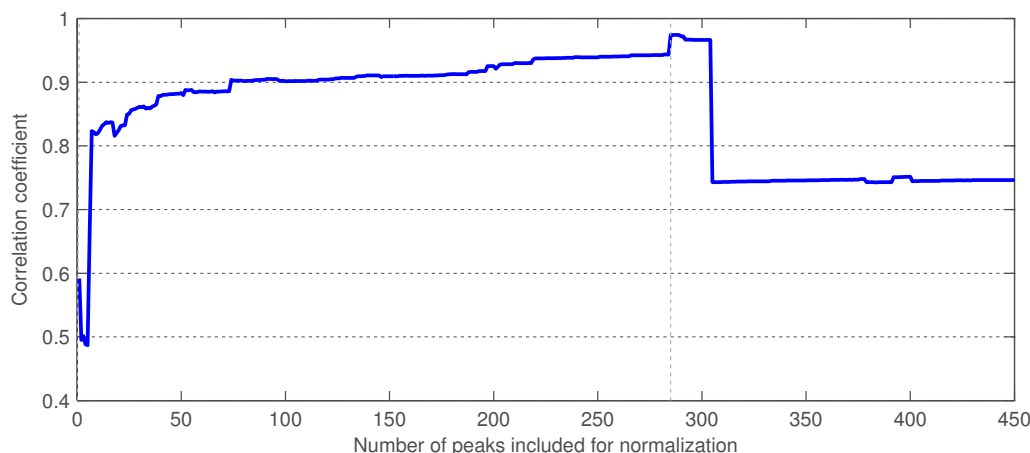


Figure 4.22: Iteratively determined correlation between selected-peaks normalized and weight-background normalized TIC signal plotted against the number of peaks included for selected-peaks normalization.

from 285 peaks could possibly be similar to a constant sum normalization (i.e. using all peaks). But it has to be kept in mind that among the 458 peaks extracted from the data most are minor components with very little contribution to the total sum. The abrupt decline of the correlation coefficient is induced by the major peak of levoglucosan (305th peak) which underlines the biasing effect of the levoglucosan peak on normalization.

To estimate the performance of the described selected-peaks normalization procedure the mean and median RSDs may be helpful which are displayed in table 4.13. For each replicate set the RSDs for each of the 458 peaks were calculated and the respective mean and median RSDs determined. Lower RSD values imply less scatter within the replicates which is one of the major scopes of normalization. The mean RSD alone, though, is easily biased by extreme values, i.e. peaks showing extensive scatter resulting in extremely high RSD values may obscure the effect of normalization. The median RSD is robust against those extreme values as long as those extremes are only present in relatively small numbers. Hence it better reflects the average RSDs of the majority of the peaks. When the results displayed in table 4.13 are reviewed large differences between the mean and the respective median RSDs can be observed indicating the presence of extreme values (*outliers*). A second conclusion which can be drawn from the displayed results is that the selected-peaks normalization reduced the overall scatter within the replicate sets more effectively than the weight-background (wbn) and constant sum normalization (csn) reflected by the lower RSD values.

## CHAPTER 4. DISCUSSION OF RESULTS

Table 4.14: Comparison of the mean and median RSD values ( $RSD_{wbn}$ ,  $RSD_{csn}$  and  $RSD_{spn285}$ ) resulting from weight-background, constant sum and selected-peaks normalization for the 9 replicate sets. For the selected-peaks normalization 285 peaks selected by the ranking order described above were used.

Sample	Mean			Median		
	$RSD_{wbn}$	$RSD_{csn}$	$RSD_{spn285}$	$RSD_{wbn}$	$RSD_{csn}$	$RSD_{spn285}$
B <sub>30</sub>	32.3	33.4	32.1	14.2	16.5	13.8
B <sub>60</sub>	35.2	32.8	31.6	15.9	13.1	11.6
A <sub>90</sub>	27.6	27.6	27.0	11.7	11.7	11.2
B <sub>90</sub>	27.8	27.2	26.5	12.8	12.2	11.4
B <sub>120</sub>	22.9	23.3	23.0	9.9	10.4	10.1
B <sub>150</sub>	27.5	26.4	25.8	11.6	10.3	10.0
B <sub>270</sub>	33.8	31.2	30.4	15.0	11.6	10.0
B <sub>330</sub>	38.1	38.7	37.7	12.4	13.5	12.3
$S_{BCTMP}$	38.2	39.0	36.9	16.3	17.3	14.6

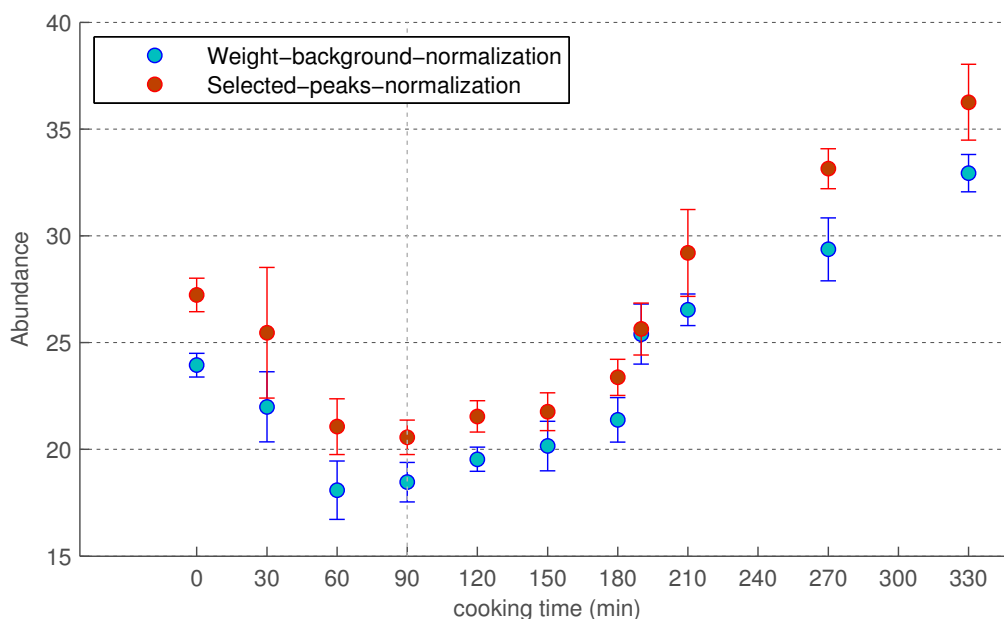


Figure 4.23: Comparison of weight-background and selected-peaks normalized TIC signals acquired for samples of the B series as a function of cooking time. Error-bars/standard deviations were calculated from 2 to 17 replicates for each sample. For display purposes all weight-background and selected-peaks normalized TIC signals were multiplied by the factor 1000 and 200, respectively.

## CHAPTER 4. DISCUSSION OF RESULTS

---

To survey whether the selected-peaks normalized TIC signals show a trend converging with weight-background normalized data the TIC signals of the B series samples were plotted against cooking time in analogy to figure 4.20. It can be observed in figure 4.22 that both trends show high similarity. Hence it may be concluded that apart from the weight-background normalization also the elaborated selected-peaks normalization conserved the systematic differences between the samples.

#### 4.2.2.6 Removal of insignificant peaks

One of the last steps of the pre-processing procedure was the removal of apparently meaningless data for the subsequent analysis, i.e. peaks without any significant discriminative ability may as well be excluded. It could be considered to perform this step in an earlier stage of pre-processing but for the univariate statistical procedures applied for this purpose prior normalization of the data was inevitable. The exclusion of meaningless variables, or vice versa, the preselection of potentially discriminative marker peaks is also commonly known as feature, variable or subset selection. But the feature selection may also be splitted into two stages. The first stage could be considered a preliminary selection applying a low threshold to remove peaks which are insignificant for the whole data set and retain all peaks which have a discriminative potential in the data analysis. Hence this weak pre-selection can rather be considered a pre-processing step. The second stage is the application of feature selection as an integral part of the data analysis where moderate to high thresholds are set for the selection of variables. This enables to greatly reduce the number of peaks and retain only the most significant markers needed for discrimination or regression. This makes particularly sense when multivariate analysis is to be conducted on several different subsets of samples, e.g. when only samples from two cooking stages are compared it is advantageous to perform the feature selection only on these analyzed samples.

For the preliminary removal of overall insignificant peaks Oneway ANOVA (analysis of variance) was considered as an appropriate tool which is applied to each variable/peak separately (hence univariate). ANOVA is a global test based on hypothesis testing using F statistic. The goal of ANOVA is to prove the absence or existence of any statistically significant difference between the means of several groups. The procedure relies on the calculation of two different estimates of variance for a sample set which are referred to as the between-sample estimate of variance and the within-sample estimate of variance, i.e. in the case of the pyrolysis data the variance between the different replicate sets is compared to the variance within each replicate set. The resulting F-value is determined by the ratio of these two estimates and a corresponding p-value is extracted from the F statistic table. The higher the F-value the more significant is the difference between at least one group and the remaining groups of samples. The p-value provides the significance level of the difference.

The generalized formula for the between-sample variance expressed as sum of squares (SS) is given by:

$$SS_{Btw} = \sum_{j=1}^p n_j (\bar{X}_j - \bar{X})^2 \quad (4.2)$$

The within-sample variance is calculated by:

$$SS_{W/in} = \sum_{j=1}^p \sum_{i=1}^{n_j} (X_{ij} - \bar{X}_j)^2 \quad (4.3)$$

where  $\bar{X}$  refers to the mean value,  $i$  is any score,  $j$  any group,  $n$  the number of scores and  $p$  the last group within the tested set.

Prior to the calculation of the F-value these two variances are divided by respective *degrees of freedom* which are determined on the basis of the total amount of measurements tested and the amount of measurements in each group. As for all statistical tests high numbers of measurements/replicates in each sample group greatly improves the confidence of the results. Therefore again only the 9 replicate sets were used for the ANOVA peak removal procedure. The threshold for rejection of variables can be arbitrarily set. But commonly a cut-off p-value of 0.05 is applied corresponding to the 95% confidence level. Hence in the case of the peak removal task analyzed peaks with  $p > 0.05$  were rejected. ANOVA has been implemented by various authors into their feature selection routines (Ebrahimi *et al.* 2007, Sinkov and Harynuk 2011).

ANOVA allows to determine if any of the analyzed measurement groups show significant differences to the others but does not provide any information how many and which groups vary significantly from each other. One test giving details on the variation of each group to each other is Tukey's honestly significant difference (HSD) test. The means of each pair of measurement groups is compared against each other including a predefined confidence level (typically 95 %). If the results are plotted the details of the variance between the groups can be reviewed. Graph 4.23 shows the result for the mean peak areas of the unknown component (represented by m/z 55) coeluting with 5-hydroxymethylfurfural which was already discussed in section 4.2.2.2 (see figure 4.14). It can be observed that the peak area means of several replicate sets show significant differences to each other, e.g. the peak area mean of the sample B<sub>30</sub> replicates (marked blue) differs significantly from the peak area means of 6 other replicate sets (marked red). In the same fashion each of the other replicate sets can be compared against the remaining replicate sets. Hence this peak may be important for discrimination.



## CHAPTER 4. DISCUSSION OF RESULTS

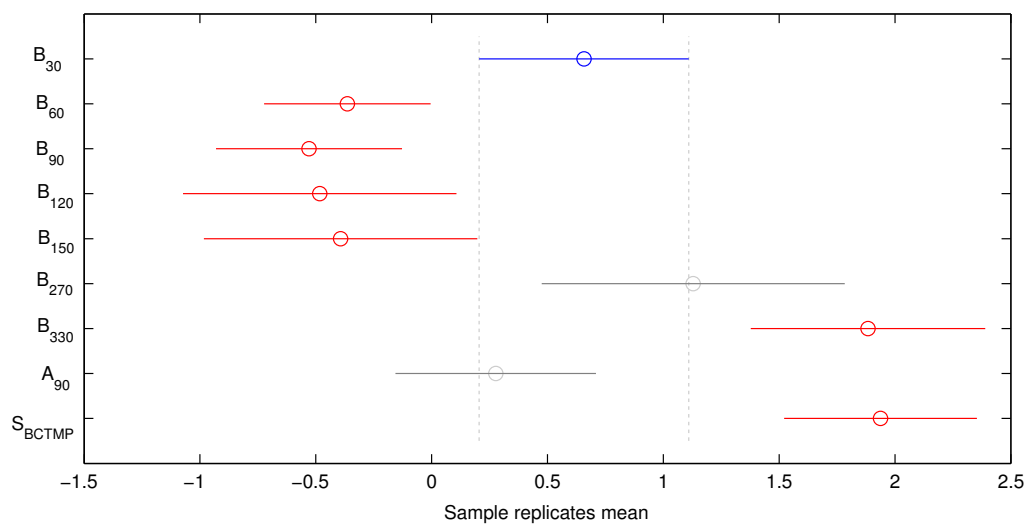


Figure 4.24: Visual representation of the results of Tukey's HSD test on the mean peak areas of ion  $m/z$  55 eluting at RT 31.38 min (ID 282). 9 replicate sets were compared against each other.

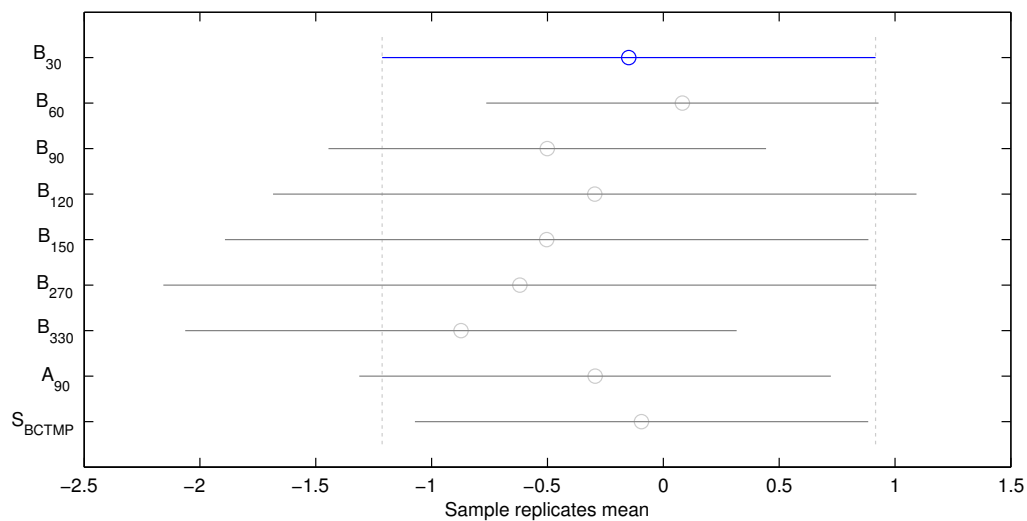


Figure 4.25: Tukey's HSD test on the mean peak areas of ion  $m/z$  44 eluting at RT 36.6 min (ID 351). This peak was discarded from the peak list.

The graph 4.24 depicts an example of a peak which was rejected by significance testing via ANOVA. This was actually a peak coeluting with the two components also discussed in section 4.2.2.2 (see figure 4.13), but of very low intensity and as shown in the plot 4.24 not having any discriminative relevance.

Surprisingly only 36 of the 458 peaks were discarded by the ANOVA method. Further 14 peaks were removed which had mainly missing data and only sporadic peak entries. Hence the final global peak list consisted of 408 potentially meaningful peaks which was much more than expected. The second stage of feature selection for extraction of the meaningful peaks for each particular multivariate analysis conducted on subsets of the data is discussed in section 4.2.3.

#### 4.2.2.7 Centering and scaling prior to MVA

For the application of PCA and PLS it is common practice to mean-center the data before analysis. This variable centering procedure shifts the axes of the coordinate system of the latent variables (e.g. principal components) into the center of the data. One benefit of mean or median centering is that it facilitates the description of variation in the analyzed data.

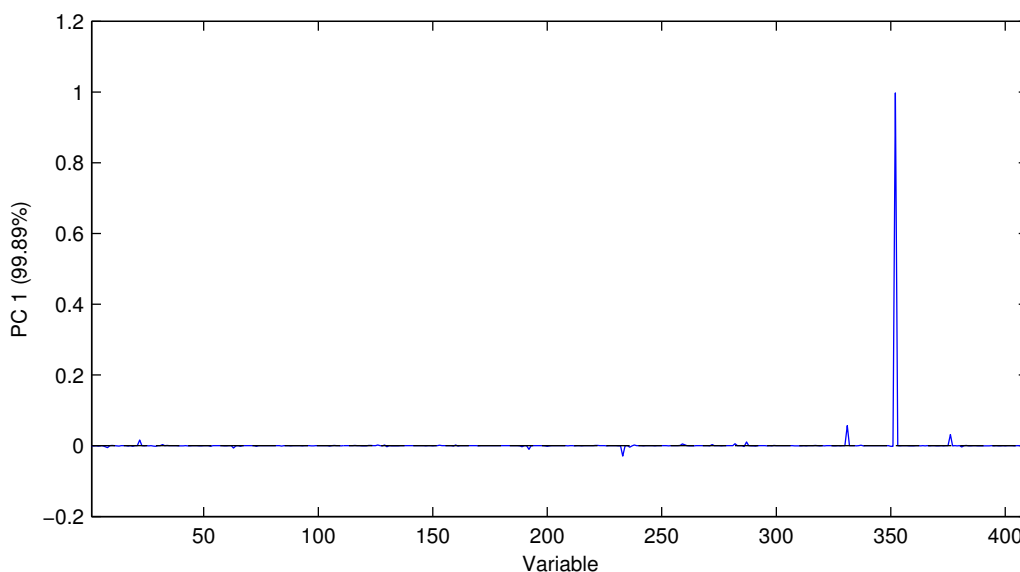


Figure 4.26: Loadings plot for PC1 of mean-centered data taken from the PCA analysis of the replicates of A<sub>210</sub>, AR1<sub>210</sub>, AR2<sub>210</sub>, B<sub>210</sub>, BR1<sub>210</sub> and BR2<sub>210</sub>.

For the multivariate analysis of the pyrolysis data two variable scaling methods were used, autoscaling and pareto scaling. When only mean-centering is applied to the data the original weight of each variable/peak is preserved, i.e. the major peaks have more influence on discrimination than the minor peaks. Although it may be of interest to reflect the importance of pyrolysis products owing to their intensity there were two reasons why scaling was advantageous or even necessary for the analysis of the pyrolysis data of pulps. Firstly, as peak areas of extracted ions were utilized instead of the peak areas of the TIC signal the actual contribution of each pyrolysis product to the pyrolysis fingerprints was biased. Each extracted ion reflects a varying proportion of the respective TIC peak. Secondly, in most measurements the levoglucosan peak deriving from cellulose was by far the most dominating peak in the pyrograms. In figure 4.25 the loadings of the 408 peaks for the first principal component (PC) of a PCA analysis is shown. The loadings

reflect the contribution of each peak to the variance of the reviewed PC and it can be seen that basically only one variable (levoglucosan) is explaining this variance obscuring any other meaningful variation.

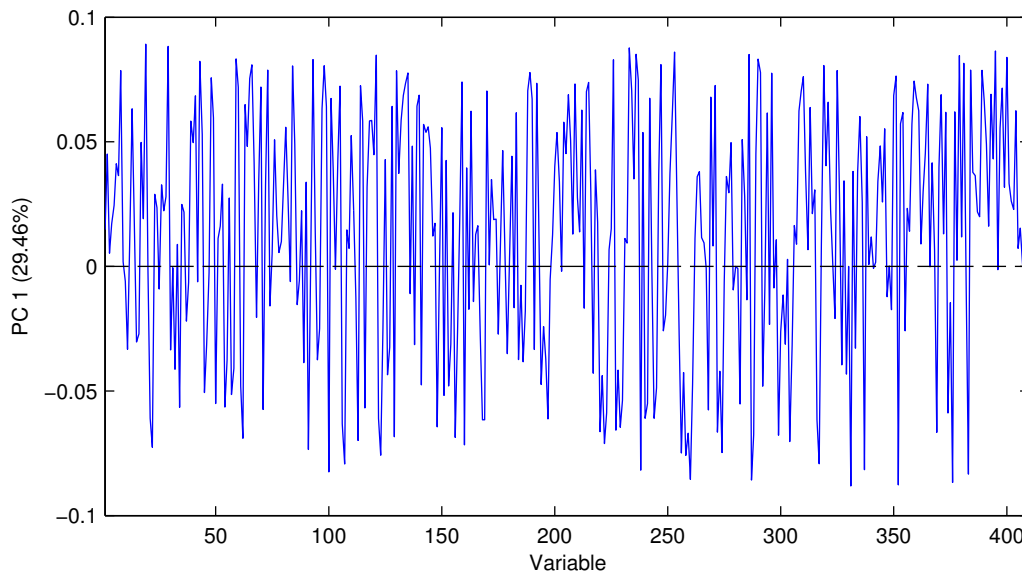


Figure 4.27: Loadings plot for PC1 of autoscaled data taken from the PCA analysis of the replicates of A<sub>210</sub>, AR1<sub>210</sub>, AR2<sub>210</sub>, B<sub>210</sub>, BR1<sub>210</sub> and BR2<sub>210</sub>.

Autoscaling is the most widely used scaling method applied. By autoscaling the columns of the data matrix are mean-centered and scaled to unit variance. As an effect all peaks/variables are put on an equal basis and affect the multivariate analysis by their variation regardless of their overall intensity. This allowed to emphasize meaningful variation of minor peaks which was of considerable importance to discriminate highly similar samples. Often the minor peaks may contain more information to explain differences. A negative effect of auto-scaling though is that also the noise in the data is enhanced resulting in more unexplained variance in the extracted PCs. In figure 4.26 the loadings plot of the auto-scaled data taken from the same PCA analysis as in figure 4.25. The influence of levoglucosan has been levelled.

Instead of using the columnwise standard deviation as for autoscaling the scaling factor for Pareto scaling is the square root of the standard deviation. This results in an intermediate between only mean-centered and autoscaled data giving some emphasis to the minor peaks but keeping up intensity differences between the peaks (see figure 4.27. This scaling method proved as

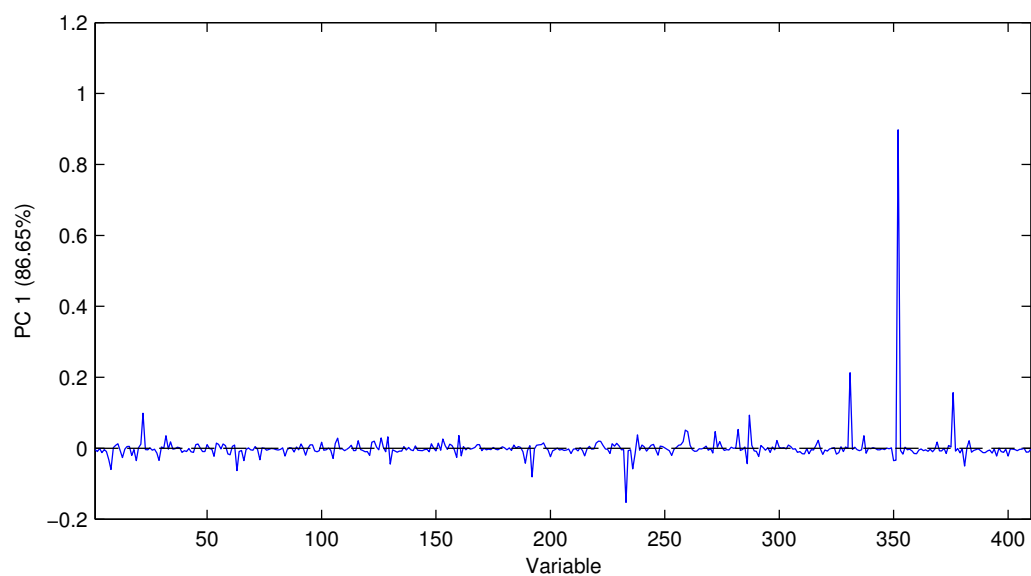


Figure 4.28: Loadings plot for PC1 of pareto scaled and mean-centered data taken from the PCA analysis of the replicates of  $A_{210}$ ,  $AR1_{210}$ ,  $AR2_{210}$ ,  $B_{210}$ ,  $BR1_{210}$  and  $BR2_{210}$ .

useful for the PCA analyses. Almost all PLS regressions worked best with autoscaling.

### 4.2.3 Exploratory data analysis

There are several common approaches for comparative or quantitative analysis of pyrolytic data. A direct comparison of peak areas of characteristic pyrolysis products may be applied, or the changes of peak area ratios between selected products within each pyrogram may be assessed. In the case of the pyrolysis data generated from the AS/AQ pulps of the delignification series the peak area changes are in many cases only subtle, hence, a straight forward comparison did not lead to any conclusion. With an increasing number of peaks being considered for evaluation these approaches may result in losing track of the data. PCA was considered by the author as a suitable tool to evaluate the pyrograms upon differences in composition.

In short terms the Principal Component Analysis transforms a set of measured variables into new *latent* variables which are called principal components. Mathematically, these principal components are a linear combination of the original variables and are determined by finding the direction of maximal variance of the original data.

#### 4.2.3.1 External interferences

Prior to analysis of structure features explaining differences between the pulp samples the data was analyzed for possible interferences biasing the results which may lead to misinterpretations. These interferences can e.g. caused by sample preparation, device fluctuations or artefacts. PCA is not only suitable for the elucidation of differences in sample properties but also to detect outliers or external interferences. Possible outliers were not searched for at this stage of analysis because too quickly measurements may be discarded although only a few peaks might be responsible for the abnormal behaviour in the multivariate analysis. This can be caused by poor automated integration and particularly when as many as 408 peaks are included with high numbers of minor peaks the chance increases. One obvious outlier was already removed prior to pre-processing by rapid visual inspection. It was considered as more appropriate to remove possible outliers in the analysis procedure before or after variable selection.

Since the sample B<sub>60</sub> was measured 17 times the sample was predestined to monitor two possible interferences. The first possible biasing influence was the milling procedure. Though all samples were milled in the same mode possible differences between different batches of the same sample being milled could be caused by differences in homogeneity. Sample B<sub>60</sub> was milled in two batches and were kept separate. The PCA analysis though did not show any perceivable difference between the two batches (results not shown here).

Hence biasing effects by milling were considered as negligible although only one sample may not be sufficient to draw this conclusion.

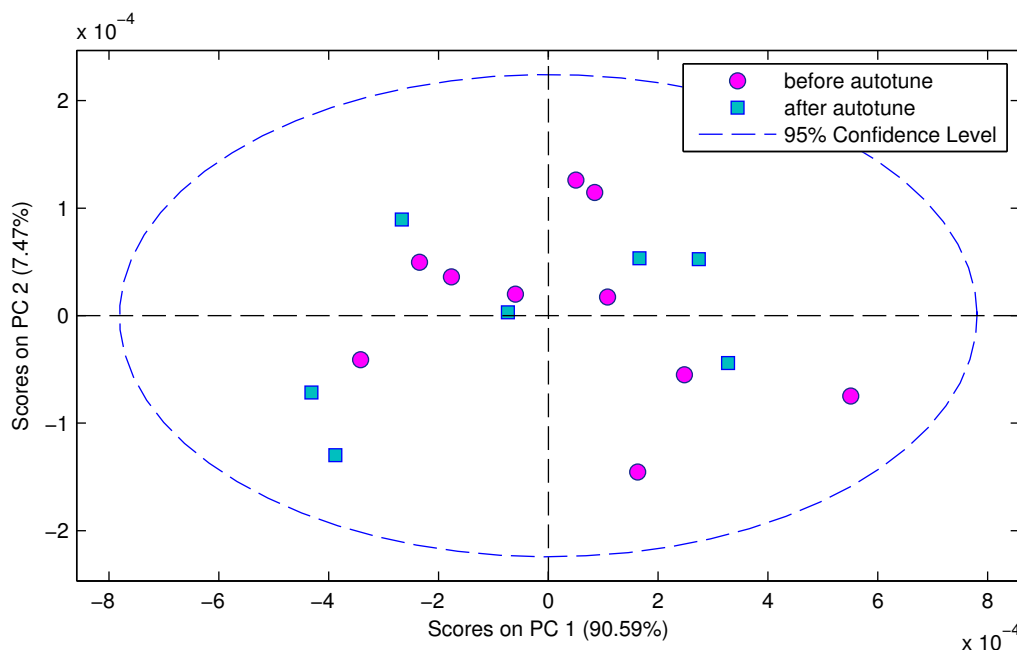


Figure 4.29: Score plot of PC1 versus PC2 of weight-background normalized and mean-centered pyrolysis data (408 peaks) of sample B<sub>60</sub>.

The second analyzed interference was the autotune performed in the middle of the measurement series which was discussed in detail in section 4.2.2.5. Although much effort has been put into minimizing the disturbance by the sensitivity leap caused by autotuning a remaining influence was feared. PCA was performed on the mean centred data (including 408 peaks) of the 17 replicates of sample B<sub>60</sub>. When the first 3 PCs were reviewed no clear discrimination between the measurements before and after autotuning was perceivable. The score plot of PC1 against PC2 displayed in figure 4.28 shows the measurements being evenly spread. PC 4 though showed finally a discrimination of the measurements before and after autotuning (not shown here).

But when PCA is performed on auto-scaled data already the score plot of PC2 against PC1 reveals the interfering effect of the autotune (figure 4.29). It can be clearly seen that the measurements are separated along PC2 which accounted for 11.34 % of the explained variance in the auto-scaled data. Hence the autotuning of the mass spectrometer caused a noticeable interfering effect

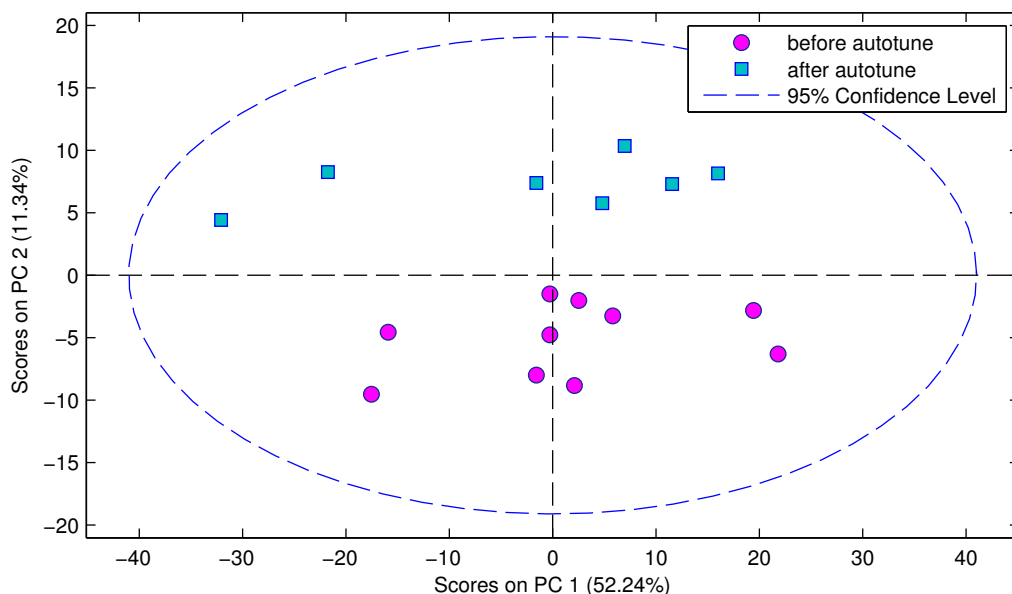


Figure 4.30: Score plot of PC1 versus PC2 of weight-background normalized and autoscaled pyrolysis data (408 peaks) of sample B<sub>60</sub>.

on the data. This was important to assess in order to explain unexpected discrimination between measurements. As the above results arose from the weight-background normalized data it was anticipated that the undesired discrimination was due to the normalization being insufficient to remove the sensitivity leap. But also PCA on the auto-scaled constant sum and selected-peaks normalized data showed similar discrimination. Rather than by the normalization the interference could most likely be explained by the high numbers of minor peaks which were included in the data set. More than  $2/3$  of the 408 included peaks were minor peaks, many of those close to the detection limit, and are more heavily influenced by sensitivity changes of the measuring device. When no scaling is applied the minor peaks have hardly any effect on the first few PCs of PCA models. But auto-scaling raises all peaks to equal importance and makes the influence of those peaks visible.

The scope of PCA was to assess differences between the samples, in particular between series A and series B samples. Hence it was interest if the effect of autotuning was still disturbing when two different samples were compared. For this purpose the two replicate sets of samples B<sub>60</sub> and B<sub>30</sub> were compared. The score plot of PC1 versus PC2 (figure 4.30) of the auto-scaled data shows an acceptable discrimination along PC1 between the two samples with the



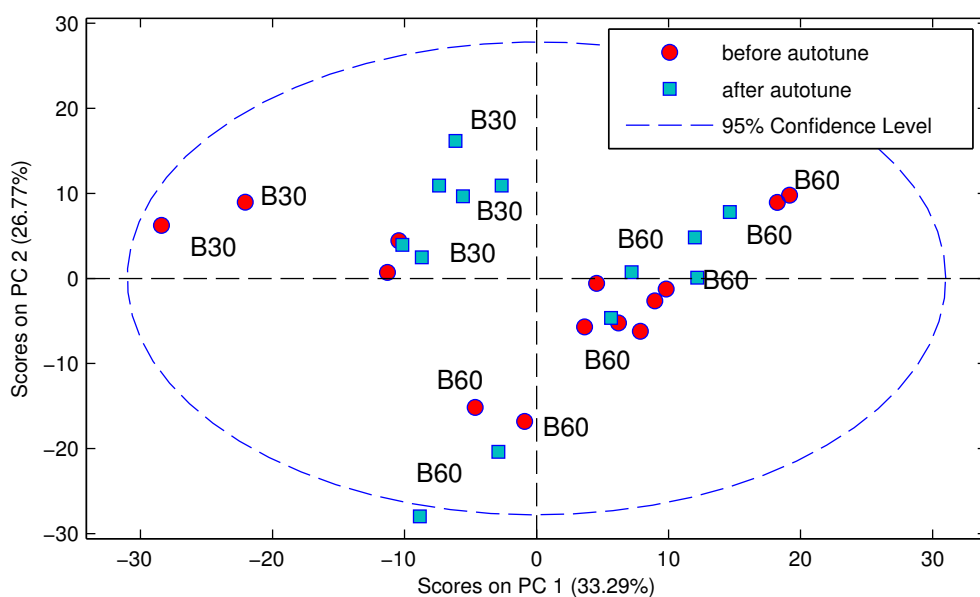


Figure 4.31: Score plot of PC1 versus PC2 of weight-background normalized and autoscaled pyrolysis data (408 peaks) of samples  $B_{30}$  and  $B_{60}$ .

$B_{60}$  replicates clustering on the right half and the  $B_{30}$  replicates on the left. The effect of autotuning is not clearly perceivable.

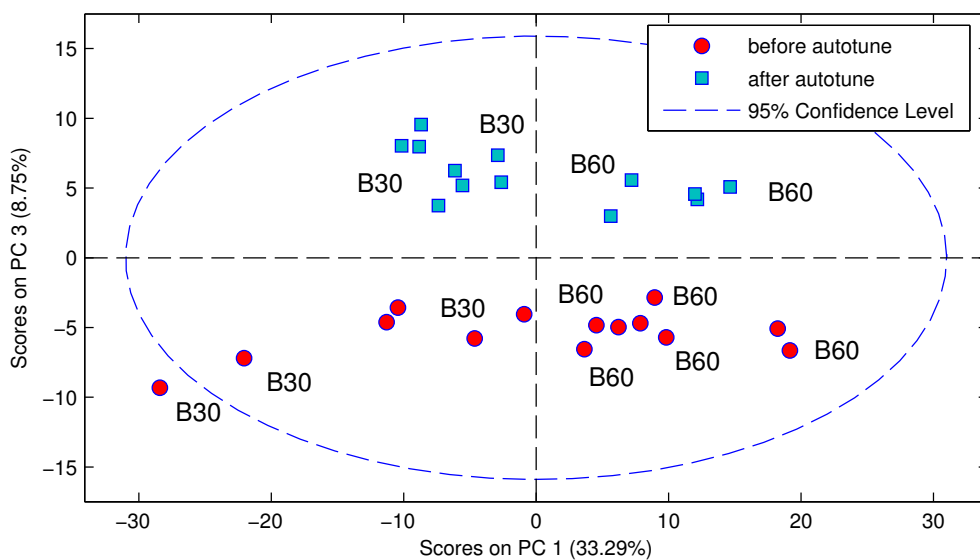


Figure 4.32: Score plot of PC1 versus PC3 of weight-background normalized and autoscaled pyrolysis data (408 peaks) of samples  $B_{30}$  and  $B_{60}$ .

## CHAPTER 4. DISCUSSION OF RESULTS

---

But when the score plot of PC1 versus PC3 is reviewed a discrimination of the measurements along PC3 due to autotuning is clearly observable. These described findings were of some importance for the course of data analysis. Apart from helping to explain inconsistencies in the data this interfering effect enforced the necessity to find strategies to still evaluate the data without discarding all minor peaks.

#### 4.2.3.2 Variable selection

Variable selection techniques are intended to aid in the reduction of the complexity of the data and in the identification of a subset of variables that show the best discriminative ability for exploratory MVA or are most suitable to achieve accurate regression models. Other than the procedure described in section 4.2.2.6 variable selection is best performed separately on each subset under study, e.g. when only the measurements of pulps from two cooking stages are compared. The intention is to reduce the number of variables/-peaks to be left only with relevant variables which explain the differences. As the thresholds or parameters of the variable selection procedures are flexible and arbitrarily set there is always the danger of removing too many variables which may have been of interest. Hence it is commonly applied several times with varying settings.

Various variable selection techniques based on mathematical methods have emerged in the past decades including genetic algorithms (GA), successive projections algorithm (SPA), interval PLS (iPLS) or ANOVA (with arbitrarily set thresholds) amongst many other techniques. These techniques are intended to perform an unbiased selection of significant variables irrespective of any prior knowledge about each variable, i.e. in case of pyrolysis data even unidentified components may be selected. In contrast hereto the manual variable selection, which has mostly been applied to pyrolysis data in studies of lignocellulosic material, is heavily biased as usually the well identified pyrolysis products are utilized for any exploratory or quantitative analysis. Obviously this approach has the major advantage that differences detected by any analysis can be interpreted much easier. But the risk of missing out possibly significant information contained in the ignored variables has to be taken into account. Often it may be useful to combine manual selection with a mathematical selection method.

If only two sample groups/classes are to be compared by PCA the application of Fisher's discriminant ratio (FDR) can be useful. This simple and straightforward selection technique is based, in analogy to ANOVA, on the calculation of the ratio of between-class scatter to within-class scatter of each variable separately irrespective of their absolute intensities. FDR is calculated by the equation:

$$FDR = \frac{(m_1 - m_2)^2}{s_1^2 + s_2^2} \quad (4.4)$$

with  $m_1$ , and  $m_2$  being the means of class 1 and class 2, and  $s_1^2$ , and  $s_2^2$  the respective variances.

The application of FDR for two-class discrimination was termed by Weiss and Indurkha (1998) *independent features* significance testing. It is suggested that variables are only retained if the significance value (FDR) is at least 2. When the significance threshold is increased the discrimination via PCA may be improved further but useful information might be lost.

A further variable selection method applied in the presented work was *interval PLS* which was primarily designed for PLS regressions applied to spectroscopic data (Norgaard *et al.* 2000). In spectroscopy (e.g. NIR) usually regions of highly collinear variables are present as the chemical information held in the measurements is expressed by several adjacent bands/scans. The iPLS algorithm is based on dividing the measurement profiles into several segments each containing a number adjacent variables. To find the relevant segments for modelling the dependent y-variables (i.e. externally determined sample properties) PLS models are calculated for each segment separately. The models are compared on the basis of the validation parameters RMSECV and RMSEP (root mean square error of cross-validation/prediction) and a selection of the most significant intervals is proposed for a previously specified validation setting.

However, the iPLS algorithm, implemented in the PLS Toolbox for MATLAB v. 7.02 (Eigenvector Research, Inc., Wenatchee, WA), may also be applied to chromatographic data with the intervals only consisting of one variable each. It can be performed in forward selection or backward elimination mode.

## CHAPTER 4. DISCUSSION OF RESULTS

### 4.2.3.3 Identification of pyrolysis products

Table 4.15: Extract of the 408 peaks found. Listed are the compounds relevant for the discussion of the results including extracted ions used for data evaluation. Fd = furan derivative, Xyl = xylose derivative, Glu = glucose derivative, H = H-lignin derivative, G = G-lignin derivative, Vs = variable selection, FDR = selected by Fisher's discriminant ratio, u = unknown structure of side chain.

ID	RT (min)	Compound	Ion m/z	marker	Vs
5	4.16	Sulfur dioxide	64		FDR
9	4.44	Methanol	32		FDR
101	18.01	4-Cyclopenten, 1,3-dione	42	Fd1	FDR
134	21.17	Unknown	73		FDR
149	21.83	Unknown (similar to 2-Hydroxy-benzaldehyde)	122	H-u	
163	22.80	Unknown phenol derivative	121	H-u	
165	23.04	Phenol	94	H	
169	23.63	Guaiacol	124	G	
176	24.48	2-Methylphenol	107	H-C	
177	24.50	Furoic acid methyl ester	39	Fd2	FDR
196	25.49	4-Methylphenol	107	H-C	
198	25.54	3-Methylphenol	107	H-C	
200	25.71	3-Methyl guaiacol	138	G-C	
201	25.73	Unknown lignin derivative	121	H-u	
202	25.78	Unknown furan derivative	98		FDR
210	26.31	Unknown lignin derivative	123	G-Cu	
213	26.55	Unknown	85		FDR
215	26.60	Unknown	43		FDR
216	26.60	4-Methyl guaiacol	123	G-C	
221	26.83	2,4-Dimethylphenol	122	H-C	
223	26.97	Unknown phenol derivative	121	H-u	
225	27.15	Unknown lignin derivative	152	G-C-Cu	
228	27.66	Unknown (similarities to 4-vinylphenol)	120	H-u	
229	27.80	Unknown	69		FDR
230	27.85	Unknown (similarities to 2,4-dimethylphenol)	107	H-u	
233	27.96	3- or 4-Ethylphenol	107	H-C-C	
236	28.38	3-Ethylguaiacol	152	G-C-C	
239	28.66	Unknown (similarities to 2,4-dimethylphenol)	107	H-u	
240	28.93	4-Ethylguaiacol	137	G-C-C	
245	29.14	Unknown	134	H-u	
256	29.89	Unknown lignin derivative	137	G-C-Cu	FDR
257	29.89	Unknown	39		FDR
267	30.44	Vinyl guaiacol	150	G-C=C	
277	31.08	Eugenol	164	G-C-C=C	
278	31.15	Unknown lignin derivative	137	G-C-Cu	
289	31.83	Unknown phenol derivative	107	H-u	
292	32.13	Unknown lignin derivative	164	G-u	
296	32.26	Unknown lignin derivative	164	G-u	
297	32.36	Unknown	111		FDR
299	32.50	Isoeugenol (cis)	164	G-C=C-C	
302	32.65	Unknown phenol derivative	77	H-u	FDR

... continued on the next page

## CHAPTER 4. DISCUSSION OF RESULTS

ID	RT (min)	Compound	Ion m/z	marker	Vs
303	32.70	Unknown phenol derivative	138	H-u	
306	33.16	Unknown phenol derivative	134	H-C=C-C	
314	33.70	1,5-Anhydro- $\beta$ -D-xylofuranose	29	Xyl	FDR
315	33.78	Isoeugenol (trans)	164	G-C=C-C	
318	33.90	Unknown	98		FDR
323	34.31	Unknown	72		FDR
325	34.39	Vanillin	151	G-C=O	FDR
327	34.71	Unknown phenol derivative	121	H-C	
328	34.72	1-(4-Hydroxy-3-methoxyphenyl)propyne	147	G-CC-C	
330	34.97	1-(4-Hydroxy-3-methoxyphenyl)allene ?	162	G-C=C=C	FDR
331	34.98	Unknown	110		FDR
334	35.05	Unknown	74		FDR
343	35.76	Homovanillin	122	G-C-C=O	FDR
346	36.13	Unknown	98		FDR
348	36.31	Acetoguaiacone	151	G-CO-C	
350	36.56	unknown lignin derivative	151	G-C-C-Cu	FDR
353	36.61	Unknown phenol derivative	121	H-C-C	
355	36.84	4-Hydroxy-benzaldehyde ?	122	H-C	
362	37.45	Guaiacyl acetone	137	G-C-CO-C	FDR
363	37.68	Homovanillyl alcohol	137	G-C-COH	
365	37.84	Unknown lignin derivative	149	G-C-C-Cu	FDR
370	38.20	Propioguaiacone	151	G-CO-C-C	
371	38.48	Unknown	121		FDR
372	38.49	Isomer of coniferyl alcohol ?	124	G-C-C-Cu	
373	38.51	Guaiacyl vinyl ketone	178	G-CO-C=C	
375	38.69	Unknown lignin derivative	151	G-C-C-Cu	FDR
387	39.39	1-[5-(2-Furanylmethyl)-2-furanyl]-ethanone	190	Fd3	FDR
388	39.49	Unknown	52	LCC*	FDR
390	39.85	Levogluconan	60	Glu1	FDR
391	39.87	3-Methoxy-2-naphthalenol	174		FDR
393	40.20	Dihydroconiferyl alcohol	137	G-C-C-COH	FDR
396	40.77	Unknown lignin derivative (phenyl coumaran)	150	G-u	FDR
401	41.11	Unknown lignin derivative (phenyl coumaran)	178	G-u	FDR
419	42.99	Coniferyl aldehyde	178	G-C=C-CO	
420	43.04	Homovanillic acid methyl ester	137	G-C-COOC	
421	42.96	Unknown saccharide derivative	29	Glu2	FDR
423	43.34	Unknown lignin derivative	136	G-u	
424	43.36	Unknown	126		FDR
428	44.94	Unknown	97		FDR
436	46.16	Unknown	85		FDR
440	49.43	Unknown lignin derivative	192	G-u	
445	53.32	Unknown lignin derivative	137	G-Gu	
452	55.30	Unknown lignin derivative	240	G-Gu	
456	57.52	Unknown lignin derivative	138	G-Gu	
460	62.49	4,4'-Dihydroxy-3,3'-dimethoxystilbene	272	G-C=C-G	

For peak identification the NIST02 MS library, literature sources (Ralph and Hatfield 1991) and an in-house library were utilized. It was not attempted to identify all 408 detected peaks. Even though the NIST libraries may contain a vast collection of identified compounds most attempts to identify some of the

## CHAPTER 4. DISCUSSION OF RESULTS

---

minor or even fairly prominent unknown peaks failed. This can be considered the downside of extracting and evaluating unknown peaks. Interpretation of results is hindered. The tentatively assumed H- and G-lignin peaks listed in table 4.2.3.3 were classified by the combinations of their major mass traces, with  $m/z$  107, 108, 121, 122 and 134 indicating towards H-lignin units and  $m/z$  124, 137, 138, 150, 151, 164, 178 and 180 indicating towards G-lignin units.

#### 4.2.3.4 Comparison of different pulping processes

Within the measurement series consisting of 160 measurements also pulp samples from three reference cooks were measured (only duplicates). Spruce was pulped to a target kappa number of approx. 30 by an ASAM, Kraft and acid Na-Sulfite process, respectively, and were meant to serve for comparison with the two cooks  $A_{330}$  and  $B_{270}$  both having also a kappa number around 30. Hence 5 cooks could be compared with respect to their lignin composition via PCA.

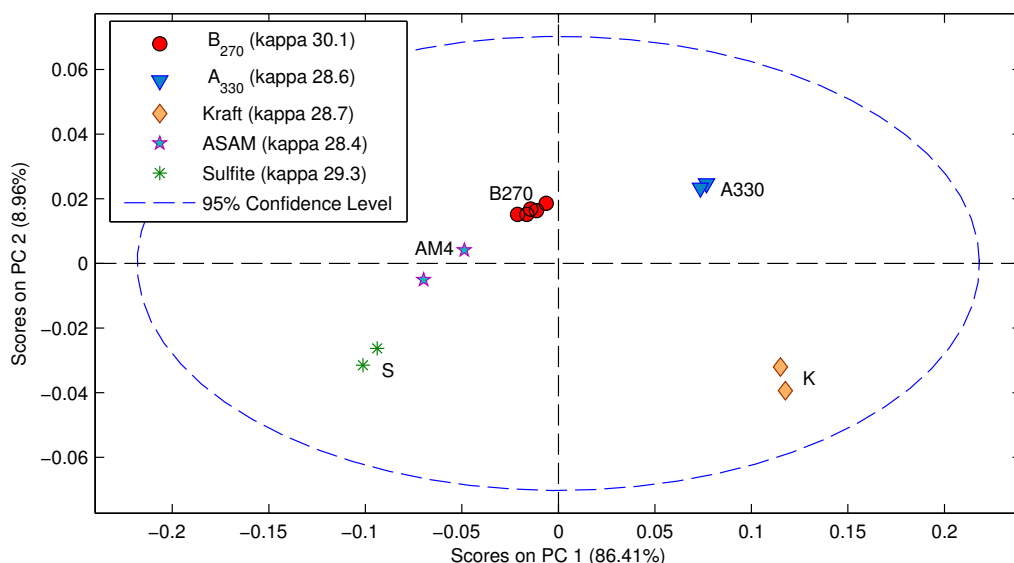


Figure 4.33: Score plot of the first two PCs for the complete pyrolysis data (408 peaks) of 5 pulp samples produced by kraft, acid sulfite, ASAM, AS/AQ and ASA process with similar kappa number. Peak areas were weight-background normalized and pareto-scaled.

When PCA was performed on all 408 pareto-scaled peak data a clear separation of the 5 cooks was possible. Foremost the score plot 4.32 of PC1 versus PC2 illustrates that the replicate measurements were sufficiently reproducible as the replicates (apart from the ASAM sample measurements) are clustered closely together. It can also be concluded that the samples from the acid sulfite and kraft process show the most pronounced differences as these two samples have the furthest distance to each other along PC1 (explaining 86.4 % of the total variance in the data). Additionally, the plot implies that the ASAM pulp has the highest compositional similarities to the acid sulfite pulp followed by the pulp  $B_{270}$  and the pulp  $A_{330}$  is closer asso-



ciated with the kraft pulp. Along PC2, explaining 9 % of the total variance, the 3 pulps from alkaline sulfite processes are separated from the sulfite and kraft sample. As the carbohydrate compositions of the three reference cooks could be expected to have pronounced differences but were not assessed a further elucidation of the differences with respect to all pyrolysis products was not followed. Instead only the lignin derived pyrolysis products were chosen for a closer analysis of the residual lignin composition which were manually selected according to the identification results listed in table 4.2.3.3.

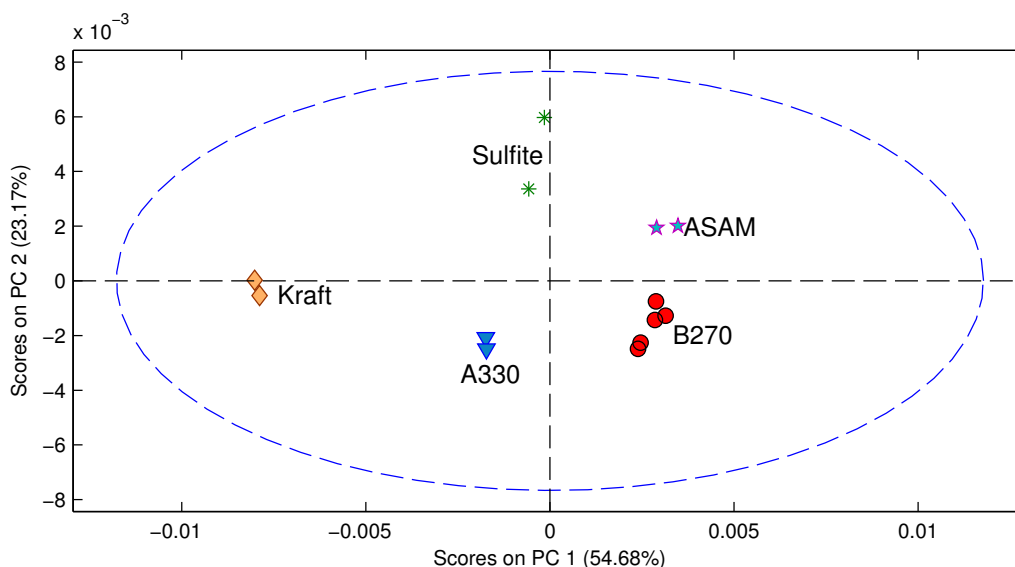


Figure 4.34: Score plot of the first two PCs for the pyrolysis data of G-lignin fragments (40 peaks) of 5 pulp samples produced by kraft, acid sulfite, ASAM, AS/AQ and ASA process with similar kappa number. Peak areas were weight-background normalized and pareto-scaled.

In most previous studies where lignin derived products were selected for multivariate analysis typically 12 - 14 major G-lignin products were utilized. Opposed hereto it was decided to include also the minor products which were tentatively identified as being derived from G-lignin. The score plot 4.33 of PC1 versus PC2 illustrates the discrimination of the 5 pulp samples utilizing the peak data of 40 G-lignin products. Again, the kraft sample can be assumed to have the least compositional resemblance with the other pulps, in this case solely with respect to the lignin composition, as the kraft sample shows the furthest distance to the other samples along PC1. Again the pulp A<sub>330</sub> seems to have the closest resemblance with the kraft pulp. Also the ASAM and B<sub>270</sub> pulp seem to have a relatively close resemblance of lignin

composition to each other and show the highest difference toward the kraft pulp sample.

The biplot 4.2.3.4 showing both the loadings (the weights of the peaks/variables) and the scores for PC1 and PC2 in parallel helps to visually explain the discrimination depicted in the score plot 4.33.

It can be seen that most loadings are clustered close to the center of the plot indicating that they have only little influence on the discrimination. Although it can be perceived that the clustering is mainly around the acid sulfite, ASAM and to some extent the B<sub>270</sub> pulp sample which are also located nearer to the center as compared to the kraft pulp sample. Performing the analysis on autoscaled data (not displayed here), resulting in similar overall weights of all variables, similar but more articulate clustering around the aforementioned samples could be noticed. This may indicate that these samples have an overall slightly higher lignin contents as compared to the kraft and A<sub>330</sub> pulp. When the kappa numbers of the pulps are reviewed (see legend in score plot 4.32) this may be a reasonable explanation. If the kappa factor for kraft pulp (approx. 0.15) is taken into account the actual difference in lignin contents between the ASAM and kraft pulp would increase assuming the kappa factor for ASAM pulps to be around 0.165. This is not reflected by the only marginal difference between the kappa numbers. But a further explanation could also be a significant difference in the contents of hexenuronic acids between the pulps which can be assumed to be highest in the kraft pulp.

Most interesting though are the pyrolysis products having significant influence on the discrimination of the 5 pulps. The loadings of the pyrolysis products located farthest away from the center indicate a high significance of those variables. In the upper right quarter homovanillin (G-C-C=O) and two unknown lignin derivatives (G-C-C-C<sub>u</sub>, G-C-CO-C) appear to be present in higher abundances in the acid sulfite and ASAM pulp in particular when compared to the kraft and A<sub>330</sub> pulp. The unknown lignin derivative denoted with G-u was a late eluting compound with the major ions m/z 192, 164, 135 and 107, which indicate that it is possibly a phenyl coumaran structure. The other unknown lignin derivative (G-C-C-C<sub>u</sub>) was tentatively considered to be a phenyl propane unit (m/z 151, 123, 108, 194).

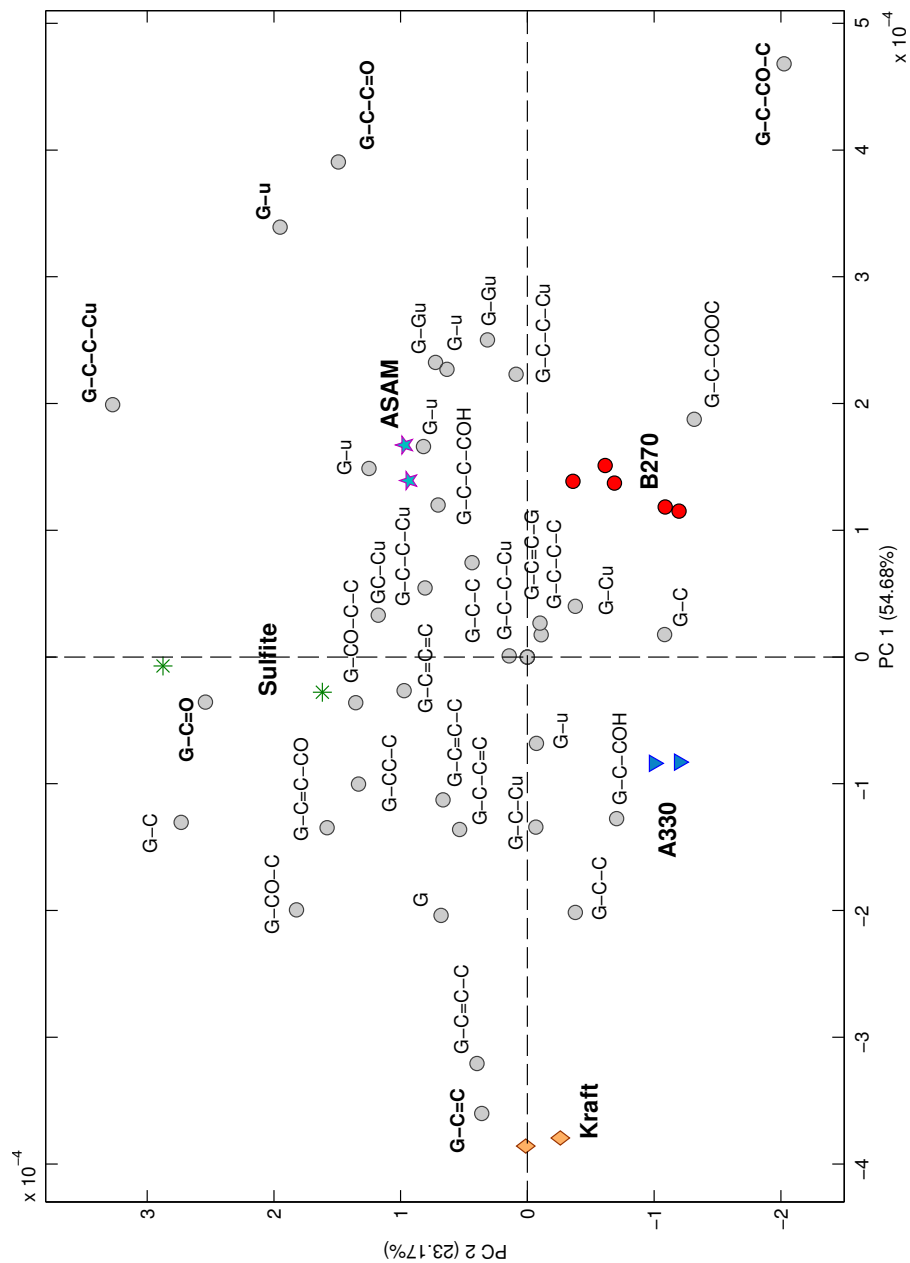
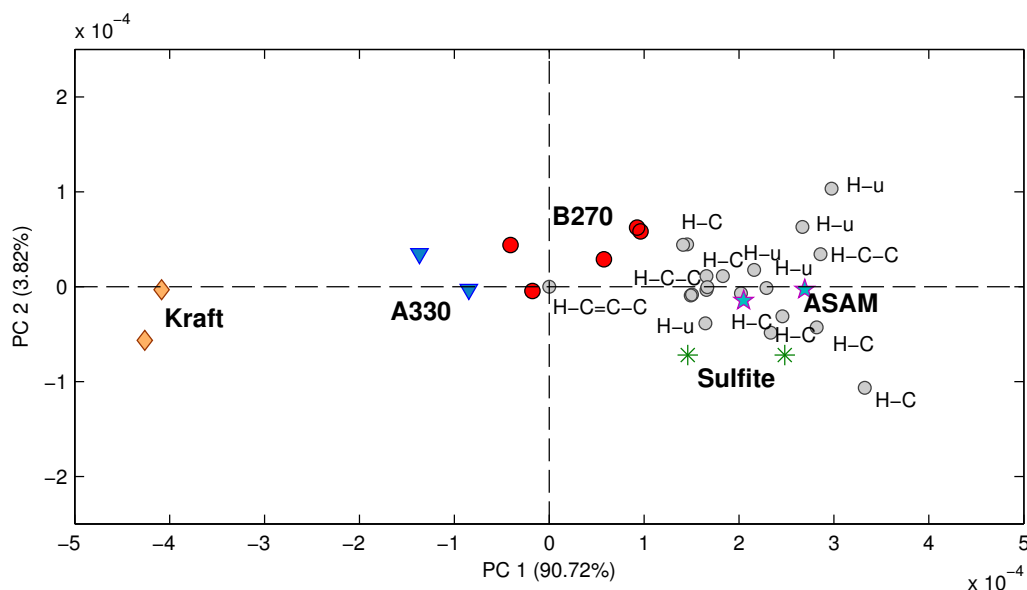


Figure 4.35: Biplot of PC1 versus PC2 for the pyrolysis data of G-lignin fragments (40 peaks) of 5 pulp samples produced by kraft, acid sulfite, ASAM, AS/AQ and ASA process with similar kappa number. Grey markers represent loadings of the variables/pyrolysis products. Assignment of loadings corresponds to assignment in table 4.2.3.3.

## CHAPTER 4. DISCUSSION OF RESULTS

On the other hand a high abundance of phenyl propane units may indicate a higher reactivity of the residual lignin. Overall most loadings of phenyl propane units are either located near the center or in the upper half of the plot so that a higher abundance of phenyl propanes in the acid sulfite and ASAM pulp can be assumed.



In addition to the G-lignin pyrolysis products also H-lignin units were examined. Although all products derived from H-lignin were expectedly of very low abundance it was wondered if they give any indication of differences in demethoxylation reactions or in the degree of lignin condensation occurring in the pulping processes. When the H-lignin fragments were evaluated together with the G-lignins on autoscaled data the H-lignin products only had negligible influence on discrimination.

As it is depicted in the biplot 4.34 basically all loadings of products possibly derived from H-lignin cluster close to the acid sulfite and particularly around the ASAM pulp. Knowing of the good bleachability of ASAM and acid sulfite pulps this observation is most likely not due to a higher amount of condensed or demethoxylated lignin in those pulps. It may rather be explained by an overall slightly higher lignin content in those pulps as already mentioned above. Another possible explanation could be that the residual lignin in ASAM and acid sulfite pulps is more accessible for pyrolytic reactions leading to less char formation. The char residues remaining in the sample cups were not determined and may vary in dependence of the sample composition.

However, the main objective was the comparison of the two AS/AQ delignification series so that the vague interpretations of the observations described above were not scrutinized any further. The results show that pulps with nearly similar lignin content including the two pulps from the delignification series can be well discriminated by PCA.

#### 4.2.3.5 Comparison of samples A<sub>210</sub> and B<sub>210</sub>

From the results presented in section 4.1.3 it was concluded that a more detailed comparison of the the two samples A<sub>210</sub> and B<sub>210</sub> could be helpful to explain the improved pulping when NaOH splitting is applied. Both samples appeared to be highly similar although the cooking conditions and the generated pulps prior to the cooking time of 210 min showed obvious differences. Also the pulps produced with longer cooking times of 270 and 330 min again showed more diverging properties. To be more specific, in comparison to series A the pulps of the last two stages of series B had a lower kappa number with almost similar pulp yield. The higher viscosities and brightnesses of the pulps of the B series were observed throughout the terminal stages including on the pulp B<sub>210</sub>. This was giving a hint towards structural differences between the pulps A<sub>210</sub> and B<sub>210</sub>. For this reason 4 further cooks were performed to verify the high similarity between the pulps A<sub>210</sub> and B<sub>210</sub>. With the aid of two replicate pulps for each of the two stages (210 min, A and B series) to be compared it was aimed to ensure more reliable results. The results of the standard tests are displayed in section 4.1.3 in table 4.7. For simplification of discussion in this subsection the two sets of samples/measurements from the cooking stage at 210 min will be referred to as series A and series B pulps.

For each of the 3 pulps A<sub>210</sub> duplicate and for the pulps R1A<sub>210</sub> and R2A<sub>210</sub> triplicate measurements, and for the pulps B<sub>210</sub>, R1B<sub>210</sub> and R2B<sub>210</sub> five replicate measurements each were conducted. PCA including all 408 peaks was performed to get a first impression. Regarding the first 3 PCs neither of the normalization and scaling techniques yielded a clear discrimination between the series A and series B pulps. The best separation was achieved when PC4 was taken into account. The scoreplot in figure 4.35 depicts a discrimination of the two pulps mainly along PC4. But additionally the series A pulps are separated into two groups by PC1. This separation was again due to the autotune and therefore an unwanted interference. Also a possible outlier could be detected (located on the confidence level border line). To enhance the discrimination between the pyrolysis data of the A and B series pulps appropriate subsets of pyrolysis products were selected.

Analogous to the approach in section 4.2.3.4 the 40 products derived from G-lignin were chosen to examine if differences in lignin composition could be detected. PCA analysis on the G-lignin subset revealed an outlier. Figure 4.36 shows the plot of the Q residuals (lack-of-fit statistic) versus Hotelling

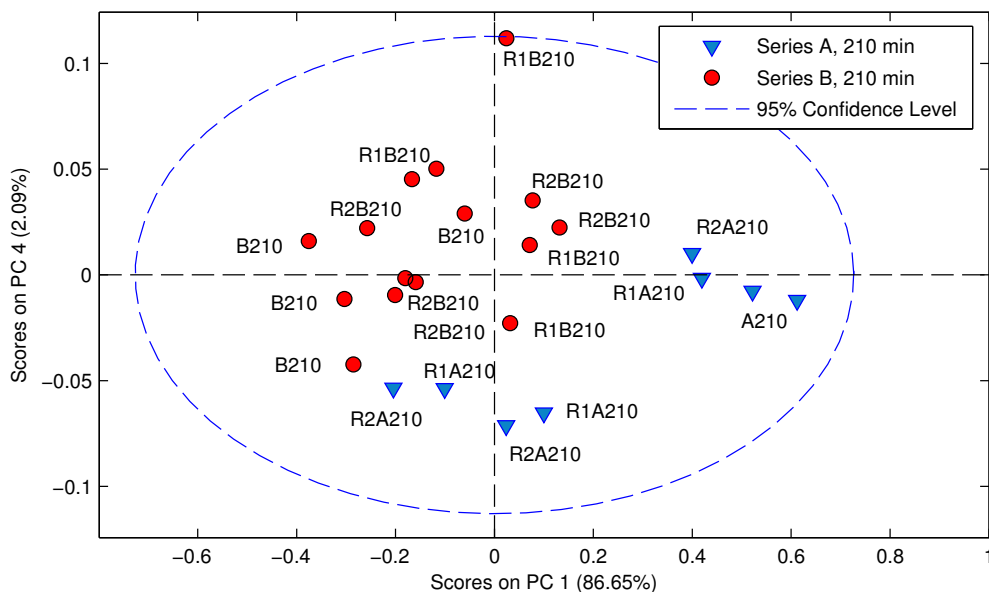


Figure 4.37: Score plot of PC1 versus PC4 for the complete pyrolysis data (408 peaks) of samples  $A_{210}$ ,  $R1A_{210}$ ,  $R2A_{210}$ ,  $B_{210}$ ,  $R1B_{210}$  and  $R2B_{210}$ . Peak areas were selected-peaks normalized and pareto-scaled.

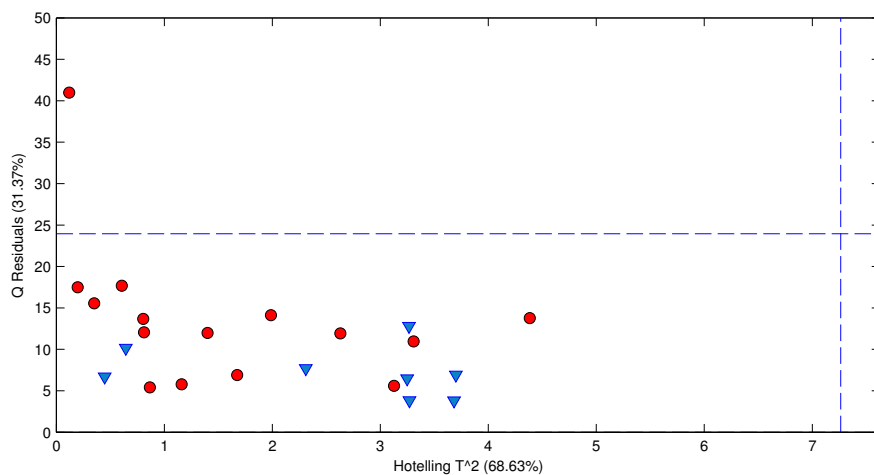


Figure 4.38: Plot of the Q residuals versus Hotelling  $T^2$  revealing outlier

$T^2$  (measure of variation in each measurement within the model) for the measurements. The blue dotted line borders the 95% confidence level. Measurements beyond the confidence level are likely outliers. The outlier depicted in the plot corresponds with the measurement presumed as an outlier in the previous PCA analysis (figure 4.35).





The biplot in figure 4.2.3.5 shows the separation of the samples of the two series achieved utilizing the 40 G-lignin derived products and loadings of the py-products. It can be perceived that the discrimination with respect to PC1 is not clear. 4 measurements of the series B samples are grouped on the left side of the plot together with the series A samples. All these 4 measurements were from the B<sub>210</sub> pulp. Though, if PC2 is taken into account these 4 B<sub>210</sub> measurements are somewhat separated along PC2 from the A series samples. A second obvious observation is that all loadings are located on the right half of the plot. This may imply that the series B samples have an overall higher lignin content and it is believed that it partly affects the discrimination. The sample B<sub>210</sub> had actually the lowest lignin content of the 3 series B pulps. However, reviewing the kappa numbers displayed in table 4.7 this can not be verified as the main reason for the discrimination. Even when a correction by the hexA content is considered lowering the kappa numbers of the series B samples by approx. 2 and of the series A samples accordingly by approx. 3 the samples R1A<sub>210</sub>, R1B<sub>210</sub> and R2B<sub>210</sub> have comparable lignin contents. Consequently, these 3 samples would be expected to cluster together. It is rather assumed that the discrimination depicted in the biplot 4.2.3.5 reflects an overall higher accessibility or lower degree of condensation of the lignin resulting in overall more monomeric lignin pyrolysis products amenable to gas chromatographic separation. It may further imply that the residual lignin in the B series pulps is better accessible for continuous degradation. This is supported by the previously discussed observation that the measurements of acid sulfite, ASAM and B<sub>270</sub> pulps yielded lignin fragments with slightly higher intensities. Both, acid sulfite and ASAM pulps are known to show better bleachability as compared to kraft pulps (see figure 4.2.3.4 and 4.34 in section 4.2.3.4). Yet, the most striking influence on the discrimination between the pulps of the two series is apparently caused by the loadings of two lignin derived products, guaiacyl acetone (G-C-CO-C) and homovanillin (G-C-C=O), located furthest right in the lower right quarter. Hence, a significantly higher abundance of these components in the pyrolysis data of the B series pulps could be concluded. Guaiacyl acetone may be taken as an indicator of an overall higher abundance of phenyl propane units in the B series pulps hinting towards a less extensive degradation of the propane side chains of the lignin monomers and a higher reactivity of the residual lignin. A possible explanation for the higher abundance of homovanillin in measurements of the B series pulps will be discussed on the biplot 4.2.3.5.

Instead of manual selection of variables like the G-lignin fragments it was wondered if an unbiased selection of the most discriminative variables would

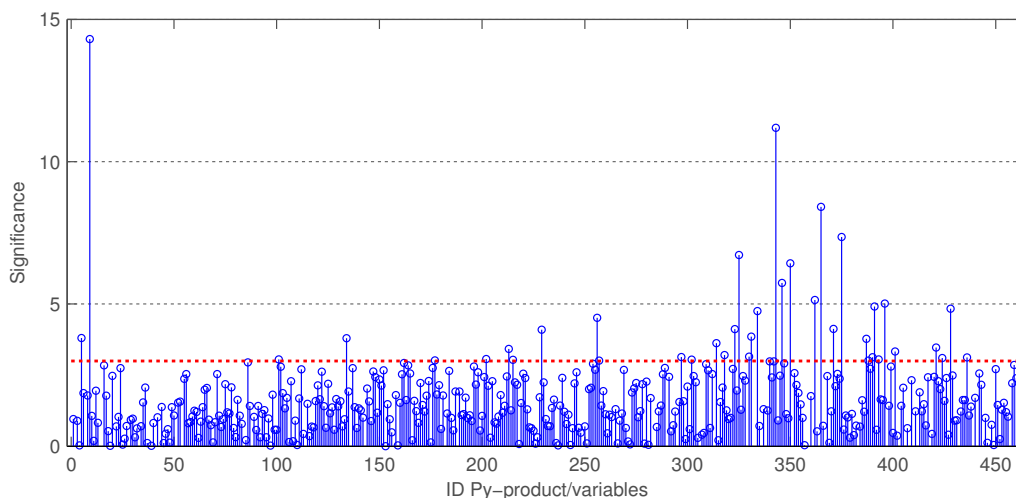


Figure 4.40: Visual presentation of results obtained from FDR peak selection with a the significance threshold of 3 (marked by horizontal red line).

lead to an improved discrimination, to the same conclusions and would possibly provide further details. For this purpose Fisher's discriminant ratio was employed on the 408 variables to select the pyrolysis products showing a significance above a given threshold. When the significance threshold was set to 2, 135 peaks were selected. To further reduce the amount of variables the threshold was increased to 3 resulting in the selection of 38 peaks. In figure 4.37 the results obtained from the significance level (marked by horizontal red line) set to 3 is visualized. All variables above the threshold line were selected regardless of the absolute intensity of each peak. Consequently major and minor peaks were treated equally. The reduction to a small subset of variables was expected to enhance the discrimination of the two sample sets. In order to highlight also the minor peaks selected by FDR PCA was conducted on autoscaled data.

It has to be emphasized here that out of the 38 selected peaks 17 were minor products with unknown identity. It is believed that most of these unknown products are never considered in any study on pyrolysis of lignocellulosic biomass. Though these 17 unknown products showed, according to the FDR selection, significant differences between series A and B measurements some may still turn out to be false positives. The pyrolysis products selected by FDR are listed in table 4.2.3.3.

When the resultant score plot of PC1 versus PC2 (figure 4.38) is reviewed it can instantly be observed that the variable selection with the aid of Fisher's discriminant ratio greatly improved the discrimination between the two sam-

ple sets along PC1. Along PC2 no obvious separation is visible which was not expected in any event as the FDR approach was applied to find the most discriminative variables for two classes. Consequently the improvement of discrimination is primarily along the most important principal component PC1. Though keeping in mind that autoscaling may also enhance noise or any interferences the trend along PC2 seems actually to be due to two effects which counteract to some extent. These two effects are the slight differences in lignin content between the replicate pulps and again the previously discussed autotune (section 4.2.3.1).

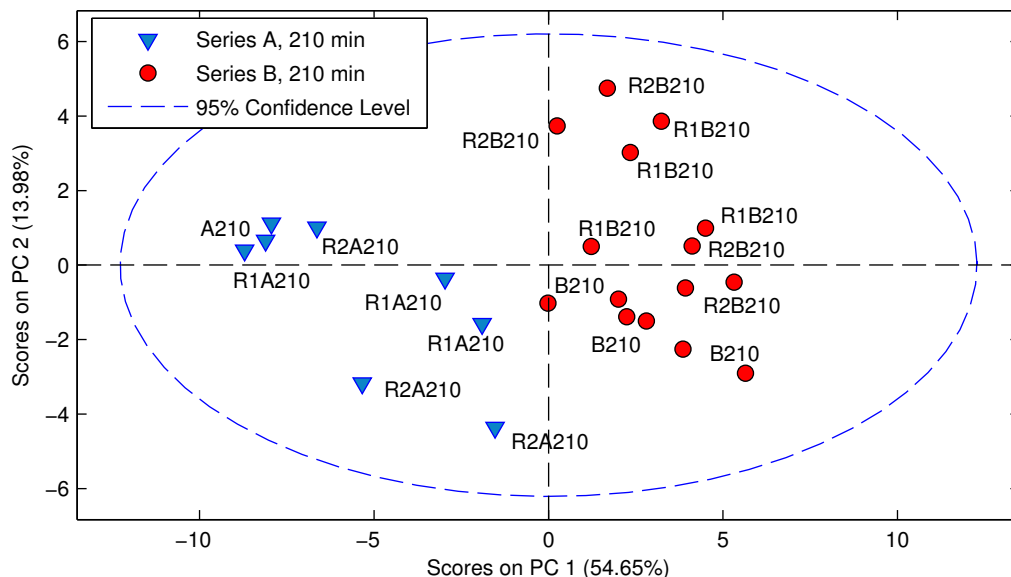


Figure 4.41: Score plot of PC1 versus PC2 for the pyrolysis data of 38 selected peaks of samples A<sub>210</sub>, R1A<sub>210</sub>, R2A<sub>210</sub>, B<sub>210</sub>, R1B<sub>210</sub> and R2B<sub>210</sub>. Peak areas were weight-background normalized and autoscaled.

The corresponding biplot in figure 4.2.3.5 confirms previous observations discussed on the PCA analysis of the G-lignin derived products but also reveals new details about the differences between the series A and B pulps. It has to be noted again that the autoscaling affects the loadings of the variables in such a way that all peaks are of similar importance for discrimination irrespective of the peak size. This explains why most loadings in the plot are located on an imaginary circle around the center. The unimportant variables which would have been located closer to the center have been removed by FDR selection.

The biplot reveals several aspects. Because of all loadings of lignin derived products being located in the upper right quarter it is believed that PC2 describes the overall differences in lignin content between the samples with the lignin content increasing in the direction from bottom to top. The external interference by the autotune obscurs this trend to some extent but it is still visible. PC1 rather describes the structural differences between the two sample sets. The assumption that the residual lignin of the series B pulps may be more reactive because of an overall lower degree of degradation of the propane side chain is impressively underlined by 6 phenylpropane derivatives. Guaiacyl acetone (G-C-CO-C), dihydroconiferyl alcohol (G-C-C-COH), 1-(4-Hydroxy-3-methoxyphenyl)allene (G-C=C=C) and three tentatively assumed C<sub>9</sub> units (G-C-C-C<sub>u</sub>) show significantly higher intensities in the measurements of the B series pulps.

Further products which shall be highlighted are methanol, sulfur dioxide and homovanillin (already highlighted in the biplot in figure 4.2.3.5). They are also positively correlated with the B series measurements and their loadings are located in the upper right quarter. Sulfur dioxide is the major product derived from the sulfonic acid groups and when table 4.7 is reviewed it can be verified that the highest degree of sulfonation out of the compared samples is found in the R1B<sub>210</sub> and R2B<sub>210</sub> pulps. Methanol is a very unspecific pyrolysis product with various possible origins. It was proposed by Shen *et al.* (2010) that methanol may derive from an elimination reaction of 4-O-methylglucuronic acids. But methanol may also evolve from the demethoxylation of the guaiacyl moieties or from the cleavage of the  $\gamma$ -carbon on the propane side chains (Evans *et al.* 1986, Kleen and Gellerstedt 1995). Loadings located close to each other can be assumed to be highly inter-correlated. The close neighbourhood to the loading of homovanillin may suggest that methanol and homovanillin are derived from the pyrolytic cleavage of a G-unit with a hydroxypropane side chain. Thus homovanillin may be a further indicator of higher abundance of phenylpropane units in the B series pulps.

Three assignable products correlating positively with the A series pulps were 1,5-Anhydro- $\beta$ -D-xylofuranose (Xyl), a main pyrolysis product derived from xylan, and two products associated with cellulose, levoglucosan (Glu1) and an unknown anhydrosugar (Glu2). From the results of the carbohydrate analyses displayed in table 4.7 of section 4.1.3 neither a significantly higher amount of xylose nor of glucose in the A series pulps can be assumed. Unfortunately analysis results for the pulp A<sub>210</sub> are missing making the analysis results even less meaningful.

When the plot in figure 4.19 in section 4.2.2.5 is recalled where the total peak areas (area sum, TIC signal) are plotted against cooking time it can be noticed that the total peak areas of the measurements of sample A<sub>210</sub> were significantly higher than those of sample B<sub>210</sub>. The two aforementioned cellulose markers (Glu1 and Glu2) are major peaks in pulp measurements and were actually mainly responsible for this difference in total peak area. Hence it is believed that a reason other than the divergence of cellulose content between the two sample sets was responsible for the intensity difference. A hypothesis is that a lower DP of cellulose may result in more monomeric glucose derived products upon pyrolysis and less char residues originating from cellulose. The lower viscosities of the A series pulps supports this hypothesis. The same may hold true for the xylan.

Another pyrolysis product that is worth to be mentioned here is an unknown product with the main fragments  $m/z$  68, 192, 109 and 39. It is believed that it is possibly derived from lignin-carbohydrate-complexes (LCCs) only formed during sulfite pulping. In fact, also 3 other products with closely similar mass spectra, whereof one is depicted in figure 4.13, B1 (section 4.2.2.2), were found only in sulfite pulps. Neither the pyrolysis of the kraft pulp nor the native wood sample yielded these 4 products. The suggestion that it might be derived from LCCs is only made on the basis of the fragment pattern of the mass spectra. It contains mass traces typical for lignin and furan derivatives. Whether sulfur is contained in the product could not be verified. One of these products (LCC\*) showed a significant difference in peak intensity between the two sample sets.

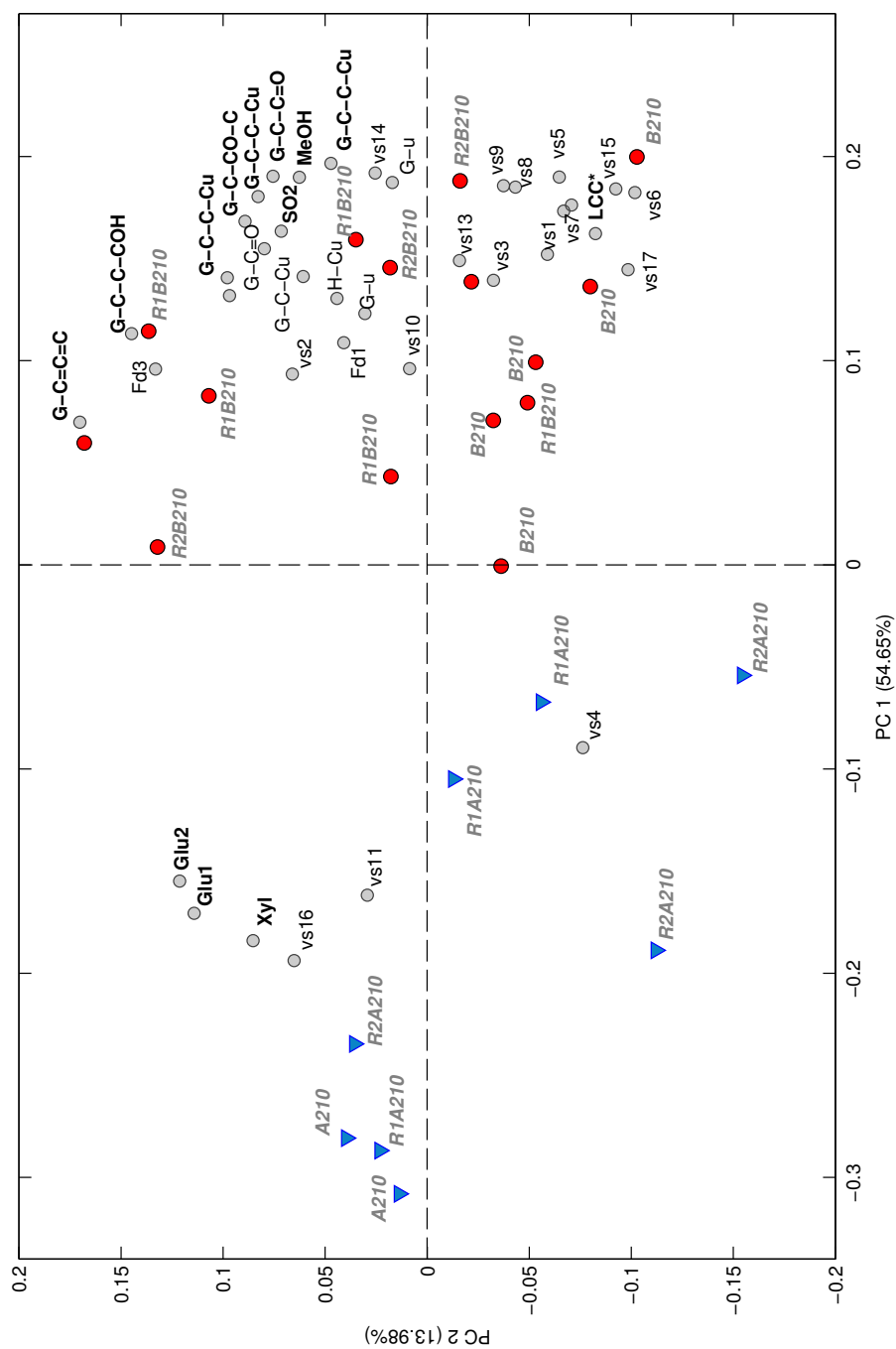


Figure 4.42: Biplot of PC1 versus PC2 for the pyrolysis data of the 38 selected peaks (by FDR) of samples A<sub>210</sub>, R1A<sub>210</sub>, R2A<sub>210</sub>, B<sub>210</sub>, R1B<sub>210</sub> and R2B<sub>210</sub>. Grey markers represent loadings of the variables/pyrolysis products. Assignment of loadings corresponds to assignment in table 4.2.3.3.

### 4.2.3.6 Comparison of the two delignification series

Another approach to evaluate the pyrolysis data was to plot the peak areas of the marker ions of single pyrolysis products against the cooking time or against the lignin content. To verify the results received by the PCA analysis it was considered as most reasonable to normalize the peak areas of the lignin fragments under study by the total lignin content at each stage of delignification. Hereby the ratio of the lignin fragment to the overall lignin content is reflected. These ratios then may be plotted against the lignin content. The vertical dotted line in all following plots against lignin content marks the cooking stage after 210 min.

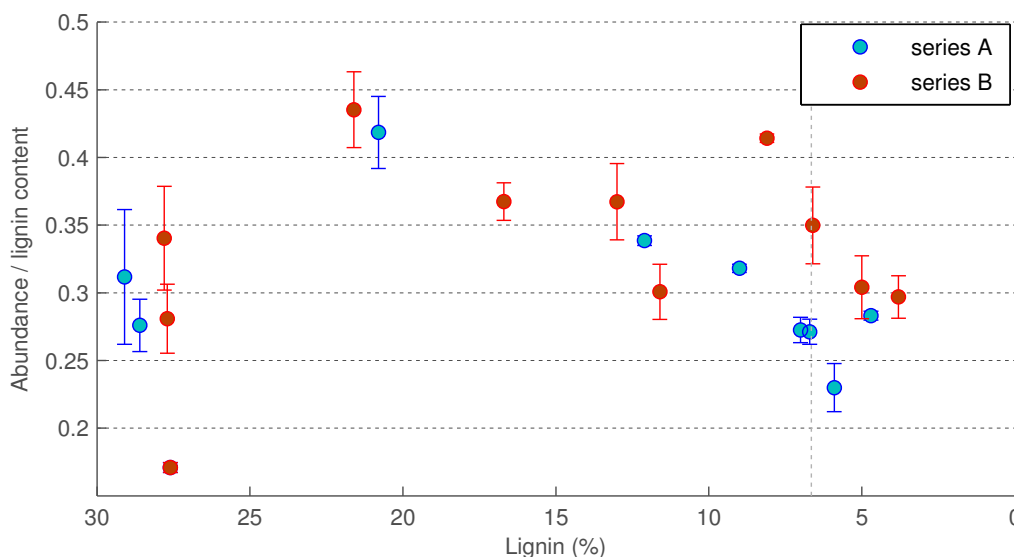


Figure 4.43: Peak areas of guaiacyl acetone marker ion  $m/z$  137, normalized by the lignin content, plotted against the lignin content

According to the PCA results the series B pulps contained higher proportions of the phenyl propane unit guaiacyl acetone. The plot in figure 4.39 verifies the observation. In all 4 last cooking stages, which were after the second addition of NaOH, the proportion of guaiacyl acetone in the residual lignin of the series B pulps was significantly higher. In the earlier stages of delignification, though, no clear difference can be noticed. It can be assumed that guaiacyl acetone is not an indicator for lignin moieties involved in  $\beta$ -O-4 structures. Such an indicator would have been expected to show a steady decline in the course of delignification.

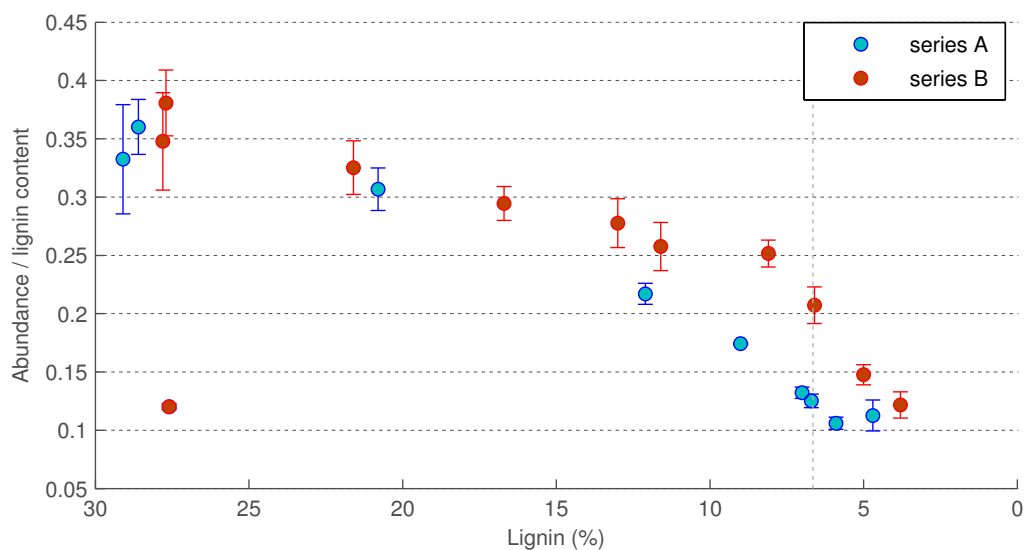


Figure 4.44: Peak areas of homovanillin marker ion  $m/z$  164, normalized by the lignin content and plotted against the lignin content.

The  $\beta$ -O-4 linkages are the primarily attacked lignin structures and are degraded steadily in the course of delignification. In contrast, homovanillin may be derived from lignin moieties involved in  $\beta$ -O-4 structures. Accordingly, in figure 4.40 a steady decline of the homovanillin fraction can be noticed.

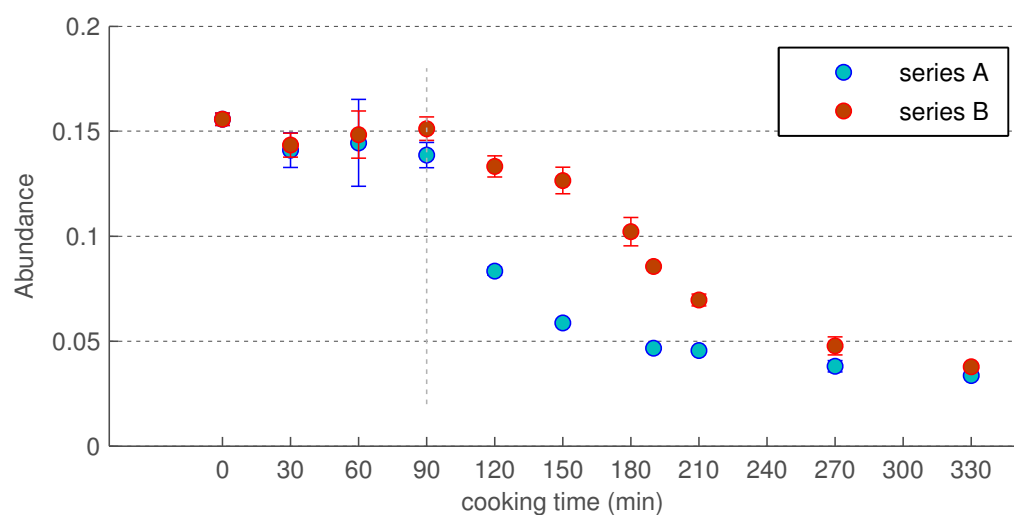


Figure 4.45: Peak areas of methanol marker ion  $m/z$  32 plotted against cooking time.



In section 4.2.3.5 it was contemplated that homovanillin may derive from phenyl propane units under pyrolytic cleavage of the  $\gamma$ -carbon releasing methanol. Although methanol may derive from several sources within lignocellulosic biomass figure 4.41 suggests that lignin is the main source of methanol detected. When the peak areas of the marker ion ( $m/z$  32) are plotted against the cooking time the decreasing trends of the abundance of methanol match considerably well to the trends of delignification for both series, depicted in figure 4.4 in section 4.1.3. It can be noticed that the abundances for series B are throughout higher in comparison to the corresponding series A stage, even at the last cooking stages. It is believed that methanol is a very good indicator for phenyl propane units present in lignin. Extensive demethoxylation reactions are not expected to have occurred, particularly not under the fairly mild cooking conditions in the first stages of series B. Here the methanol abundances were highest which indicates that pyrolytic cleavages of the  $\gamma$ -carbon of propane side chains are the primary source of methanol.

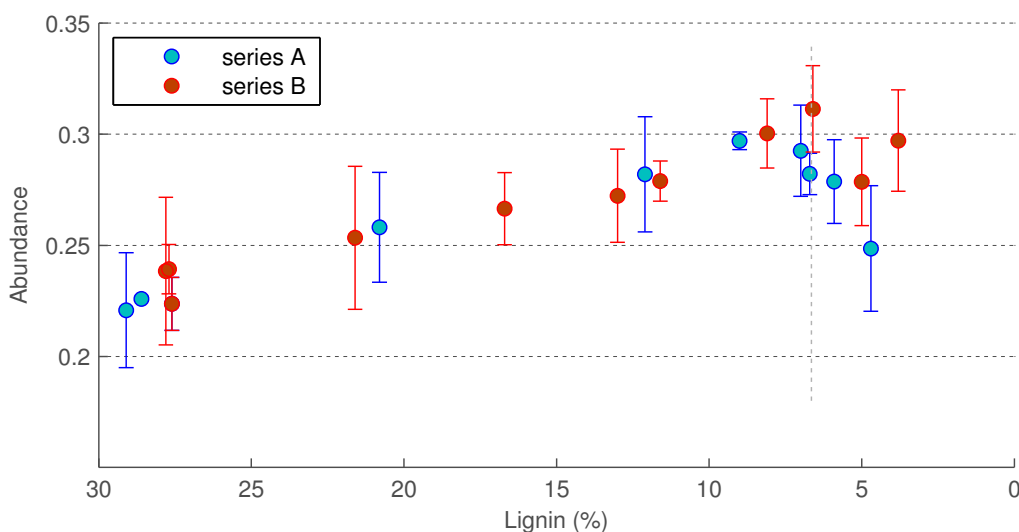


Figure 4.46: Peak areas of 3-hydroxybenzaldehyde marker ion  $m/z$  121 plotted against lignin content.

In softwoods only low proportions (3 - 5 %) of p-hydroxyphenyl (H) lignin units are found. Compared to S- and G-lignin units these are known to show a higher degree of condensation and to be more resistant towards degradation. Because of the overall low abundance of these moieties they have been hardly considered in pulping studies on wood. In particular when Py-

GC/MS is employed for analysis care may have to be taken to choose phenol, methylphenols or dimethylphenols as markers for H-lignin, even though they are usually the most abundant H-lignin components found in pyrolysis data of pulps. It has been reported that these phenolic components may also derive from carbohydrates (Moldoveanu 1998). In figure 4.42 the extracted ion for 3-hydroxybenzaldehyde is plotted against the lignin content. It can be observed that the abundance stayed more or less constant in the course of the cooking series, only a slight increase is noticeable. If the product was derived from polysaccharides it would be expected to increase towards the end of the delignification.

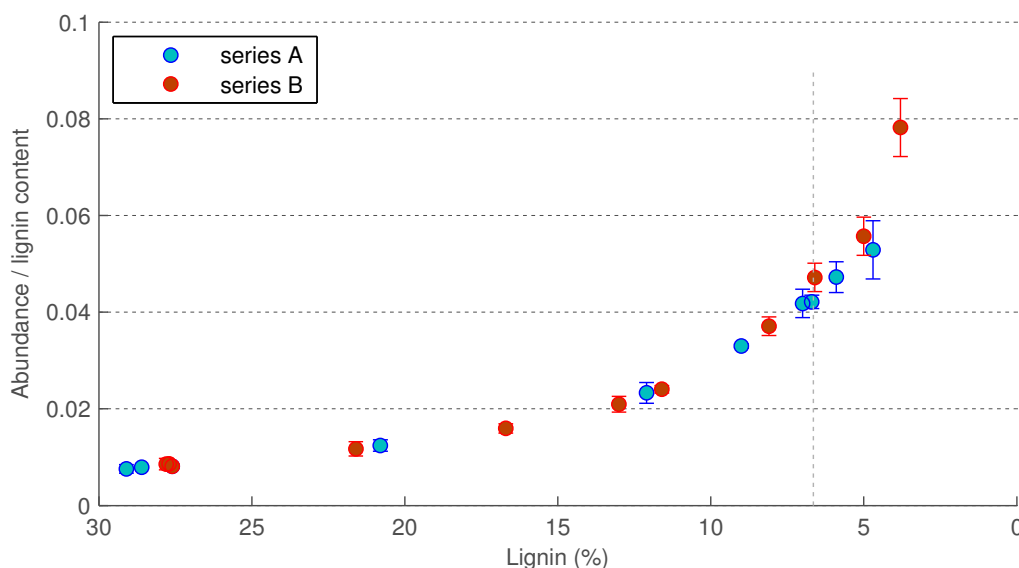


Figure 4.47: Peak areas of 3-hydroxybenzaldehyde marker ion  $m/z$  121, normalized by the lignin content and plotted against lignin content.

When the ratio of 3-hydroxybenzaldehyde to overall lignin content is reviewed a more or less exponential increase of the H-lignin fraction becomes apparent (figure 4.43). Several H-lignin monomers, including 4-hydroxybenzaldehyde and phenol, showed a similar trend. For some H-lignin monomers, however, the trend was less pronounced. One example depicted in figure 4.44.

It could not clearly be verified whether the phenolic compounds, tentatively assumed as H-lignin markers, were derived from lignin or polysaccharides. But the low correlation of these compounds with well identified products

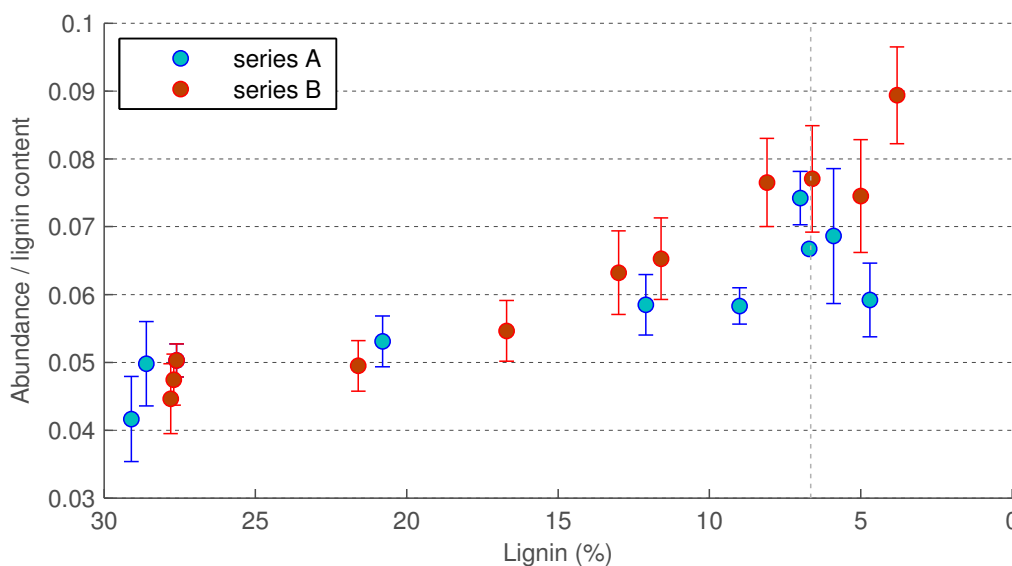


Figure 4.48: Peak areas of 4-methylphenol marker ion  $m/z$  107, normalized by the lignin content and plotted against lignin content.

derived from polysaccharides supports the assumption that these products originate from lignin.

In figure 4.45 the trend of the overall most prominent pyrolysis product is illustrated. It was discussed before (4.2.3.5) that samples with similar cellulose content may show considerable differences in the abundance of levoglucosan. From the plot it can be concluded that these differences are rather due to structural or compositional differences between the samples than to random scatter of the abundance. Only the replicates of one sample of series A showed a considerably low reproducibility of the levoglucosan (depicted by the large errorbar).

Some further details of interest could be derived from the pyrolysis data. As already discussed in section 4.1.3 the rapid decline of the pH in the cooks of series B was attributed to the almost exhaustive cleavage of the acetyl groups of the glucomannans. Figure 4.46 illustrates that Py-GC/MS is well suited to monitor the fate of the acetyl groups. Already after the first cooking stage only approx. 15 % of the initial abundance of acetic acid could be found. All subsequent stages showed a fairly constant level of acetic acid. It can be noticed that in the first 5 cooking stages the abundances for series B

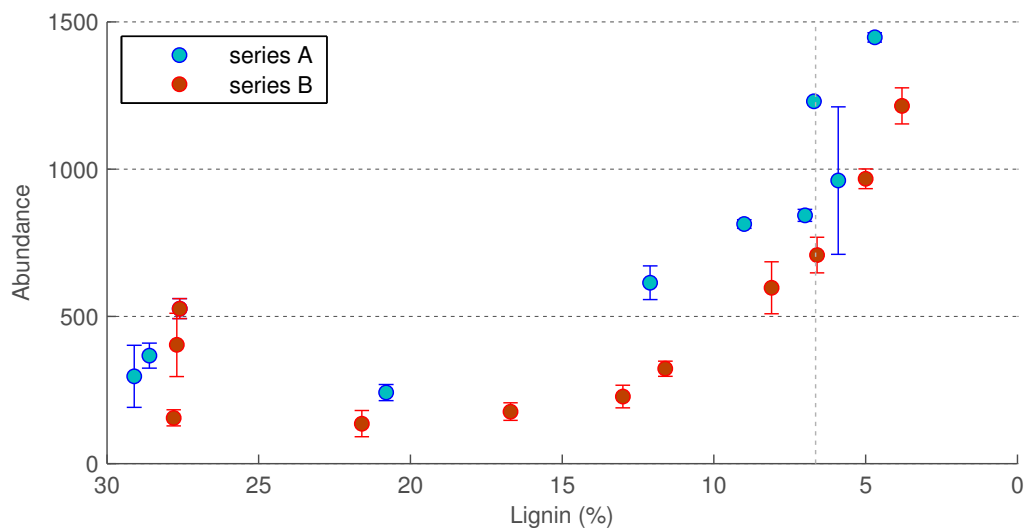


Figure 4.49: Peak areas of levoglucosan marker ion  $m/z$  60 plotted against lignin content

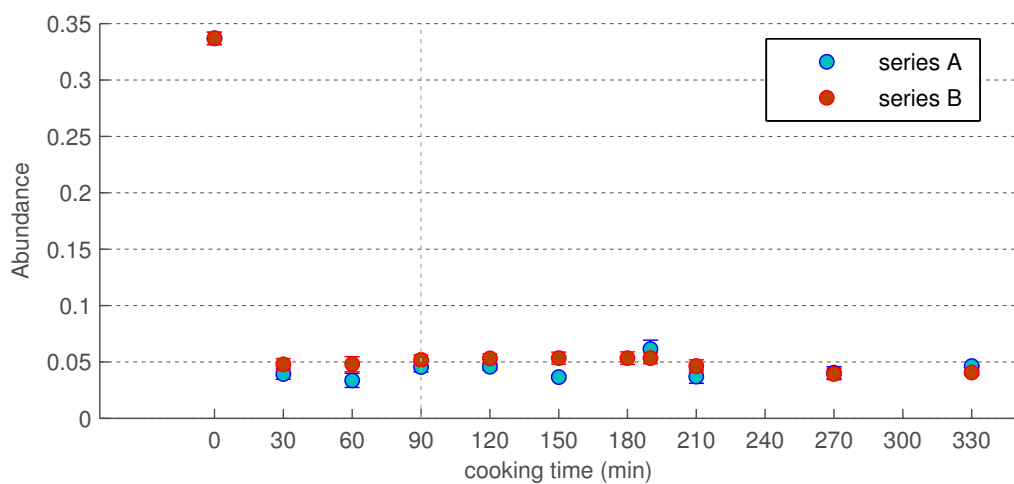


Figure 4.50: Peak areas of acetic acid marker ion  $m/z$  43 plotted against cooking time

were slightly higher. This may be attributed to comparably mild cooking conditions and the higher glucomannan content.

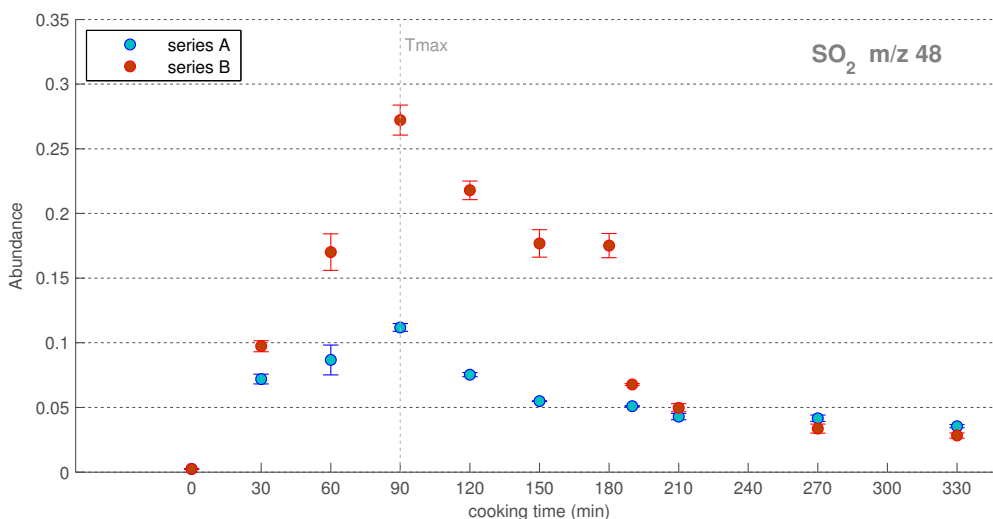


Figure 4.51: Peak areas of sulfur dioxide marker ion  $m/z$  64 plotted against cooking time.

It has been shown by van Loon *et al.* (1993) that sulfur dioxide may be used as an indicator for the contents of sulfonic acid groups in lignosulfonates. Also for pulps Py-GC/MS has proven to be very suitable to monitor the degree of sulfonation. At a pyrolysis temperature of  $500^{\circ}\text{C}$   $\text{SO}_2$  is the only major pyrolysis product associated with sulfonic acids. When the abundance of  $\text{SO}_2$  is plotted against cooking time the difference in the degree of sulfonation within the first 6 cooking stages becomes apparent (figure 4.47). These differences were already discussed in section 4.1.3.2. When the errorbars are reviewed a high reproducibility of the marker ion for  $\text{SO}_2$  can be assumed.

Another interesting observation was the detection of anthraquinone in the pulps. In figure 4.48 the abundance of the marker ion ( $m/z$  180) is plotted against cooking time. It can be noticed that AQ was not detected in the pulps of the last 3 cooking stages. A further observation was that both series showed distinct systematic differences in the abundances of AQ. In series A the abundance of AQ increased more rapidly than in series B. The maximum abundance was reached directly after the heating-up period and rapidly declined hereafter. Additionally, the maximum abundance was nearly 2-fold higher than the maximum in series B. In series B a slower and more

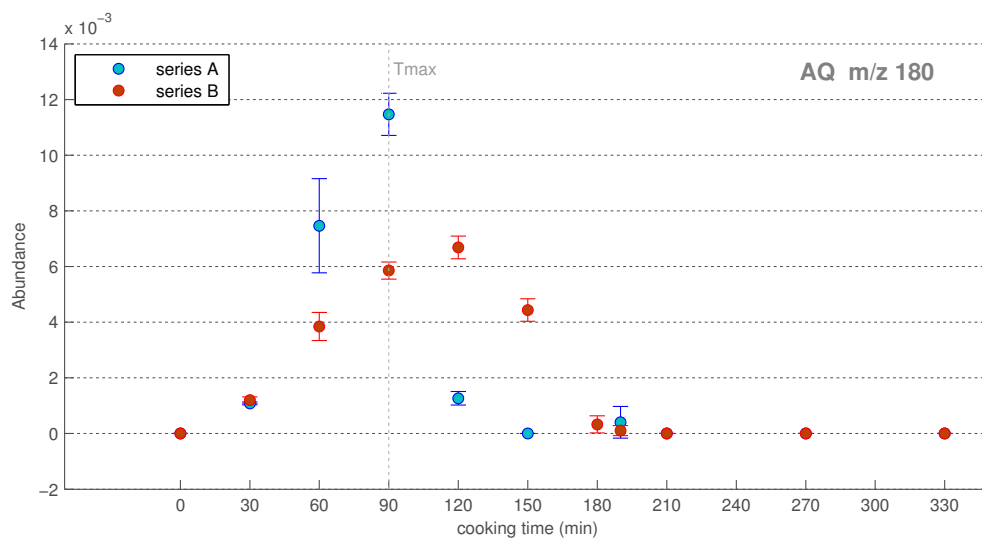


Figure 4.52: Peak areas of anthraquinone marker ion m/z 180 plotted against cooking time.

moderate increase and decline of AQ in pulp could be perceived. These observation may be explained by the differences of the pH profiles and the rates of delignification in the course of the two delignification series. The high NaOH concentration in series A promoted the swelling of the fibers and the penetration of the chemicals. The implication of this observation may be that the more rapid delignification in the first stages of the A series was due to both, higher NaOH concentration and quicker AQ penetration.

## 4.2.4 Quantitative data analysis

### 4.2.4.1 Quantification of sulfonic acid groups

Only a brief section shall be dedicated to the quantification of sulfite pulp constituents. As it was mentioned before the initial intention of the application of Py-GC/MS was to test whether sulfonic acid groups could be quantified. The conductometric method of Katz *et al.* (1984) is fairly time-consuming and therefore not appealing when large-scale studies are intended. SO<sub>2</sub> has proven as a suitable marker for sulfonic acid groups and no other pyrolysis products could be found which directly derived from those. Hence, the most straightforward approach was to try quantification by means of external calibrations. Because of considerable overlap with other early eluting peaks, again the marker ion  $m/z$  64 was utilized as extracted ion. The determined values from the conductometric titration were utilized as reference and appropriate pulp samples with known sulfonic acid group content were selected as calibrants. The pulps chosen were B<sub>60</sub>, A<sub>90</sub>, B<sub>90</sub>, B<sub>330</sub> and a spruce BCTMP which covered the whole range of sulfonic acid group content of the available pulps.

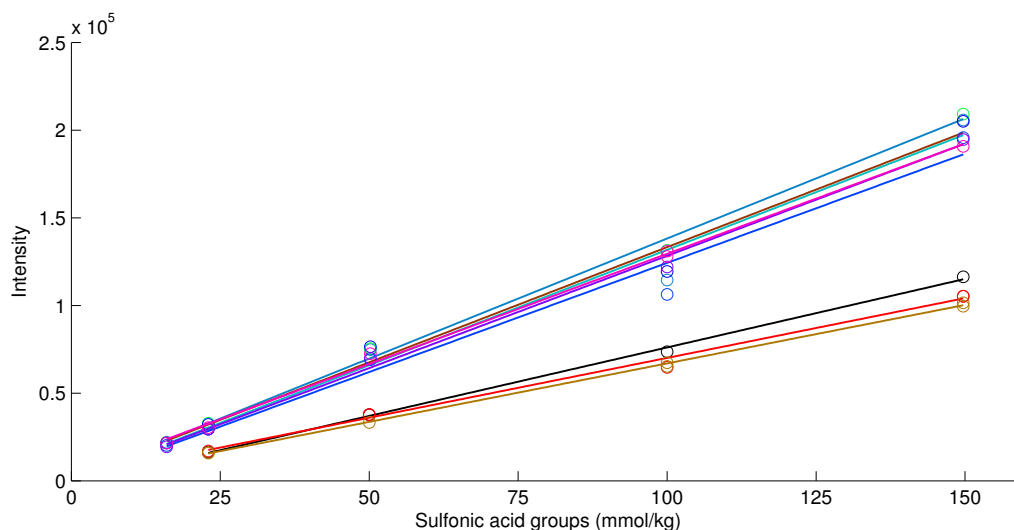


Figure 4.53: 9 calibration curves for SO<sub>2</sub>.

In figure 4.49 9 calibration curves measured within the series of 160 measurements are plotted. The peak areas of  $m/z$  64 were normalized by sample weight. Two sets of calibration curves with similar slopes can be perceived which can be explained by the previously discussed *autotune* in the middle of

## CHAPTER 4. DISCUSSION OF RESULTS

---

the series. It can also be seen that the measurements of the sample B<sub>60</sub> (100 mmol/kg sulfonic acid groups) apparently showed a too low response which may have been due to inaccurate values acquired by the reference method.

Table 4.16:  $R^2$  and slopes of 9 calibration curves for SO<sub>2</sub> marker ions m/z 48, 64 and 66.

Cal.	$R^2$	Slope	$R^2$	Slope	$R^2$	Slope
	m/z 48	m/z 48	m/z 64	m/z 64	m/z 66	m/z 66
1	0.999	345.52	0.999	781.52	0.999	36.66
2	0.998	304.51	0.994	681.76	0.994	32.12
3	0.999	296.78	0.999	667.22	0.999	31.31
4	0.989	615.07	0.980	1316.12	0.978	62.18
5	0.996	606.16	0.996	1369.69	0.998	66.18
6	0.989	560.74	0.986	1313.59	0.988	63.99
7	0.990	571.24	0.977	1245.21	0.975	57.39
8	0.994	575.07	0.996	1280.39	0.995	61.24
9	0.998	561.69	0.998	1258.39	0.997	60.78

In table 4.14 the coefficients of determination and the slopes of the regression curves are listed for the three major ions m/z 48, 64 and 66 of sulfur dioxide. Overall high coefficients of determination were received for all 3 ions. It was concluded that the external calibration approach may be well suited to determine sulfonic acid groups. However, when it was tested on the remaining samples some it showed overall acceptable results with deviations between 2 and 18 %. It could not be assessed whether the highly deviating measurements were due to inaccurate reference values or due to measurement deviations. The conductometric titration method, though, is considered as highly accurate. The normalization techniques discussed in section 4.2.2.5 were not tried on the data. It is believed that the method is a rapid, but less accurate method, to assess the sulfonic acid group content in larger sample sets. If more than 4 or 5 calibration samples had been employed the accuracy may have been improved.



#### 4.2.4.2 Quantification of pulp constituents

Another approach for quantification is the application of multivariate regression methods. As already described in the literature review wood and pulp constituents have been quantified by several authors by means of Py-GC/MS using partial-least-squares regression. In all works, as far as known, only the major or well identified peaks were utilized as variables.

An alternative approach is to employ variable selection algorithms to select the most feasible pyrolysis products for quantification. To test if the 408 peaks extracted may be helpful to find appropriate variables to quantify the constituents the variable selection method iPLS was applied. For preliminary testing the algorithm was employed on 19 calibration samples. The 19 samples were taken from the two delignification series. And for this first trial the means of the normalized replicate measurements were calculated and utilized as calibration data. The iPLS algorithm can be conducted in several modes. For the trial it was set to perform an exhaustive search for the best variable set for each of the constituents lignin, cellulose, mannose, xylose, galactose, arabinose, 4-O-methylglucuronic acid and also for the sulfonic and carboxylic acids. The search was constrained to only use a maximum of 5 latent variables (LVs). Afterwards PLS calibration models were calculated for each constituent to be predicted. In addition, all three normalization methods described in section 4.2.2.5 were compared. The results are displayed in table 4.2.4.2.

A good predictability of lignin and cellulose content has been shown before. But when the correlation coefficients of cross validation ( $R_{cv}^2$ ) and the root mean square errors of cross validation (RMSECV) were reviewed surprisingly good values were found for galactose and carboxylic acids. And also all other constituents appeared to be predictable by means of PLS.

However, the results may be misleading and are overly optimistic. The most important process in setting up PLS models is the validation of the models. For this purpose independent validation sample sets with known composition are needed. Also, it is recommended to apply the variable selection procedure to several subsets of the calibration sets. Hereby more robust models may be built which have lower  $R_{cv}^2$  and higher RMSECV values but may not fail as quickly.

But several likely conclusions could be drawn from the PLS trial: pulp constituents, including carboxylic acids, may be quantified by Py-GC/MS. The selected-peaks normalized data showed the best results. Several minor unknown pyrolysis products were selected for each constituent to be quantified.

Table 4.17: Comparison of results of PLS calibration on pyrolysis data normalized by weight-background, constant sum and selected peaks normalization. Pulp constituents including sulfonic and carboxylic acids were used as y-variables. For each of the constituents iPLS variable selection has been performed separately for 5 LVs. IPLS algorithm and PLS models were calculated on autoscaled data.  $R^2_{cv}$  and RMSECV were based on Venetian blinds cross validation.

normalization		Lignin	Glucose	Xylose	Mannose	Galactose	Arabinose	COOH	Me-O-4	SO <sub>3</sub> H
constant sum	LV	3	3	5	5	5	3	3	5	3
	No. of peaks	7	19	6	8	5	8	20	8	4
	$R^2_{cv}$	0.996	0.999	0.944	0.965	0.991	0.913	0.983	0.908	0.98
	RMSECV	0.557	0.434	0.142	0.427	0.044	0.061	4.709	0.079	5.734
weight-background	LV	3	5	4	5	5	5	5	5	5
	No. of peaks	6	11	9	6	6	9	13	12	7
	$R^2_{cv}$	0.996	0.999	0.954	0.995	0.985	0.936	0.991	0.946	0.974
	RMSECV	0.578	0.412	0.128	0.155	0.057	0.053	3.266	0.061	6.453
selected-peaks	LV	5	5	5	5	5	5	4	5	5
	No. of peaks	7	13	7	6	6	12	23	11	8
	$R^2_{cv}$	0.999	0.999	0.954	0.989	0.996	0.977	0.995	0.977	0.989
	RMSECV	0.222	0.329	0.128	0.243	0.028	0.032	2.427	0.041	4.185

# Chapter 5

## Summary

In the work of Rose (2003) it was sought to modify the AS/AQ process as such as to yield pulps with properties close to ASAM pulps without the use of any organic solvent. Amongst other findings it was discovered that a low ratio of NaOH to Na<sub>2</sub>SO<sub>3</sub> in the initial stage and a significant elevation of the NaOH concentration after the heating-up period enhanced the performance of the AS/AQ process in particular when applied to softwoods. The degree of delignification and the strength properties of the obtained pulps were significantly improved. This modification was termed NaOH splitting. The focus of the work was the optimization of the cooking conditions and analyses of the strength properties and bleachability of the pulps. Although the work was accompanied by standard analytical methods, the reason for the improvements and the impact particularly on the residual lignin by the aforementioned modification was not elucidated in detail.

**The main objective** of the presented work was based on the aforementioned study of Rose (2003) and was conducted on spruce as the raw material. Compositional and structural aspects explaining the improved pulp properties by the elaborated process modifications were to be assessed in order to evaluate whether further improvements could be reached.

To elucidate the effect of the NaOH splitting on the composition and the chemical structure of the pulp components, two delignification series were conducted; one under conventional (series A) and one under modified AS/AQ pulping conditions (series B). Except for the cooking temperature, cooking time and the time of the second NaOH charge, all cooking parameters were adopted from the work of Rose (2003). The total cooking time of 330 min, including the heating-up period, was split into 10 time intervals. According to the intervals, cooks were terminated for both series after 30, 60, 90, 120,

150, 180, 190, 210, 270 and 330 min. For the series with NaOH splitting, the time of second NaOH addition was set to 180 min. Hence 10 pulps for each series were obtained that were to be analysed.

**The standard analyses** employed on the pulps of the two delignification series verified all findings of the former work but also revealed new insights. Until the addition of the second NaOH charge in series B, significant differences between the two series could be observed. The rate of delignification in series A was considerably higher than in series B, reflected by the quicker decrease of yield and kappa number.

On the other hand the selectivity of delignification of series B within the first 180 min of the cooking time was notably higher than for series A. This implied that much more of the polysaccharides, in particular the glucomannans, were preserved in series B. A major reason for the differences was apparent: in terms of severity, the significant difference of the initial NaOH concentrations between the two delignification series had a considerable impact on the courses of the cooks. Within the heating-up period the pH in series B decreased dramatically, and was 3 units lower than for series A throughout the cooking interval B<sub>90</sub> - B<sub>180</sub> (0 - 90 min at  $T_{max}$ ). A high NaOH concentration as in series A is known to promote both, lignin and polysaccharide degradation.

An observation that was not expected was the enormous difference between the two series in the degree of sulfonation of the lignin. At the cooking time of 60 min at  $T_{max}$  the degree of sulfonation in series B was highest and 2.5 times higher than in the corresponding pulp of series A. Thus, until the addition of the second NaOH charge in series B, a combination of two major effects may have led to a higher selectivity of delignification: lower severity and a higher degree of sulfonation. The high degree of sulfonation indicated a high proportion of sulfidolytic degradation of lignin. These are known to take place within a wide pH range.

After the addition of the second NaOH charge in series B the obvious compositional differences between the two series rapidly diminished. At the cooking stage after 120 min at  $T_{max}$  the compositional data revealed almost identical properties of the pulps A<sub>210</sub> and B<sub>210</sub>. Kappa numbers, yields, carbohydrate composition and the degree of sulfonation were basically equal. However, the viscosity and brightness of the pulp B<sub>210</sub> were higher. The comparison of the two terminal cooking stages revealed again compositional results diverging between the two series. Here the improvement by the process modification

became apparent. For pulp at the terminal stage of series A ( $A_{330}$ ), a kappa number of 28.6, a viscosity of 1066 ml/g and a brightness of 23.1 %ISO were determined. The corresponding pulp of series B had a kappa number of 23.3, and the viscosity and brightness were assessed to be 1221 ml/g and 30.6 %ISO. The yield of pulp  $B_{330}$ , however, was slightly lower than for the pulp  $A_{330}$ .

From the obtained results it was concluded that the key to finding structural differences responsible for the improvements lay in the three last cooking stages. Foremost, the pulps  $A_{210}$  and  $B_{210}$  were considered as most appropriate to serve as subjects for a detailed study. For this purpose 2 replicate cooks for each of the two series, terminated after 210 min, were conducted. Most of the results assessed for the pulps  $A_{210}$  and  $B_{210}$  could be reproduced, only the degrees of sulfonation of the two sets of replicate pulps ( $R1A_{210}$   $R2A_{210}$ ,  $R1B_{210}$  and  $R2B_{210}$ ) were apparently higher and diverging. This was attributed to the fact that the replicate cooks were employed on a new charge of spruce raw material which may also have had a different initial moisture content.

Although other analytical approaches were considered it was decided to concentrate solely on **pyrolysis - gas chromatography/mass spectrometry** to assess structural differences between the pulps. Py-GC/MS can be considered as a rapid and high-throughput analytical method that provides fingerprints with high information content. In particular for the analysis of residual lignin Py-GC/MS seemed to be appropriate as minor components can still be detected without preceding isolation procedures. The presented section on Py-GC/MS was based on the detailed analysis on a series consisting of 160 measurements. It included the measurements of all pulps of the delignification series and replicate cooks, native spruce wood and 4 pulps from reference cooks. All samples were measured at least as duplicates whereas 9 samples were measured between 6 and 17 times.

Considerable effort has been put into the **pre-processing of the pyrolysis data**. It was realised that proper pre-processing was the key to extract reliable and unbiased information from the data. Unfortunately, the batch-wise pre-processing of chromatographic data was not trivial. No evaluation software was available to solve all desired pre-processing tasks. With the aid of several software solutions and self-written scripts in MATLAB a semi-automated pre-processing chain has been elaborated to enable reproducible processing of large-scale data sets. The pyrograms were smoothed, background corrected and subjected to peak detection and deconvolution. All

detected peaks were filtered and merged to a global peak list containing 458 peaks. The peak list included several hundreds of minor peaks of unknown identity whereof many were overlapping and coeluting. Hereafter one representative ion for each peak was extracted and the ion peak areas determined batch-wise for all measurements. Particular attention had to be put on the normalization of the data. No internal standard was used and normalization only by sample-weight was inapplicable because sensitivity fluctuations of the measuring device or sensitivity leaps caused e.g. by an autotune (a routine service procedure) are not compensated. Two normalization techniques, termed weight-background and selected-peaks normalization, were elaborated which functioned well on the analysed data set.

It was anticipated that numerous peaks of the global peak list were uninformative for the data analysis. ANOVA was applied on the replicate measurements of the aforementioned 9 samples to assess which peaks may have discriminative potential. Surprisingly, only 36 peaks were discarded by ANOVA analysis. A further 14 peaks were manually removed because of extensive amounts of missing entries. Hence, 408 peaks remained as the basis for subsequent data analysis.

Almost all studies on lignocellulosic biomass are restricted to the major and well identified peaks which sum up to around 80 to 120 peaks. It has the major advantage that the interpretation of the results is more straightforward and the effort on processing of the data is moderate. The intention of extracting as many peaks as possible irrespective of their intensities was to have an unbiased view on the data and to assess whether any of the commonly ignored peaks may appear as important for the discrimination of samples by multivariate analysis.

The pyrolysis data was evaluated by **principal component analysis (PCA)** and directly by comparison of differences in peak intensities of marker ions. For PCA prior manual and algorithm-based variable selection with the aid of Fisher's discriminant ratio were employed. The manually selected peaks included all lignin derived products found in the data. Many products were tentatively assumed to originate from lignin on basis of mass traces ( $m/z$ ) with which they are associated. The second variable selection approach was solely on the basis of the discriminative significance of the peaks for the intended comparison. It could be shown that nearly half of the 38 selected peaks by FDR were unknown minor peaks.

Several **conclusions** could be drawn from the analyses. Foremost, it was ascertained that the pulps derived from the modified process, contained overall more phenylpropane units, i.e. the propane side chains of the lignin monomers were degraded to a lower extent. This may imply that the residual lignin was more susceptible to degradation reactions. However the difference diminished towards the end. The focus was primarily on the guaiacyl moieties but also the fate of p-coumaryl moieties (H-lignin) as a function of total lignin content was assessed. Apparently, some H-lignin fragments showed a more or less exponential increase towards the terminal cooks for both series. This may point towards an increase of the fraction of condensed and demethoxylated lignin structures in the residual lignin.

It could also be illustrated that the relative degree of sulfonation and the relative amount of anthraquinone retained in the pulps, can be assessed by Py-GC/MS. Concerning the pyrolysis products derived from the polysaccharides further details may be revealed by this analytical approach, but the focus in the presented study was on lignin.

From the results obtained for the two delignification series by means of Py-GC/MS a **possible improvement of the modified AS/AQ process** may be proposed. Within the scope of a subsequent bleaching sequence it may be advantageous to terminate the cooks at an earlier stage, e.g. when a kappa number of 30 to 40 is reached. The tendency of the residual lignin at this stage towards further selective degradation may be considerably higher. In addition, the rapid increase of the H-lignin fraction towards the end of the cooks may be avoided.

# Bibliography

- ADLER, E., *Lignin Chemistry - Past, Present and Future*, Wood Science and Technology, 11, 3, (1977), 169–218
- ALVES, A., GIERLINGER, N., SCHWANNINGER, M. and RODRIGUES, J., *Analytical pyrolysis as a direct method to determine the lignin content in wood Part 3. Evaluation of species-specific and tissue-specific differences in softwood lignin composition using principal component analysis*, Journal of Analytical and Applied Pyrolysis, 85, 1-2, (2009), 30–37
- ALVES, A., SCHWANNINGER, M., PEREIRA, H. and RODRIGUES, J., *Analytical pyrolysis as a direct method to determine the lignin content in wood - Part 1: Comparison of pyrolysis lignin with Klason lignin*, Journal of Analytical and Applied Pyrolysis, 76, 1-2, (2006), 209–213
- ATAK, D., HEITNER, C. and KARNIS, A., *Ultrahigh yield pulping of eastern black spruce .2.*, Svensk Papperstidning, 83, 5, (1980), 133–141
- BACKA, S., BROLIN, A. and NILSSON, T., *Characterisation of fungal degraded birch wood by FTIR and Py-GC*, Holzforschung, 55, 3, (2001), 225–232
- BAUCHER, M., HALPIN, C., PETIT-CONIL, M. and BOERJAN, W., *Lignin: Genetic engineering and impact on pulping*, Critical Reviews In Biochemistry and Molecular Biology, 38, 4, (2003), 305–350
- BEATSON, R. P., *Determination of Sulfonate Groups and Total Sulfur. In: Methods in Lignin Chemistry*, Springer, chap. 7, 1992, 473–484
- BECERRA, V. and ODERMATT, J., *Detection and quantification of traces of bisphenol A and bisphenol S in paper samples using analytical pyrolysis-GC/MS*, The Analyst, 137, 9, (2012), 2250–9
- BEHRENDTS, V., TREDWELL, G. D. and BUNDY, J. G., *A software complement to AMDIS for processing GC-MS metabolomic data*, Analytical Biochemistry, 415, 2, (2011), 206–208



## BIBLIOGRAPHY

---

- BIASCA, K. L., *A study of the kinetics of delignification during the early stage of alkaline sulfite anthraquinone pulping*, Ph.D. thesis, GeorgiaTech, Institue of Paper Science and Technology, 1989
- BLAIN, T. J., *Anthraquinone Pulping - 15 Years Later*, Tappi Journal, 76, 3
- BOCCHINI, P., GALLETTI, G. C., CAMARERO, S. and MARTINEZ, A., *Absolute quantitation of lignin pyrolysis products using internal standard*, Journal of Chromatography A, 773, (1997), 227–232
- BREDENBERG, J. B., MASUKU, C. P. and VUORI, A., *Thermal-reactions of the Bonds In Lignin .2. Thermolysis of Dihydrodehydrodiisoeugenol*, Holzforschung, 43, 2, (1989), 115–120
- BREMER, J., *Quantifizierung der Gerüstsubstanzen von Lignocellulosen durch analytische Pyrolyse-Gasschromatographie/ Massenspektrometrie*, Ph.D. thesis, University of Hamburg, Department of Biology, 1991
- BRERETON, R. G., *Chemometrics: Data Analysis for the Laboratory and Chemical Plant*, John Wiley & Sons, 2003
- BREZNY, R., MIHALOV, V. and KOVACIK, V., *Low-temperature Thermolysis of Lignins .1. Reactions of Beta-o-4 Model Compounds*, Holzforschung, 37, 4, (1983), 199–204
- BRITT, P. F., BUCHANAN, A. C., THOMAS, K. B. and LEE, S. K., *Pyrolysis Mechanisms of Lignin - Surface-immobilized Model-compound Investigation of Acid-catalyzed and Free-radical Reaction Pathways*, Journal of Analytical and Applied Pyrolysis, 33, (1995), NAGOYA UNIV
- BROECKLING, C. D., REDDY, I. R., DURAN, A. L., ZHAO, X. C. and SUMNER, L. W., *MET-IDEA: Data extraction tool for mass spectrometry-based metabolomics*, Analytical Chemistry, 78, 13, (2006), 4334–4341
- BRUNOW, G., KILPELÄINEN, I., SIPILÄ, J., SYRJÄNEN, K., KARHUNEN, P., SETÄLÄ, H. and RUMMAKKO, P., *Oxidative Coupling of Phenols and the Biosynthesis of Lignin; in: Lignin and Lignan Biosynthesis*, American Chemical Society, ACS Symposium Series 697, Washington DC, USA, chap. 10, 1998, 131–147
- BRUNOW, G. and LUNDQUIST, K., *Functional groups and bonding patterns in lignin (including the lignin-carbohydrate complexes) In: Lignin and Lignans: Advances in Chemistry*, CRC Press, chap. 7, 2010, 267–299

## BIBLIOGRAPHY

---

- BRÄNNVALL, E., *Pulping Technology. In: Pulping Chemistry and Technology*, De Gruyter, chap. 6, Pulp and Paper Chemistry and Technology, 2009
- BUCHERT, J., TELEMAN, A., HARJUNPAA, V., TENKANEN, M., VIKARI, L. and VUORINEN, T., *Effect of Cooking and Bleaching On the Structure of Xylan Conventional Pine Kraft Pulp*, Tappi Journal, 78, 11, (1995), 125–130
- BÖTTCHER, J. H., *Quantitative Analyse von Holz und Holz- Komponenten mittels FTIR-Spektroskopie unter Anwendung Multivariater Statistischer Verfahren*, Ph.D. thesis, Universität Hamburg, Fachbereich Biologie, 1993
- CAMARERO, S., BOCCHINI, P., GALLETTI, G. C. and MARTA, A. T., *Pyrolysis-Gas Chromatography / Mass Spectrometry Analysis of Phenolic and Etherified Units in Natural and Industrial Lignins*, Rapid Communications in Mass Spectrometry, 636, (1999), 630–636
- CAPPELEN, H. and SCHÖÖN, N.-H., *Determination of sulfonic acid groups in unbleached sulfite pulps.*, Svensk Papperstidning, 69, 9, (1966), 322–325
- CHAMBERS, R. E. and CLAMP, J. R., *Assessment of Methanolysis and Other Factors Used In Analysis of Carbohydrate-containing Materials*, Biochemical Journal, 125, 4, (1971), 1009–&
- CHEN, H. T., FUNAOKA, M. and LAI, Y. Z., *The influence of anthraquinone in sulfite delignification of norway spruce. 2. Phenolic hydroxyl group formation.*, Holzforschung, 48, (1994a), 140–145
- CHEN, H. T., GHAZY, M., FUNAOKA, M. and LAI, Y. Z., *The influence of anthraquinone in sulfite delignification of norway spruce. 1. Liquor pH and sulfonation*, Cellulose Chemistry and Technology, 28, 1, (1994b), 47–54
- CHOI, J. W., FAIX, O. and MEIER, D., *Characterization of residual lignins from chemical pulps of spruce (Picea abies L.) and beech (Fagus sylvatica L.) by analytical pyrolysis-gas chromatography/mass spectrometry*, Holzforschung, 55, 2, (2001), 185–192
- CLIFFORD, D., STONE, G., MONTOLIU, I., REZZI, S., MARTIN, F.-P., GUY, P., BRUCE, S. and KOCHHAR, S., *Alignment Using Variable Penalty Dynamic Time Warping*, Analytical Chemistry, 81, 3, (2009), 1000–1007
- DIXON, S. J., BRERETON, R. G., SOINI, H. A., NOVOTNY, M. V. and PENN, D. J., *An automated method for peak detection and matching in large gas chromatography-mass spectrometry data sets*, Journal of Chemometrics, (2007), 325–340

## BIBLIOGRAPHY

---

- DORRESTIJN, E., LAARHOVEN, L. J. J., ARENDS, I. W. C. E. and MULDER, P., *The occurrence and reactivity of phenoxyl linkages in lignin and low rank coal*, Journal of Analytical and Applied Pyrolysis, 54, 1-2, (2000), 153–192
- DOUEK, M. and ING, J., *Determination of Sulfur and Chlorine In Pulp and Paper Samples By Combustion Ion Chromatography*, Journal of Pulp and Paper Science, 15, 2, (1989), J72–J78
- EBRAHIMI, D., LI, J. and HIBBERT, D. B., *Classification of weathered petroleum oils by multi-way analysis of gas chromatography-mass spectrometry data using PARAFAC2 parallel factor analysis.*, Journal of Chromatography A, 1166, 1-2, (2007), 163–70
- EKEBERG, D., FLAETE, P., EIKENES, M., FONGEN, M. and NAESS-ANDRESEN, C., *Qualitative and quantitative determination of extractives in heartwood of Scots pine ( Pinus sylvestris L .) by gas chromatography*, Journal of Chromatography A, 1109, (2006), 267–272
- ERICKSON, M., LARSSON, S. and MIKSCH, G. E., *Gaschromatographische Analyse von Ligninoxidationsprodukten. VIII. Zur Struktur des Lignins der Fichte*, Acta Chemica Scandinavica, 27, 3, (1973), 903–914
- EVANS, R. J., MILNE, T. A. and SOLTYS, M. N., *Direct Mass-spectrometric Studies of the Pyrolysis of Carbonaceous Fuels .3. Primary Pyrolysis of Lignin*, Journal of Analytical and Applied Pyrolysis, 9, 3, (1986), 207–236
- FABBRI, D., CHIAVARI, G., PRATI, S., VASSURA, I. and VANGELISTA, M., *Gas chromatography/mass spectrometric characterisation of pyrolysis/silylation products of glucose and cellulose*, Rapid Communications In Mass Spectrometry, 16, 24, (2002), 2349–2355
- FAHMI, R., BRIDGWATER, A. V., THAIN, S. C., DONNISON, I. S., MORRIS, P. M. and YATES, N., *Prediction of Klason lignin and lignin thermal degradation products by Py-GC/MS in a collection of Lolium and Festuca grasses*, Journal of Analytical and Applied Pyrolysis, 80, 1, (2007), 16–23
- FAIX, O., BREMER, J., SCHMIDT, O. and STEVANOVIC, T., *Monitoring of chemical-changes in white-rot degraded beech wood by pyrolysis-gas chromatography and fourier-transform infrared spectroscopy*, Journal of Analytical and Applied Pyrolysis, 21, 1-2, (1991), 147–162

## BIBLIOGRAPHY

---

- FAIX, O., MEIER, D. and FORTMANN, I., *Pyrolysis-gas Chromatography-mass Spectrometry of 2 Trimeric Lignin Model Compounds With Alkyl-aryl Ether Structure*, Journal of Analytical and Applied Pyrolysis, 14, 2-3, (1988), 135–148
- FAIX, O., MEIER, D. and FORTMANN, I., *Thermal-degradation Products of Wood - Gas-chromatographic Separation and Mass-spectrometric Characterization of Monomeric Lignin Derived Products*, Holz Als Roh-und Werkstoff, 48, 7-8, (1990), 281–285
- FAIX, O., MEIER, D. and GROBE, I., *Studies On Isolated Lignins and Lignins In Woody Materials By Pyrolysis-gas Chromatography-mass Spectrometry and Off-line Pyrolysis-gas Chromatography With Flame Ionization Detection*, Journal of Analytical and Applied Pyrolysis, 11, (1987), 403–416
- FENGEL, D. and WEGENER, G., *Wood: Chemistry, Ultrastructure, Reactions*, Walter de Gruyter, Berlin, Germany, 1984
- FILLEY, T. R., CODY, G. D., GOODELL, B., JELLISON, J., NOSER, C. and OSTROFSKY, A., *Lignin demethylation and polysaccharide decomposition in spruce sapwood degraded by brown rot fungi*, Organic Geochemistry, 33, 2, (2002), 111–124
- FU, Q., ARGYROPOULOS, D. S., TILOTTA, D. C. and LUCIA, L. A., *Understanding the pyrolysis of CCA-treated wood*, Journal of Analytical and Applied Pyrolysis, 81, 1, (2008), 60–64
- GABRIELSSON, J. and TRYGG, J., *Recent developments in Multivariate calibration*, Critical Reviews In Analytical Chemistry, 36, 3-4, (2006), 243–255
- GALLETTI, G. C. and BOCCHINI, P., *Pyrolysis/Gas Chromatography/Mass Spectrometry Of Lignocellulose*, Rapid Communications In Mass Spectrometry, 9, 9, (1995), 815–826
- GALLETTI, G. C., CARNACINI, A., BOCCHINI, P. and ANTONELLI, A., *Chemical-Composition Of Wood Casks For Wine Aging As Determined By Pyrolysis/GC/MS*, Rapid Communications In Mass Spectrometry, 9, 14, (1995), 1331–1334
- GELLERSTEDT, G., *The reactions of lignin during sulfite pulping*, Svensk Papperstidning-Nordisk Cellulosa, 79, 16, (1976), 537–543
- GELLERSTEDT, G., *Chemistry of Chemical Pulping. In: Pulping Chemistry and Technology*, De Gruyter, chap. 5, Pulp and Paper Chemistry and Technology, 2009

## BIBLIOGRAPHY

---

- GELLERSTEDT, G. and LI, J. B., *An HPLC method for the quantitative determination of hexeneuronic acid groups in chemical pulps*, Carbohydrate Research, 294, (1996), 41–51
- GENUIT, W., BOON, J. J. and FAIX, O., *Characterization of Beech Milled Wood Lignin By Pyrolysis-gas Chromatography Photoionization Mass-spectrometry*, Analytical Chemistry, 59, 3, (1987), 508–513
- GERBER, L., ELIASSEN, M., TRYGG, J., MORITZ, T. and SUNDBERG, B., *Multivariate curve resolution provides a high-throughput data processing pipeline for pyrolysis-gas chromatography/mass spectrometry*, Journal of Analytical and Applied Pyrolysis, 95, 2010, (2012), 95–100
- GIERER, J., *Chemistry of delignification .1. General concept and reactions during pulping*, Wood Science and Technology, 19, 4, (1985), 289–312
- GUERRA, A., ELISSETCHE, J. P., NORAMBUENA, M., FREER, J., VALENZUELA, S., RODRIGUEZ, J. and BALOCCHI, C., *Influence of Lignin Structural Features on Eucalyptus globulus Kraft Pulping*, Industrial & Engineering Chemistry Research, 47, 22, (2008), 8542–8549
- GUSTAVSSON, C. A. S. and AL-DAJANI, W. W., *The influence of cooking conditions on the degradation of hexenuronic acid, xylan, glucomannan and cellulose during kraft pulping of softwood*, Nordic Pulp and Paper Research Journal, 15, 2
- HARDELL, H.-L. and NILVEBRANT, N.-O., *Analytical pyrolysis of spruce milled wood lignins in the presence of tetramethylammonium hydroxide*, Nordic Pulp And Paper Research Journal, , 211996, (1996), 121–126
- HATCHER, P. G., NANNY, M. A., MINARD, R. D., DIBLE, S. D. and CARSON, D. M., *Comparison of two thermochemolytic methods for the analysis of lignin in decomposing gymnosperm wood: The CuO oxidation method and the method of thermochemolysis with tetramethylammonium hydroxide (TMAH)*, Organic Geochemistry, 23, 10, (1995), 881–888
- HÜBSCHMANN, H. J., *Handbuch der GC/MS: Grundlagen und Anwendung*, John Wiley & Sons, 1996
- IBARRA, D., DEL RIO, J. C., GUTIERREZ, A., RODRIGUEZ, I. M., ROMERO, J., MARTINEZ, M. J. and MARTINEZ, A. T., *Chemical characterization of residual lignins from eucalypt paper pulps*, Journal of Analytical and Applied Pyrolysis, 74, 1-2, (2005), 116–122

## BIBLIOGRAPHY

---

- IBARRA, D., ISABEL CHAVEZ, M., RENCORET, J., DEL RIO, J. C., GUTIERREZ, A., ROMERO, J., CAMARERO, S., MARTINEZ, M. J., JIMENEZ-BARBERO, J. and MARTINEZ, A. T., *Lignin modification during Eucalyptus globulus kraft pulping followed by totally chlorine-free bleaching: A two-dimensional nuclear magnetic resonance, fourier transform infrared, and pyrolysis-gas chromatography/mass spectrometry study*, Journal of Agricultural and Food Chemistry, 55, 9, (2007), 3477–3490
- INGRUBER, O. V., *Pulp and Paper Manufacture Vol. 4: Sulfite science and technology*, The Joint Textbook Committee of the Paper Industry (TAPPI/CPPA), chap. VIII, 1985, 24–49
- INGRUBER, O. V., STRADAL, M. and HISTED, J. A., *Alkaline Sulfite Anthraquinone Pulping Of Eastern Canadian Woods*, Pulp and Paper Magazine Canada, 83, 12, (1982), 79–&
- IRWIN, W. J., *Analytical Pyrolysis: A Comprehensive Guide*, M. Dekker, New York, 1982
- JIANG, Z. H., VAN LIEROP, B. and BERRY, R., *Hexenuronic acid groups in pulping and bleaching chemistry*, Tappi Journal, 83, 1, (2000), 167–175
- JOHANSSON, E., WOLD, S. and SJODIN, K., *Minimizing Effects of Closure On Analytical Data*, Analytical Chemistry, 56, 9, (1984), 1685–1688
- JOHNSON, K. J., WRIGHT, B. W., JARMAN, K. H. and SYNOVEC, R. E., *High-speed peak matching algorithm for retention time alignment of gas chromatographic data for chemometric analysis*, Journal Of Chromatography A, 996, 1-2, (2003), 141–155
- JONSSON, P., JOHANSSON, A. I., GULLBERG, J., TRYGG, J., A, J., GRUNG, B., MARKLUND, S., SJOSTROM, M., ANTTI, H. and MORITZ, T., *High-throughput data analysis for detecting and identifying differences between samples in GC/MS-based metabolomic analyses*, Analytical Chemistry, 77, 17, (2005), 5635–5642
- JONSSON, P., JOHANSSON, E. S., WUOLIKAINEN, A., LINDBERG, J., SCHUPPE-KOISTINEN, I., KUSANO, M., SJOSTROM, M., TRYGG, J., MORITZ, T. and ANTTI, H., *Predictive metabolite profiling applying hierarchical multivariate curve resolution to GC-MS data - A potential tool for multi-parametric diagnosis*, Journal of Proteome Research, 5, 6, (2006), 1407–1414

## BIBLIOGRAPHY

---

- KATZ, S., BEATSON, P. and SCALLAN, A. M., *The determination of strong and weak acidic groups in sulfite pulps*, Svensk Papperstidning, 87, 6, (1984), R48–R53
- KAWAMOTO, H. and SAKA, S., *Role of side-chain hydroxyl groups in pyrolytic reaction of phenolic beta-ether type of lignin dimer*, Journal of Wood Chemistry and Technology, 27, 2, (2007), 113–120
- KESSLER, W., *Multivariate Datenanalyse*, Wiley, 2007
- KESSLER, W. and KESSLER, R., *Multivariate Curve Resolution - Integration von Wissen in Chemometrische Modelle*, Chemie Ingenieur Technik, 82, 4, (2010), 441–451
- KETTUNEN, J., VIRKOLA, N. E. and YRJALA, I., *Effect Of Anthraquinone On Neutral Sulfite And Alkaline Sulfite Cooking Of Pine*, Paperi Ja Puu-Paper And Timber, 61, 11, (1979), 685–&
- KLEEN, M. and GELLERSTEDT, G., *Influence of inorganic species on the formation of polysaccharide and lignin degradation products in the analytical pyrolysis of pulps*, Journal of Analytical and Applied Pyrolysis, 35, 1, (1995), 15–41
- KLEEN, M., LINDBLAD, G. and BACKA, S., *Quantification of Lignin and Carbohydrates In Kraft Pulps Using Analytical Pyrolysis and Multivariate Data-analysis*, Journal of Analytical and Applied Pyrolysis, 25, (1993), 209–227
- KLEEN, M. and LINDSTROM, K., *Polysaccharides and lignins in newsprint process waters studied by pyrolysis-gas chromatography/mass spectrometry*, Nordic Pulp And Paper Research Journal, 2, (1994), 111–118
- KLEIN, M. T. and VIRK, P. S., *Model Pathways In Lignin Thermolysis .1. Phenethyl Phenyl Ether*, Industrial & Engineering Chemistry Fundamentals, 22, 1, (1983), 35–45
- KORDSACHIA, O. and PATT, R., *Untersuchungen zum Aufschluss von Buche nach dem ASAM-Verfahren und zur Bleiche der Zellstoffe in unterschiedlichen Sequenzen*, Papier, 41, 7, (1987), 340–351
- KURODA, K., ASHITANI, T., FUJITA, K. and HATTORI, T., *Thermal behavior of beta-1 subunits in lignin: Pyrolysis of 1,2-diarylpropane-1,3-diol-type lignin model compounds*, Journal of Agricultural And Food Chemistry, 55, 8, (2007), 2770–2778

## BIBLIOGRAPHY

---

- KURODA, K. I., *Pyrolysis-trimethylsilylation analysis of lignin: preferential formation of cinnamyl alcohol derivatives*, Journal of Analytical and Applied Pyrolysis, 56, 1, (2000), 79–87
- KVALHEIM, O. M., BRAKSTAD, F. and LIANG, Y., *Preprocessing of Analytical Profiles in the Presence of Homoscedastic or Heteroscedastic Noise*, Analytical Chemistry, 66, 1, (1994), 43–51
- LABBE, N., RIALS, T. G., KELLEY, S. S., CHENG, Z. M., KIM, J. Y. and LI, Y., *FT-IR imaging and pyrolysis-molecular beam mass spectrometry: new tools to investigate wood tissues*, Wood Science and Technology, 39, 1, (2005), 61–U19
- LAPIERRE, C., MONTIES, B. and ROLANDO, C., *Thioacidolysis of Lignin - Comparison With Acidolysis*, Journal of Wood Chemistry and Technology, 5, 2, (1985), 277–292
- LAPIERRE, C., POLLET, B., MONTIES, B. and ROLANDO, C., *Thioacidolysis of Spruce Lignin - Gc-ms Analysis of the Main Dimers Recovered After Raney-nickel Desulfuration*, Holzforschung, 45, 1, (1991), 61–68
- LAPIERRE, C., POLLET, B., PETIT-CONIL, M., TOVAL, G., ROMERO, J., PILATE, G., LEPLÉ, J. C., BOERJAN, W., FERRET, V., DE NADAI, V. and JOUANIN, L., *Structural alterations of lignins in transgenic poplars with depressed cinnamyl alcohol dehydrogenase or caffeic acid O-methyltransferase activity have an opposite impact on the efficiency of industrial kraft pulping*, Plant Physiology, 119, 1, (1999), 153–163
- LI, J. B. and GELLERSTEDT, G., *On the structural significance of the kappa number measurement*, Nordic Pulp and Paper Research Journal, 13, 2, (1998), 153–158
- LIANG, Y., XIE, P. and CHAU, F., *Chromatographic fingerprinting and related chemometric techniques for quality control of traditional Chinese medicines*, Journal of separation science, 33, (2010), 410–421
- LIMA, C. F., BARBOSA, L. C. A., MARCELO, C. R., SILVÉRIO, F. O. and COLODETTE, J. L., *Comparison between analytical pyrolysis and nitrobenzene oxidation for determination of syringyl/guaiacyl ratio in Eucalyptus spp. lignin*, BioResources, 3, (2008), 701–712
- LOMMEN, A., *MetAlign: Interface-Driven, Versatile Metabolomics Tool for Hyphenated Full-Scan Mass Spectrometry Data Preprocessing*, Analytical Chemistry, 81, 8, (2009), 3079–3086



## BIBLIOGRAPHY

---

- LU, F. and RALPH, J., *Solution-State NMR of Lignocellulosic Biomass*, Journal of Biobased Materials and Bioenergy, 5, 2, (2011), 169–180
- LU, F. C. and RALPH, J., *Derivatization followed by reductive cleavage (DFRC method), a new method for lignin analysis: Protocol for analysis of DFRC monomers*, Journal of Agricultural and Food Chemistry, 45, 7, (1997), 2590–2592
- MANN, D. G. J., LABBE, N., SYKES, R. W., GRACOM, K., KLINE, L., SWAMIDOSS, I. M., BURRIS, J. N., DAVIS, M. and STEWART, C. N. J., *Rapid Assessment of Lignin Content and Structure in Switchgrass (Panicum virgatum L.) Grown Under Different Environmental Conditions*, Bioenergy Research, 2, 4, (2009), 246–256
- MANSFIELD, S. D., KIM, H., LU, F. and RALPH, J., *Whole plant cell wall characterization using solution-state 2D NMR*, Nature protocols, 7, 9, (2012), 1579–89
- MARQUES, A. V., PEREIRA, H., MEIER, D. and FAIX, O., *Quantitative-analysis of Cork (quercus-suber L) and Milled Cork Lignin By Ftir Spectroscopy, Analytical Pyrolysis, and Total Hydrolysis*, Holzforschung, 48, (1994), 43–50
- MASSART, D., VANDEGINSTE, B., BUYDENS, L., DE JONG, S., LEWI, P. J. and SMEYERS-VERBEKE, J., *Handbook of Chemometrics and Qualimetrics: Part A*, no. 20A in Data Handling in Science and Technology, Elsevier, 1997
- MASUKU, C. P., VUORI, A. and BREDENBERG, J. B., *Thermal-reactions of the Bonds In Lignin .1. Thermolysis of 4-propylguaiacol*, Holzforschung, 42, 6, (1988), 361–368
- MASURA, V., *A mathematical model for neutral sulfite pulping of various broadleaved wood species*, Wood Science and Technology, 32, (1998), 1–13
- MCDONOUGH, T. J., VAN DRUNEN, V. J. and PAULSON, T. W., *Sulphite-anthraquinone pulping of southern pine for bleachable grades*, J. Pulp Pap. Sci., 11, 6, (1985), J167–J176
- MCGOVERN, J. N., *Neutral sulfite semichemical pulping*, Paper Trade Journal, (1952), 179–184
- MCLAFFERTY, F. W., *Performance Prediction and Evaluation of Systems For Computer Identification of Spectra*, Analytical Chemistry, 49, 9, (1977), 1441–1443

## BIBLIOGRAPHY

---

- MEIER, D., FORTMANN, I., ODERMATT, J. and FAIX, O., *Discrimination of genetically modified poplar clones by analytical pyrolysis-gas chromatography and principal component analysis*, Journal of Analytical and Applied Pyrolysis, 74, 1-2, (2005), 129–137
- MOLDOVEANU, S. C., *Analytical Pyrolysis of Natural Organic Polymers*, Techniques and Instrumentation in Analytical Chemistry, 20, (1998), 510
- MULLER-HAGEDORN, M., BOCKHORN, H., KREBS, L. and MULLER, U., *A comparative kinetic study on the pyrolysis of three different wood species*, Journal of Analytical and Applied Pyrolysis, 68-9, (2003), 231–249
- NIMZ, H., *Beech Lignin - Proposal of A Constitutional Scheme*, Angewandte Chemie-international Edition In English, 13, 5, (1974), 313–321
- NORGAARD, L., SAUDLAND, A., WAGNER, J., NIELSEN, J. P., MUNCK, L. and ENGELSEN, S. B., *Interval partial least-squares regression (iPLS): A comparative chemometric study with an example from near-infrared spectroscopy*, Applied Spectroscopy, 54, 3, (2000), 413–419
- NUNES, C. A., LIMA, C. F., BARBOSA, L. C. A., COLODETTE, J. L., GOUVEIA, A. F. G. and SILVÉRIO, F. O., *Determination of Eucalyptus spp lignin S/G ratio: a comparison between methods*, Bioresource technology, 101, 11, (2010), 4056–61
- O'CONNELL, A., HOLT, K., PIQUEMAL, J., GRIMA-PETTENATI, J., BOUDET, A., POLLET, B., LAPIERRE, C., PETIT-CONIL, M., SCHUCH, W. and HALPIN, C., *Improved paper pulp from plants with suppressed cinnamoyl-CoA reductase or cinnamyl alcohol dehydrogenase*, Transgenic Research, 11, 5, (2002), 495–503
- ODERMATT, J., MEIER, D., LEICHT, K., MEYER, R. and RUNGE, T., *Approaches to applying internal standards for the quantification of paper additives by Py-GC/MSD*, Journal of Analytical and Applied Pyrolysis, 68-69, (2003), 269–285
- OHI, H., FUKAGAWA, N., MESHITSUKA, G. and ISHIZU, A., *Reduction of Carbohydrate Depolymerization By Sulfite During Quinone Pulping and Oxygen Delignification*, Mokuzai Gakkaishi, 35, 12, (1989), 1105–1109
- ONA, T., SONODA, T., SHIBATA, M. and FUKAZAWA, K., *Small-scale Method To Determine the Contents of Wood Components From Multiple Eucalypt Samples*, Tappi Journal, 78, 3, (1995), 121–126

## BIBLIOGRAPHY

---

- OTTO, M., *Chemometrics*, Wiley, 2007
- PATT, R., KNOBLAUCH, J., FAIX, O., KORDSACHIA, O. and PULS, J., *Lignin and Carbohydrate Reactions In Alkaline Sulfite, Anthraquinone, Methanol (asam) Pulping*, Papier, 45, 7, (1991), 389–396
- PATT, R. and KORDSACHIA, O., *Herstellung von Zellstoffen unter Verwendung von alkalischen Sulfitlösungen mit Zusatz von Anthrachinon und Methanol*, Papier, 40, 10A, (1986), V1–V8
- PATT, R. and KORDSACHIA, O., *Pulp. In: Ullmann's Encyclopedia of Industrial Chemistry*, Weinheim: VCH Verlagsgesellschaft mbH, vol. A 18, 1991, 647–594
- PATT, R., KORDSACHIA, O. and KNOBLAUCH, J., *The ASAM process—alkaline sulfite, anthraquinone, methanol pulping*, in *Proc. ISWPC, Paris, S. 355-360*
- PATT, R., KORDSACHIA, O. and ROSE, B., *Progress in alkaline sulfite AQ pulping (AS/AQ)*, in *Proc. 7th International Conference on New Available Technologies, Stockholm*, Stockholm: SPCI The Swedish Association of Pulp and Paper Engineers 2002, 26–30
- PENG, J. P., LU, F. C. and RALPH, J., *The DFRC method for lignin analysis. 4. Lignin dimers isolated from DFRC-degraded loblolly pine wood*, Journal of Agricultural and Food Chemistry, 46, 2, (1998), 553–560
- PIERCE, K. M., KEHIMKAR, B., MARNEY, L. C., HOGGARD, J. C. and SYNOVEC, R. E., *Review of chemometric analysis techniques for comprehensive two dimensional separations data*, Journal of Chromatography A, 1255, (2012), 3–11
- POUWELS, A. D. and BOON, J. J., *Analysis of beech wood samples, its milled wood lignin and polysaccharide fractions by curie-point and platinum filament pyrolysis mass-spectrometry*, Journal of Analytical and Applied Pyrolysis, 17, 2, (1990), 97–126
- RALPH, J. and HATFIELD, R. D., *Pyrolysis-GC-MS characterization of forage materials*, Journal of Agricultural and Food Chemistry, 39, 8, (1991), 1426–1437
- RALPH, J., LUNDQUIST, K., BRUNOW, G., LU, F., KIM, H., PAUL, F., MARITA, J. M., HATFIELD, R. D., RALPH, S. A., CHRISTENSEN, J. H. and BOERJAN, W., *Lignins : Natural polymers from oxidative coupling of 4-hydroxyphenyl- propanoids*, Phytochemistry Reviews, (2004), 29–60

## BIBLIOGRAPHY

---

- REALE, S., DI TULLIO, A., SPRETI, N. and DE ANGELIS, F., *Mass spectrometry in the biosynthetic and structural investigation of lignins*, Mass Spectrometry Reviews, 23, 2, (2004), 87–126
- RENCORET, J., GUTIERREZ, A. and DEL RIO, J. C., *Lipid and lignin composition of woods from different eucalypt species*, Holzforschung, 61, 2, (2007), 165–174
- RENCORET, J., MARQUES, G., GUTIÉRREZ, A., IBARRA, D., LI, J., GELLERSTEDT, G., SANTOS, J. I., JIMÉNEZ-BARBERO, J., MARTÍNEZ, Á. T. and DEL RÍO, J. C., *Structural characterization of milled wood lignins from different eucalypt species*, Holzforschung, 62, 5, (2008), 514–526
- ROCKLIN, R. D. and POHL, C. A., *Determination of Carbohydrates By Anion-exchange Chromatography With Pulsed Amperometric Detection*, Journal of Liquid Chromatography, 6, 9, (1983), 1577–1590
- RODRIGUES, J., MEIER, D., FAIX, O. and PEREIRA, H., *Determination of tree to tree variation in syringyl / guaiacyl ratio of Eucalyptus globulus wood lignin by analytical pyrolysis*, Journal of Analytical and Applied Pyrolysis, 48, (1999), 121–128
- ROSE, B., *Modifikation von alkalischen Sulfitverfahren zur Herstellung hochwertiger Zellstoffe*, Ph.D. thesis, Universität Hamburg, 2003
- ROVIO, S., KUITUNEN, S., OHRA-AHO, T., ALAKURTTI, S., KALLIOLA, A. and TAMMINEN, T., *Lignin oxidation mechanisms under oxygen delignification conditions. Part 2: Advanced methods for the detailed characterization of lignin oxidation mechanisms*, Holzforschung, 65, 4, (2011), 575–585
- RUTKOWSKA, E. W., WOLLBOLDT, P., ZUCKERSTATTER, G., WEBER, H. K. and SIXTA, H., *Characterization of Structural Changes In Lignin During Continuous Batch Kraft Cooking of Eucalyptus Globulus*, Bioresources, 4, 1, (2009), 172–193
- RYDHOLM, S., *Pulping Processes*, Interscience Publishers: New York, London, Sydney, 1965
- SANTOS, R. B., CAPANEMA, E. A., BALAKSHIN, M. Y., CHANG, H.-M. and JAMEEL, H., *Effect of Hardwoods Characteristics On Kraft Pulping Process: Emphasis On Lignin Structure*, Bioresources, 6, 4, (2011), 3623–3637

## BIBLIOGRAPHY

---

- SARKANEN, K. V., *Lignins: Occurrence, formation, structure and reactions*, John Wiley & Sons, Inc., New York, 1971
- SARKANEN, K. V. and HERGERT, H. L., *Classification and distribution. In: Lignins – Occurrence, Formation, Structure and Reactions.*, John Wiley & Sons, Inc., New York, 1971, 43–94
- SEVASTYANOVA, O., LI, J. and GELLERSTEDT, G., *On the reaction mechanism of the thermal yellowing of*, Nordic Pulp and Paper Research Journal, 21, (2006), 1–5
- SHEN, D. K., GU, S. and BRIDGWATER, A. V., *The thermal performance of the polysaccharides extracted from hardwood : Cellulose and hemicellulose*, Carbohydrate Polymers, 82, (2010), 39–45
- SILVA, T. C. F., GOMIDE, J. L. and SANTOS, R. B., *Evaluation of Chemical Composition and Lignin Structural Features of Simarouba Versicolor Wood On Its Pulping Performance*, Bioresources, 7, 3, (2012), 3910–3920
- SINKOV, N. A. and HARYNUK, J. J., *Cluster resolution: a metric for automated, objective and optimized feature selection in chemometric modeling*, Talanta, 83, 4, (2011), 1079–87
- SINNER, M. and PULS, J., *Non-corrosive Dye Reagent For Detection of Reducing Sugars In Borate Complex Ion-exchange Chromatography*, Journal of Chromatography, 156, 1, (1978), 197–204
- SINNER, M., SIMATUPANG, M. H. and DIETRICH, H. H., *Automated Quantitative-analysis of Wood Carbohydrates By Borate Complex Ion-exchange Chromatography*, Wood Science and Technology, 9, 4, (1975), 307–322
- SIXTA, H., *Comparative Evaluation of Different Concepts of Sulfite Pulping Technology*, Das Papier, 5, (1998), 239–249
- SIXTA, H., *Handbook of Pulp*, vol. 1, Wiley-VCH, Weinheim, 2006
- SJÖBERG, J., KLEEN, M., DAHLMAN, O., AGNEMO, R., FABRIKER, D. and SUNDVALL, H., *Analyses of carbohydrates and lignin in the surface and inner layers of softwood pulp fibers obtained employing various alkaline cooking processes*, Nordic Pulp & Paper Research Journal, 17, 3, (2002), 295–301

## BIBLIOGRAPHY

---

- SJÖBERG, J., KLEEN, M., DAHLMAN, O., AGNEMO, R. and SUNDVALL, H., *Fiber surface composition and its relations to papermaking properties of soda-anthraquinone and kraft pulps*, Nordic Pulp & Paper Research Journal, 19, 3, (2004), 392–396
- SJÖSTRÖM, E., *Wood Chemistry: Fundamentals and Applications*, Academic Press, 2 edn., 1993
- SJÖSTRÖM, E., *Do Hexenuronic Acid Groups Represent the majority of the Carboxyl Groups in Kraft Pulps?*, Journal of Wood Chemistry and Technology, 26, (2006), 283–288
- SJÖSTRÖM, E. and ENSTRÖM, B., *A method for the separate determination of sulpho and carboxyl groups in sulphite pulps*, Svensk Papperstidning, 69, 3, (1966), 55–59
- SJÖSTRÖM, E. and WESTERMARK, U., *Chemical Composition of Wood and Pulps: Basic Constituents and Their Distribution In: Analytical Methods in Wood Chemistry, Pulping, and Papermaking*, Springer, chap. 1, 1998, 1–19
- SJÖSTRÖM, K., *Influence of ionic strength on kraft cooking and subsequent TCF-bleaching*, Nordic Pulp And Paper Research Journal, 14, 3
- SKOV, T. and BRO, R., *Solving fundamental problems in chromatographic analysis*, Analytical and Bioanalytical Chemistry, 390, (2008), 281–285
- STEIN, S. E., *An integrated method for spectrum extraction and compound identification from gas chromatography/mass spectrometry data*, Journal of the American Society For Mass Spectrometry, 10, 8, (1999), 770–781
- SULLIVAN, J. and DOUEK, M., *Determination of Carbohydrates In Wood, Pulp and Process Liquor Samples By High-performance Anion-exchange Chromatography With Pulsed Amperometric Detection*, Journal of Chromatography A, 671, 1-2, (1994), DIONEX CORP; MILLIPORE, WATERS CHROMATOGRAPHY DIV
- SUNDBERG, A. and HOLMBOM, B., *Fines in spruce TMP, BTMP and CTMP - chemical composition and sorption of mannans*, Nord. Pulp Pap. Res. J., 19, 2, (2004), 176–182
- SUNDBERG, A., SUNDBERG, K. and HOLMBOM, B., *Determination of hemicelluloses and pectins in wood and pulp fibres by acid methanolysis and gas chromatography*, Nordic Pulp and Paper Research Journal, 11, 4, (1996), 216–219

## BIBLIOGRAPHY

---

- TELEMAN, A., HARJUNPÄÄ, V., TENKANEN, M., BUCHERT, J., HAUSALO, T., DRAKENBERG, T. and VUORINEN, T., *Characterisation of 4-deoxy-beta-L-threo-hex-4-enopyranosyluronic acid attached to xylan in pine kraft pulp and pulping liquor by  $^1\text{H}$  and  $^{13}\text{C}$  NMR spectroscopy.*, Carbohydrate research, 272, 1, (1995), 55–71
- THYSELL, E., POHJANEN, E., LINDBERG, J., SCHUPPE-KOISTINEN, I., MORITZ, T., JONSSON, P. and ANTTI, H., *Reliable profile detection in comparative metabolomics*, Omics-a Journal of Integrative Biology, 11, 2, (2007), 209–224
- TUSKAN, G., WEST, D., BRADSHAW, H. D., NEALE, D., SEWELL, M., WHEELER, N., MEGRAW, B., JECH, K., WISELOGEL, A., EVANS, R., ELAM, C., DAVIS, M. and DINUS, R., *Two high-throughput techniques for determining wood properties as part of a molecular genetics analysis of hybrid poplar and loblolly pine*, Applied Biochemistry and Biotechnology, 77-9
- UCAR, G., MEIER, D., FAIX, O. and WEGENER, G., *Analytical pyrolysis and FTIR spectroscopy of fossil Sequoiadendron giganteum (Lindl.) wood and MWLs isolated hereof*, Holz als Roh- und Werkstoff, 63, 1, (2005), 57–63
- VAN DE MEENT, D., DE LEEUW, J. W., SCHENCK, P. A., WINDIG, W. and HAVERKAMP, J., *Quantitative-analysis of Bio-polymer Mixtures By Pyrolysis Mass-spectrometry*, Journal of Analytical and Applied Pyrolysis, 4, 2, (1982), 133–142
- VAN LOON, W. M. G. M., BOON, J. J. and DE GROOT, B., *Qualitative-analysis of chlorolignins and lignosulfonates in pulp-mill effluents entering the river rhine using pyrolysis mass-spectrometry and pyrolysis-gas chromatography mass-spectrometry*, Journal of Analytical and Applied Pyrolysis, 20, (1991), 275–302
- VAN LOON, W. M. G. M., BOON, J. J. and DE GROOT, B., *Quantitative-Analysis Of Sulfonic-Acid Groups In Macromolecular Lignosulfonic Acids And Aquatic Humic Substances By Temperature-Resolved Pyrolysis Mass-Spectrometry*, Environmental Science & Technology, 27, 12, (1993), 2387–2396
- VANE, C. H., ABBOTT, G. D. and HEAD, I. M., *The effect of fungal decay (Agaricus bisporus) on wheat straw lignin using pyrolysis-GC-MS in the presence of tetramethylammonium hydroxide (TMAH)*, Journal of Analytical and Applied Pyrolysis, 60, 1, (2001), 69–78

## BIBLIOGRAPHY

---

- VINCIGUERRA, V., NAPOLI, A., BISTONI, A., PETRUCCI, G. and SGHERZI, R., *Wood decay characterization of a naturally infected London plane-tree in urban environment using Py-GC/MS*, Journal of Analytical and Applied Pyrolysis, 78, 1, (2007), 228–231
- VIVÓ-TRUYOLS, G. and SCHOENMAKERS, P. J., *Automatic Selection of Optimal Savitzky-Golay Smoothing*, Analytical chemistry, 78, 13, (2006), 4598–4608
- WAMPLER, T. P., *Applied pyrolysis handbook*, Marcel Dekker, Inc., 1995
- WATANABE, T., KAWAMOTO, H. and SAKA, S., *Radical chain reactions in pyrolytic cleavage of the ether linkages of lignin model dimers and a trimer*, Holzforschung, 63, 4, (2009), 424–430
- WEISS, S. and INDURKHYA, N., *Predictive Data Mining: A Practical Guide*, The Morgan Kaufmann Series in Data Management Systems Series, Morgan Kaufmann, 1998
- WESTERMARK, U. and SAMUELSSON, B., *A spectrophotometric method for the determination of sulfonic acids in wood material*, Nordic Pulp and Paper Research Journal, 8, (1993), 358–359
- WINDIG, W., KISTEMAKER, P. G. and HAVERKAMP, J., *The Effects of Sample Preparation, Pyrolysis and Pyrolyzate Transfer Conditions On Pyrolysis Mass-spectra*, Journal of Analytical and Applied Pyrolysis, 1, 1, (1979), 39–52
- WOLD, S., *Chemometrics; What do we mean with it, and what do we want from it?*, Chemometrics and Intelligent Laboratory Systems, 30, 1, (1995), 109–115
- YAMAZAKI, N. and NAKANO, J., *On the formation of sulfonated carbohydrates during various sulfite cookings*, Mokuzai Gakkaishi, 18, (1972), 85–89
- YOKOI, H., ISHIDA, Y., OHTANI, H. and TSUGE, S., *Characterization of within-tree variation of lignin components in Eucalyptus camaldulensis by pyrolysis - gas chromatography*, The Analyst, 124, (1999), 669–674
- YOKOI, H., NAKASE, T. and ISHIDA, Y., *Discriminative analysis of Eucalyptus camaldulensis grown from seeds of various origins based on lignin components measured by pyrolysis-gas chromatography*, Journal of Analytical and Applied Pyrolysis, 57, (2001), 145–152



## BIBLIOGRAPHY

---

- ZHANG, L. M. and GELLERSTEDT, G., *Achieving quantitative assignment of lignin structure by combining  $^{13}\text{C}$  and HSQC NMR techniques*, in *Sixth European Workshop on lignocellulosics and Pulp*
- ZHANG, Y. J., SJOGREN, B., ENGSTRAND, P. and HTUN, M., *Determination of Charged Groups In Mechanical Pulp Fibers and Their Influence On Pulp Properties*, *Journal of Wood Chemistry and Technology*, 14, 1, (1994), 83–102

# List of Figures

2.1	Cellulosestructure . . . . .	10
2.2	Softwood glucomannan structure . . . . .	10
2.3	Softwood xylan structure . . . . .	11
2.4	Lignin linkage structures . . . . .	14
4.1	Effect of time $t_2$ of second NaOH charge on the kappa number and viscosity . . . . .	41
4.2	PH profile over the course of the two delignification series . . .	44
4.3	Pulp yields of series A and B as a function of cooking time . .	45
4.4	Lignin content of pulps as a function of cooking time . . . . .	46
4.5	Dissolved lignin as a function of pulp yield . . . . .	48
4.6	Carbohydrate composition as a function of cooking time for series A and series B . . . . .	50
4.7	Degree of sulfonation in pulps of series A and B . . . . .	54
4.8	Flowchart pre-processing . . . . .	62
4.9	Effect of smoothing and baseline correction for a small section of a pyrogram . . . . .	63
4.10	Effect of BC processing on TIC signal of large peak . . . . .	64
4.11	Effect of BC processing on TIC signal of small peak . . . . .	65
4.12	Effect of BC processing illustrated on extracted ions . . . . .	66
4.13	Effect of deconvolution on overlapping peaks . . . . .	68
4.14	Effect of deconvolution on coeluting peaks . . . . .	69
4.15	Overlay of two peak . . . . .	71
4.16	Comparison of coeluting peaks extracted from a pyrogram at the initial and the terminal cooking stage . . . . .	72
4.17	Selection of representative ions . . . . .	76
4.18	Selection of representative ions for 4-ethylguaiaicol and methyl pyruvate . . . . .	79
4.19	Comparison of 5 different signals across the 160 measurements conducted . . . . .	82

## LIST OF FIGURES

---

4.20	BC processed and weight-background normalized TIC signals acquired for samples of the delignification series . . . . .	84
4.21	Iteratively determined correlation between selected-peaks normalized and weight-background normalized TIC signal plotted against the number of peaks included for selected-peaks normalization . . . . .	87
4.22	Comparison of weight-background and selected-peaks normalized TIC signals acquired for samples of the B series as a function of cooking time . . . . .	88
4.23	Tukey's HSD test on the mean peak areas of ion m/z 55 eluting at RT 31.38 min . . . . .	91
4.24	Tukey's HSD test on the mean peak areas of ion m/z 44 eluting at RT 36.6 min . . . . .	92
4.25	Loadings plot for PC1 of mean-centered data taken from the PCA analysis of the replicate pulp samples . . . . .	94
4.26	Loadings plot for PC1 of autoscaled data taken from the PCA analysis of the replicate pulp samples . . . . .	95
4.27	Loadings plot for PC1 of pareto scaled and mean-centered data taken from the PCA analysis of the replicate pulp samples . . . . .	96
4.28	Score plot of PC1 versus PC2 of weight-background normalized and mean-centered pyrolysis data (408 peaks) of sample B <sub>60</sub> . . . . .	98
4.29	Score plot of PC1 versus PC2 of weight-background normalized and autoscaled pyrolysis data (408 peaks) of sample B <sub>60</sub> . . . . .	99
4.30	Score plot of PC1 versus PC2 of weight-background normalized and autoscaled pyrolysis data (408 peaks) of samples B <sub>30</sub> and B <sub>60</sub> . . . . .	100
4.31	Score plot of PC1 versus PC3 of weight-background normalized and autoscaled pyrolysis data (408 peaks) of samples B <sub>30</sub> and B <sub>60</sub> . . . . .	100
4.32	Score plot of the first two PCs for the complete pyrolysis data (408 peaks) of 5 pulp samples . . . . .	105
4.33	Score plot of the first two PCs for the pyrolysis data of G-lignin fragments (40 peaks) of 5 pulp samples . . . . .	106
4.34	Biplot of PC1 versus PC2 for the pyrolysis data of H-lignin fragments (20 peaks) of 5 pulp samples produced by kraft, acid sulfite, ASAM, AS/AQ and ASA process with similar kappa number . . . . .	108
4.35	Score plot of PC1 versus PC4 for the complete pyrolysis data (408 peaks) of samples A <sub>210</sub> , R1A <sub>210</sub> , R2A <sub>210</sub> , B <sub>210</sub> , R1B <sub>210</sub> and R2B <sub>210</sub> . . . . .	111

## LIST OF FIGURES

---

4.36	Plot of the Q residuals versus Hotelling $T^2$ revealing outlier . .	111
4.37	Visual presentation of results obtained from FDR peak selection	113
4.38	Score plot of PC1 versus PC2 for the pyrolysis data of 38 selected peaks of samples A <sub>210</sub> , R1A <sub>210</sub> , R2A <sub>210</sub> , B <sub>210</sub> , R1B <sub>210</sub> and R2B <sub>210</sub> . . . . .	114
4.39	Peak areas of guaiacyl acetone marker ion m/z 137, normalized by the lignin content, plotted against the lignin content . . . .	117
4.40	Peak areas of homovanillin marker ion m/z 164, normalized by the lignin content and plotted against the lignin content . .	118
4.41	Peak areas of methanol marker ion m/z 32 plotted against cooking time . . . . .	118
4.42	Peak areas of 3-hydroxybenzaldehyde marker ion m/z 121 plotted against lignin content . . . . .	119
4.43	Peak areas of 3-hydroxybenzaldehyde marker ion m/z 121, normalized by the lignin content and plotted against lignin content . . . . .	120
4.44	Peak areas of 4-methylphenol marker ion m/z 107, normalized by the lignin content and plotted against lignin content . . . .	121
4.45	Peak areas of levoglucosan marker ion m/z 60 plotted against lignin content . . . . .	122
4.46	Peak areas of acetic acid marker ion m/z 43 plotted against cooking time . . . . .	122
4.47	Peak areas of sulfur dioxide marker ion m/z 64 plotted against cooking time . . . . .	123
4.48	Peak areas of anthraquinone marker ion m/z 180 plotted against cooking time . . . . .	124
4.49	9 calibration curves for SO <sub>2</sub> . . . . .	125

# List of Tables

2.1	Relative chemical composition of soft- and hardwoods . . . . .	9
2.2	Linkages found in soft- and hardwoods . . . . .	15
2.3	Influence of NaOH splitting on AS/AQ pulping of spruce . . .	19
4.1	composition of <i>Picea abies</i> raw material . . . . .	38
4.2	Chemical composition of pulping liquor . . . . .	42
4.3	Comparison of results of series A and B . . . . .	43
4.4	Carbohydrate composition of the pulps of series A and B . . .	51
4.5	Sulfonic and carboxylic acid groups content in pulps of series A and B . . . . .	53
4.6	Degree of sulfonation of 4 pulps with kappa numbers of approx. 30 . . . . .	56
4.7	Analysis results for replicate pulps (210 min) . . . . .	57
4.8	Results for the RSDs calculated for 6 normalized ion peak areas	66
4.9	Path of generation of the global peak list . . . . .	70
4.10	Two examples for selection of representative ion on basis of mean correlation coefficients . . . . .	78
4.11	RSDs of sample B <sub>60</sub> calculated for 10 replicates within the first, 7 replicates within last 80 measurements . . . . .	83
4.12	RSDs of BC processed TIC signals for 5 different sets of sample replicate . . . . .	84
4.13	Comparison of the mean and median RSD values (RSD <sub>wn</sub> , RSD <sub>csn</sub> and RSD <sub>spn285</sub> ) resulting from weight-background, con- stant sum and selected-peaks normalization for the 9 replicate sets . . . . .	88
4.14	R <sup>2</sup> and slopes of 9 calibration curves for SO <sub>2</sub> marker ions m/z 48, 64 and 66 . . . . .	126